Apical Ectodermal Ridge (AER) activity and Limb outgrowth during Vertebrate Development

Ana Raquel Viegas Tomás

TESI DOCTORAL UPF
2010

Thesis Director: Joaquín Rodríguez León

Centre de Medicina Regenerativa de Barcelona (CMRB) /
Facultad de Medicina de la Universidade de Extremadura (UNEX)

Aos meus Pais…

TABLE OF CONTENTS

ACKNOWLEDGEMENTS

I would like to acknowledge the funding from Fundação para a Ciência e Tecnologia (SFRH / BD / 32346 / 2006) and from Fundação Calouste Gulbenkian, that allowed me to complete the work presented in this thesis.

I would like to acknowledge the institutions where this work has been developed, for having accepted me as a PhD student at their labs: to the Centre de Medicina Regenerativa de Barcelona at the Parc de Recerca Biomedica de Barcelona; and to the Departamento de Anatomía, Biología Celular y Zoología de la Facultad de Medicina da Universidad de Extremadura at Badajoz. And also to Instituto Gulbenkian de Ciência, that has always been, and will be, my “home”.

"O caminho faz-se caminhando."
At the end of this road, I cannot move on without thanking to all the people that came along on my journey, or just cross my path along these years. This thesis has also a bit of them, since one way or another, I have grown because of, and thanks to, them... you.

First of all, I would like to thank to Joaquín Rodríguez. Not in a million years I will find a BOSS like you! As my mother would say: "Nem com uma candeia acessa...!"
I cannot find the words to begin to thank you... maybe I'll just do a cheesecake and we leave it like this... ; Now seriously, thank you for every tip, every advice, for sharing your knowledge and for showing me how to proper science! For the opportunity to work in fancy places with "heavy machinery" and in the smaller ones, and teaching me that you can do great science in both places (you just have less cultural opportunities available...)
For your friendship, THANK YOU, BOSS!

At the CMRB, a big thank to you all for accepting “la portuguesa” with arms wide open, especially to Adriana and Dani (gracias, amigos! Demasiadas horas cerrados en la “chicken” han hecho esto - que jamás me olvide de vosotros); to my fellow “becarios” at CMRB, the postdocs and amazing technical staff, and administrative staff, that I cannot name all because they are too many… Thank you.

At UNEX, A Yolanda y Domingo. Os agradezco muchissimo. A todo el personal en el departamento por hacer com que me sienta “en casa”. Gracias!

At IGC, Catarina (sem palavras, obrigada!), um obrigado colectivo a todos os Organogénicos: um obrigado por tudo, *in situs* e caipirinhas, tudo faz parte do pacote! Agradeço em pessoa e ao vivo!

Surely there are a lot more people to thank, but time and space contingencies do not allow me.

Aos meus pais, que sempre me apoiaram nestas minhas “aventuras” não consigo passar a palavras o quanto eu vos estou grata!

LIST OF ABREVIATIONS

AER - Apical ectodermal ridge
AMV - Avian Myeloblastos virus
Amp - Ampicilin
AP - Anterior-posterior
ATP - Adenosine 5'-triphosphate
BAMBI - BMP and Activin receptor membrane bound inhibitor
BMP - Bone Morphogenetic Proteins
bp - base pairs
BSA - Bovine serum albumin
cDNA - complementar DNA
CIP - Calf Intestinal phosphatase
DEPC - Diethyl pyrocarbonate
DNA - Deoxyribonucleic acid
dNTPs - Deoxynucleotide Triphosphates
dpf - days post fertilization
dsRNA - double stranded RNA
DV - Dorsal-ventral
E. coli - Escherichia coli
ERK - Extracellular signal-regulated kinase
EST - Expressed Sequence Tag
EtOH - Ethanol
FBS - Foetal Bovine Serum
FGF - Fibroblast Growth Factor
Fw - Primer Forward
g - grama
GFP - Green Fluorescent Protein
HH - Hamburger & Hamilton staging of chicken embryo development
HBSS - Hank´s Balanced Salt Solution
h - hours
HOX - Homeodomain transcription factors
hpf - hours post-fertilization
IM - Intermediate mesoderm
iRNA - interference RNA
ISH - *In situ* Hybridisation
LPM - Lateral plate mesoderm
MABT - Maleic Acid Buffer plus Tween
MCS - Multiple Cloning Site
MetOH - Methanol
MKP - MAP Kinase fosfatase
mRNA - Messenger RNA
NBT/BCIP - Nitro Blue Tetrazolium/ 5-Bromo 4 Chloro-3Indolyphosphate

NTMT - NaCl, Tris, $MgCl_2$ and Tween solution
ON - Overnight
PBS - Phosphate Buffered saline
PCD - Programmed Cell Death
PCR - Polymerase Chain Reaction
PD - Proximal-distal
PFA - Paraformaldehyde
PI3K - phosphoinositide-3 kinase
PK - Proteinase K
pmol - picomol
PSM - Presomitic mesoderm
PZ - Progress Zone
RA - Retinoic acid
RAR - Retinoic acid receptors
RISC - RNA induced silencing complex
RNA - Ribonucleic Acid
RNApol - RNA Polymerase
RNase - RiboNuclease
rpm - rotations per minute
rRNA - ribosomal RNA
RT - Room Temperature
RT-PCR - Reverse Transcriptase Polymerase Chain Reaction
Rw - Primer Reverse
SAP - Shrimp Alkaline Phosphatase
Shh - Sonic Hedgehog
siRNA - Small Interfering RNA
tRNA - transfer RNA
TaqPol - Taq Polymerase
TGFβ - Transforming Growth Factor Beta
Tm - Melting temperature
ZPA - Zone of polarizing activity

SUMMARY

Limb outgrowth is controlled by a specialized group of cells called the apical ectodermal ridge (AER), a thickening of the limb epithelium, at its distal tip. This specialized thickening of ectodermal cells is responsible for maintaining the underlying mesenchymal cells in an undifferentiated and proliferative state, and its structure is preserved through a fine-tuned balance between proliferation and apoptosis. This equilibrium is genetically controlled but little is known about the molecules involved in this process. Several authors have been shown that both fibroblast growth factor (FGF) and Erk pathway activation are crucial for AER function. Recently, FLRT3, a transmembrane protein able to interact with FGF receptors, has been implicated in the triggering of ERK activity by FGFs. In this thesis, we show that *flrt3* expression is restricted to the AER, co-localizing its expression with *fgf8* and pERK activity. Loss-of-function studies demonstrates that silencing of *flrt3* affects the integrity of the AER and, subsequently, its proper function during limb bud outgrowth. Our data also indicate that *flrt3* expression is not regulated by FGF activity in the AER, whereas ectopic WNT3A is able to induce *flrt3* expression. Overall, our findings confirm *flrt3* as a key player during chicken limb development, being necessary but not sufficient for proper AER formation and maintenance under the control of BMP and WNT signalling.

During limb bud development, AER structure is maintained through a fine-tuned balance between proliferation and programmed cell death and this equilibrium is genetically controlled, although little is known about the molecules involved in that process.

In this thesis we present evidences involving *oct4*, required to establish and maintain the pluripotent cell population necessary for embryogenesis in mouse and human, in the control of the proliferative balance within the AER cells. Overexpression of *otc4* in the limb ectoderm disrupts the ratio apoptosis/proliferation and, moreover, *oct4* expression is under the control of wnt-canonical pathway. We also describe a special

localization and behaviour of proliferating cells in the AER in response to *oct4* activity. We, therefore, describe a role for *oct4* as a factor able to maintain a niche of cells that is responsible for the renewal of the AER.

RESUMEN

El crecimiento del esbozo de la extremidad está controlado por un grupo especializado de células denominado Cresta Ectodérmica Apical (CEA), un engrosamiento del epitelio del miembro en su borde más distal. Este engrosamiento es responsable del mantenimiento de las células del mesodermo distal en un estado indiferenciado y proliferativo. Diferentes estudios muestran que la actividad de los factores de crecimiento fibroblástico (FCF) y de la vía Erk son cruciales para la correcta funcionalidad de la CEA. Recientemente se ha implicado a FLRT3, una proteína transmembranal capaz de interaccionar con los receptores de los FCF, en la activación de la vía Erk por los mismos. En esta tesis describimos cómo la expresión de *flrt3* se restringe a la CEA, colocalizándose su expresión con *fgf8* y la actividad de la vía Erk. Los experimentos de pérdida de función demuestran que la inhibición de *flrt3* afecta la integridad de la CEA y, consecuentemente, a su función durante el desarrollo del esbozo del miembro. Nuestros datos también indican que la expresión de *flrt3* no está regulada a través de los FCF en la CEA, sin embargo, la activación ectópica de WNT3A es capaz de inducir la expresión de *flrt3*. En conjunto, nuestros resultados demuestran que *flrt3* es una molécula clave durante el desarrollo de las extremidades de pollo, siendo necesaria, pero no suficiente, para la correcta formación y mantenimiento de la CEA bajo el control de la señalización a través de BMP y WNT.

Durante el desarrollo de las extremidades, la estructura de la CEA se mantiene a través de un fino control del balance entre la proliferación y apoptosis. Este equilibrio se encuentra genéticamente controlado aunque se sabe muy poco acerca de las moléculas involucradas en este proceso.

En esta tesis presentamos evidencias en las que *oct4*, molécula necesaria para establecer y mantener la población de células pluripotentes necesarias durante la embriogénesis en ratón y humanos, controla la tasa de proliferación en las células de la CEA. La expresión ectópica de *oct4* en el ectodermo del esbozo de la extremidad

perturba la razón entre la apoptosis y la proliferación y, además, su expresión está controlada por la actividad de la vía canónica de los Wnt. También describimos en este trabajo la localización y comportamiento especiales de las células de la CEA en proliferación como respuesta a la actividad de *oct4*. Por consiguiente, podemos inferir que el rol de *oct4* será el de un factor necesario para mantener un nicho celular responsable por la renovación de la CEA.

INTRODUCTION

The main goal of Developmental Biology is the study of how the interaction of complex signalling networks drives the initial relative simplicity of a fertilized egg to become an organized and complexly patterned organism.
During organogenesis coordinated proliferation, patterning and differentiation of cells result in formation of organs and tissues. These coordinated events are orchestrated by a small group of cells with organizer properties that instruct the surrounding cells with respect to their fate and differentiation potential. However, the temporal and spatial regulation of the several individual developmental programs is tightly regulated and precisely coordinated.
In this context, limb development can be a powerful model to understand the general mechanisms of patterning and cell differentiation. Since limbs are not vital for embryonic life, one can experimentally remove or transplant parts of the developing limb without interfering with the vital process of the organism.

I Overview of vertebrate limb development

Signalling centers are specialized groups of cells located at the primordia of tissues and organs that pattern these structures for proper morphogenesis. Formation and maintenance of signalling centers is firmly regulated, spatially and temporally, being the vertebrate limb a paradigm in the study of these centers (Capdevila and Izpisua Belmonte, 2001; Niswander, 2003).

The limb patterning is coordinated along three axes during the embryonic development in vertebrates: proximal-distal (PD), starting from the shoulders and ending at the digit tips, anterior-posterior (AP), from the first to the little (fifth) digits, and dorsal-ventral (DV), from the back of the hands/ feet to the palms/ soles. As a result, three limb segments are formed: (1) the stylopod that contains the

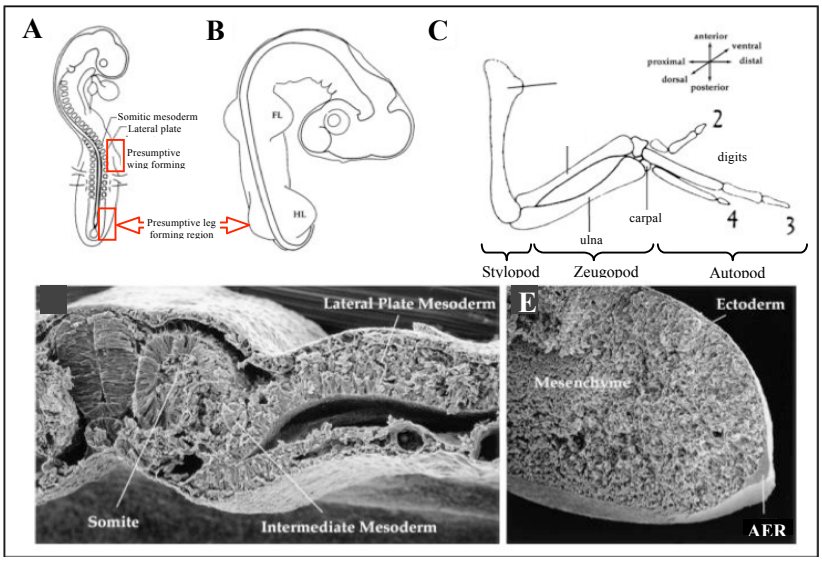

Figure 1. (A-C) Schematic representation of the primordia of the wing and leg bud and their skelectical constituition. (D-E) Scanning electron microscopy of the developing chicken limb bud. Adapted from Gilbert, 2003.

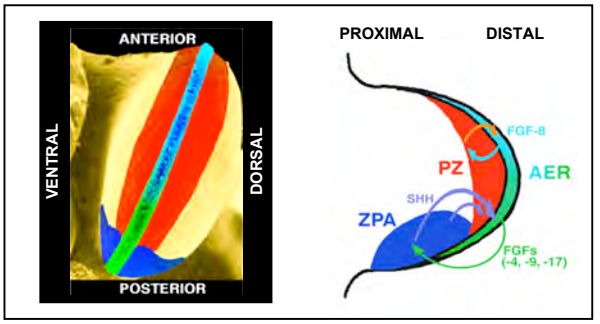

Figure 2. Schematic representation of the signalling centers the control limb outgrowth (adaptado de http://pages.unibas.ch/anatomie/zeller/).

humerus and femur, (2) the zeugopod in the middle containing the radius and ulna or tibia and fibula, and (3) the autopod at the tip composed of carpal/ tarsal, metacarpal/ metatarsal bones and fingers/ toes (Fig. 1C). Any one of these limb compartments has a unique tri-dimensional structure distinguishing it from all the other limb components. This specific pattern is under the tight control of spatio-temporally

synchronized and simultaneously orchestrated signals of three important centres (Fig. 2): the Apical Ectodermal Ridge (AER), the Zone of Polarizing Activity (ZPA) and the non-AER ectoderm (Mariani and Martin, 2003; Niswander, 2003; Tickle, 2006)

I.1 Proximodistal limb bud development

Proximal-distal outgrowth of the vertebrate limb bud is regulated by the AER, which forms along the dorsal-ventral (DV) axis of the embryo. This structure is formed soon after the initial budding as an epithelial rim at the distal border of the limb bud. The major function of the AER is to promote the PD outgrowth and patterning by keeping the most distal underlying mesenchyme in a proliferative and undifferentiated state. After the AER specification, only *Ffg8* expression is initially observed, equally distributed from anterior to posterior but this instructive role for PD pattering is mediated by the production of another four Fibroblast growth factors (FGFs): *Ffg4*, *Ffg2*, *Ffg9* and *Ffg17*. *These FGFs* are later activated in the posterior AER part and subsequently expand in an anterior direction during the progression of the limb development. It was demonstrated that the AER-Fgfs are essential for the limb bud development and, moreover, that they are also capable of inducing distal cell identity by activation of *Hoxa11* and *Hoxa13*. This indicates the presence of an FGF-dependent distal fate specification of cells giving rise to the zeugopod and autopod (Niswander, 1992; Mahmood et al., 1995; Savage and Fallon, 1995; Martin, 1998; Lewandoski et al., 2000; Montero et al., 2001; Sun et al., 2002; Mariani and Martin, 2003; Boulet et al., 2004; Kurose et al., 2004).

I.2 Limb bud positioning, initiation and early outgrowth

The first morphological indication for limb development is a rapidly growing bulge in the lateral body wall at the positions where future upper and lower limbs will emerge (Fig. 1A). This early limb bud is composed of proliferating mesenchymal cells from the lateral plate mesoderm covered by ectoderm (Fig.1D). The part of the

body flank where it appears is called the “limb field”. In chicken, this occurs around stage 12HH (Capdevila and Izpisua Belmonte, 2001; Towers and Tickle, 2009a).
Several data indirectly suggest that Hox genes expressed in the intermediate mesoderm probably mark the exact position of the limb field. In fact, the expression boundaries of several Hox genes such as *Hoxc6*, *Hoxc8* and *Hoxb5* in the lateral plate mesoderm (LPM) occur exactly at the forelimb (or pectoral fins in fish) prospective field. Also the absence of forelimbs in some snakes is well correlated with specific changes in Hox gene expression domains in both the paraxial mesoderm and the LPM (Rancourt et al., 1995; Cohn et al., 1997; Capdevila and Izpisua Belmonte, 2001).

The upper and lower limbs share common morphogenic events and morphological regulation during their development. However, there is also an obvious need for functional and corresponding morphogenic difference between them. *Tbx4* and *Tbx5* genes, both T-box transcription factors, were found to be specifically expressed in the lower and upper limbs, respectively (Gibson-Brown et al., 1996). Their expression in the corresponding limb field is detected prior to the limb bud initiation (Isaac et al., 1998). In addition, there is a synchronized interaction between them, as *Tbx5* down-regulates *Tbx4* in the forelimbs. On the other hand, *Pitx1*, another gene specifically expressed only in the lower limbs, up-regulates the *Tbx4* expression levels in the hind limbs. Thus, they seem to be specific regulators controlling limb identity (Rodriguez-Esteban et al., 1999; Takeuchi et al., 1999; Logan, 2003).

Experiments in zebrafish suggest that retinoic acid (RA) signalling is required and sufficient to initiate forelimb development, acting upstream of *Tbx5* (Gibert et al., 2006). Other parallel pathways may also be involved in the control of the upper/ lower limb identities. It is possible that *Hox* genes participate in this process as in general they are important for the AP body patterning (Nelson et al., 1996). It was demonstrated that TBX5 and TBX4 differentially regulate *hox9* genes during wing/leg specification (Takeuchi et al., 1999). The same authors also suggest that a

regulatory loop between *Hox9* and Tbx genes is necessary not only to specify limb identity but also to its initiation. According to them, *Wnt2b* and *Wnt8c*, are specifically regulated by *Tbx5* and *Tbx4*, respectively, activating the FGF pathway in earlier stages of limb development (Fig. 3A) (Takeuchi et al., 2003).

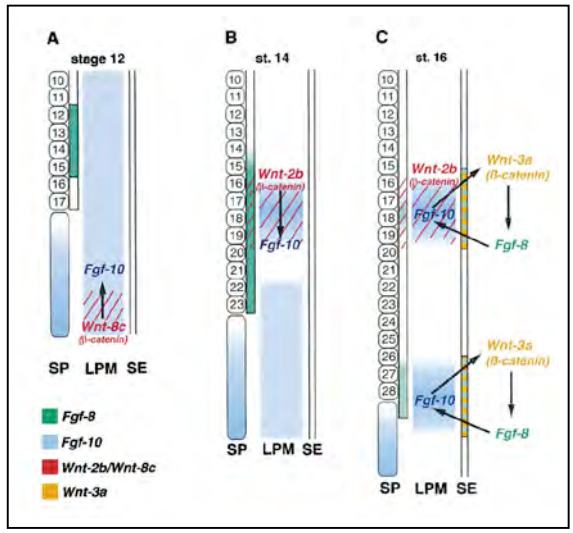

Figure 3. Simplified model proposed by Kawakami et al., 2001 for the establishment and maintenance of the *fgf10/fgf8*.

I.2.1 Establishment and maintenance of the *fgf8/fgf10* positive feedback loop

Currently, there are no clear data about the molecular mechanisms that initiate the limb bud formation (Fernandez-Teran and Ros, 2008; Zeller et al., 2009).

FGFs and WNT ligands can induce ectopic limb development when applied in the flank field of the embryo (Cohn et al., 1997; Kawakami et al., 2001). Several years ago, experiments of implantation of a bead soaked in FGF8 or FGF10 have proved that both *fgf8* and *fgf10* can induce ectopic limbs (Fig. 4)(Ohuchi et al., 1997) what was further proved with mutants for *fgf10*, which had completely truncated limbs (Sekine et al., 1999). A hypothesis suggests that Wnts induce *Fgf10* mesenchymal

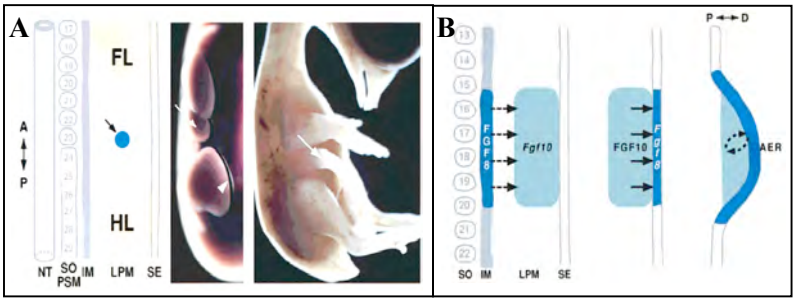

Figure 4. (A) FGF8 can induce an ectopic limb in the flank between the fore- and the hindlimb; **(B)** Limb induction model in which intermediate mesoderm (IM) plays a key role in limb bud induction by producing FGFs that are segregated to the lateral plate mesoderme (LPM), that in turn will signal to superficial mesoderm (SE). Adapted from Martin et al., 2001.

expression (Fig.3). Later, *fgf10*, with the support of *bmp4*, will prompt the AER establishment by the initiation of *fgf8* expression in prospective AER progenitors and creation of a growth-promoting mesenchymal-ectodermal feedback-loop between *fgf8*, produced by the AER-progenitors, and *fgf10* from the progress zone (Fig.4B) (Crossley et al., 1996; Ohuchi et al., 1997; Sekine et al., 1999; Benazet and Zeller, 2009).

Additionally, two members of the wnt family, *wnt2b* and *wnt8c*, are expressed in the presumptive forelimb and hindlimb regions of the LPM (Fig. 3), respectively, just prior to limb outgrowth. These two secreted proteins can induce *fgf10* that in turn will activate and maintain the expression of *fgf8* in the AER. Besides this, *Fgf8* induction in the AER by FGF10 is mediated by the expression of another wnt gene (*wnt3a*). Therefore, the positive-feedback loop, in which *fgf8* expression in the AER maintains the expression of *fgf10* in the underlying mesenchyme is established, and the three *wnt* genes that signal through β-catenin act as key molecular mediators of the FGF regulatory loop that controls both limb initiation and AER induction (Kawakami et al., 2001; McQueeney et al., 2002).

At the receptor level, this loop is mediated by FGFR2b and *wnt3a* in the AER, and FGFR2c and *wnt2b* in the LPM (Xu et al., 1998; Sekine et al., 1999; Lonai, 2003)

and is maintained until AER regresses, keeping the distal region of the limb mesenchyme, the Progress Zone (PZ) and the AER in an undifferentiated and proliferative state (Yang and Niswander, 1995; Capdevila and Izpisua Belmonte, 2001; ten Berge et al., 2008)

Beyond the range of these proliferative signals, the mesenchymal cells delay their proliferation, start to express *sox9* and initiate production of cartilaginous precursors of the future bones (Hill et al., 2005; Suzuki et al., 2008)

I.2.2 Retinoic acid and the promotion of Proximal-Distal (PD) outgrowth

Retinoic acid (RA) effect on limb bud initiation has long been established, however, its role on proximo-distal limb patterning has been target of a controversy in the last years. Retinoic Acid is synthesized in the proximal mesenchyme, mainly by RALDH2, and spreads into the distal limb bud, where it is degraded by CYP26, creating a gradient of RA concentration throughout the limb (Okamoto et al., 1990; Yashiro et al., 2004).

It was believed that these AER-FGF morphogenic activities were a result of direct FGF antagonism with RA signalling from the most proximal limb bud mesechyme (Mercader et al., 2000). As a result, the RA induced *Meis1* and *Meis2* expression remains restricted within the proximal territory of the future stylopod (Capdevila et al., 1999; Mercader et al., 2000; Niederreither et al., 2002). However, recent genetic studies suggest that the AER-FGFs determine the PD limb axis early in the limb development and the specified progenitor pools progressively expand during the later phases of the limb patterning (Dudley et al., 2002; Galloway et al., 2009). Zhao and collegues show that, in mice, RA signalling is not required for limb expression of *Shh* and *Meis2*. Moreover, they say that RA action is required outside the limb field in the body axis during forelimb induction, but that RA is unnecessary at later stages when hindlimb budding and patterning occurs (Zhao et al., 2009).

BOX 1 - Models for proximodistal limb bud axis development

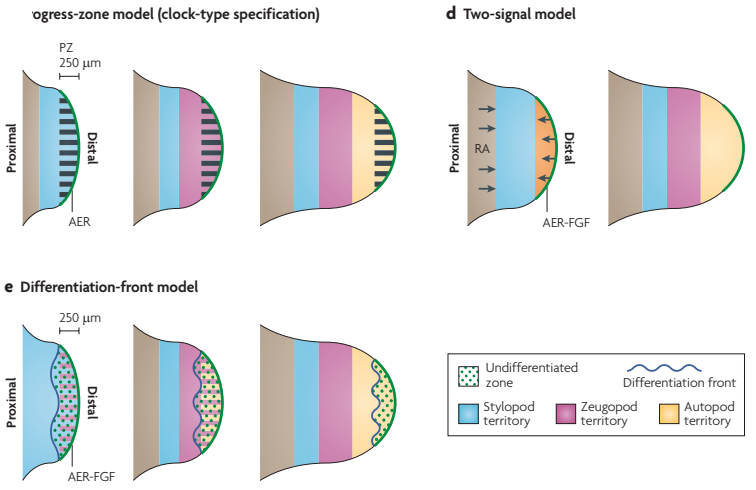

The progress zone (PZ) model was formulated to explain the limb skeletal phenotypes that result from the manipulation of chicken limb buds (Saunders J. W., 1948). It was proposed that the mesenchyme that underlies the AER contains unspecified progenitors (the PZ is indicated by black stripes)(Summerbell et al., 1973), the fates of which are controlled by AER signals. As limb bud outgrowth progresses distally, proximal cells no longer receive AER signals. The time of their 'exit' from the PZ determines their proximodistal (PD) identity (that is, there is 'clock-type' specification). Mesenchymal cells that exit early generate proximal elements, whereas cells that remain in the PZ for longer form more distal structures.

The two-signal model was proposed based on molecular analysis of chicken limb bud development (Mercader et al., 2000). During the onset of limb bud development, the proximal region (blue) is probably specified by retinoic acid (RA) signalling from the flank, and the distal region (orange) is specified by AER-derived fibroblast growth factor (AER-FGF) signalling. The zeugopod arises from the more proximal distal cells, and the autopod primordia is formed by the most distal mesenchymal cells (Mariani and Martin, 2003).

The differentiation-front model (Tabin and Wolpert, 2007) postulates that PD identities are determined as the proliferating mesenchyme leaves the undifferentiated zone - that is, when the mesenchyme is no longer under the influence of AER-FGF signalling. After cells have crossed the differentiation front (blue wavy line) they only express genes that mark the identity of a particular segment (for example, *Meis1* expression in the stylopod territory, homeobox A11 (*Hoxa11*) expression in the zeugopod territory and *Hoxa13* expression in the autopod territory).
Adapted from Zeller et al., 2009.

I.3 Establishment of dorso-ventral (DV) polarity and patterning

Another aspect of the crosstalk between the mesenchyme and the ectoderm is the establishment of DV limb polarity, a compulsory condition for AER formation. An important signalling centre in this process is the non-AER limb ectoderm where WNT and BMP signals are key components in the dorsalization of both the ectoderm and the mesoderm (Wang et al., 2004).

Once limb is growing, the dorsal ectoderm expressed *wnt7a* activates mesodermal *lmx1b* expression, which in turn is sufficient to pre-pattern dorsal identity of all components of the developing limbs (Riddle, 1993; Parr, 1995; Vogel et al., 1996; Loomis et al., 1998).

Different studies have shown that *en-1* plays a role during migration and compaction of AER cells restricting the expression of *r-fng* and *wnt-7a* to the dorsal ectoderm (Logan, 1997; Loomis et al., 1998), while Wnt/ß-catenin signalling is required to maintain the AER after AER initiation and maturation (Kengaku et al., 1998; Barrow et al., 2003). In fact, *Wnt*-7a instructs the dorsal mesoderm to adopt dorsal characteristics, such as *lmx-1* expression, which in turn specifies dorsal pattern. Thus, *en-1* has a dual function in AER positioning and ventral specification and hence acts to coordinate the two processes (Johnson and Tabin, 1997).

BMP signalling, besides being essential for AER induction, as revealed by loss and gain-of-function experiments, is also necessary and sufficient to regulate *en-1* expression in the ventral ectoderm. Therefore, the loss of BMP signalling from the early limb bud ectoderm results in failure of AER formation and bi-dorsal limbs (Ahn et al., 2001; Pizette et al., 2001; Soshnikova et al., 2003; Wang et al., 2004). Finally, in the context of axis coordination, *Wnt7a* in the dorsal ectoderm directly regulates the *Shh* expression within the ZPA (Parr, 1995)

I.4 ZPA and the regulation of Anterior-Posterior (AP) patterning

The specification of the AP axis of the limb is the earliest change from the pluripotent condition of limb mesenchyme. This axis is patterned by a group of

mesenchymal cells located in the posterior region of the limb bud. Classical grafting experiments led to the detection of a limb organizer located in the posterior limb bud mesenchyme, the Zone of Polarizing Activity (ZPA). Its function is to define the AP limb axis by instructing limb bud mesodermal cells of their final fate depending on their AP position (Capdevila and Izpisua Belmonte, 2001).

BOX2 - Models for anteroposterior limb bud axis development

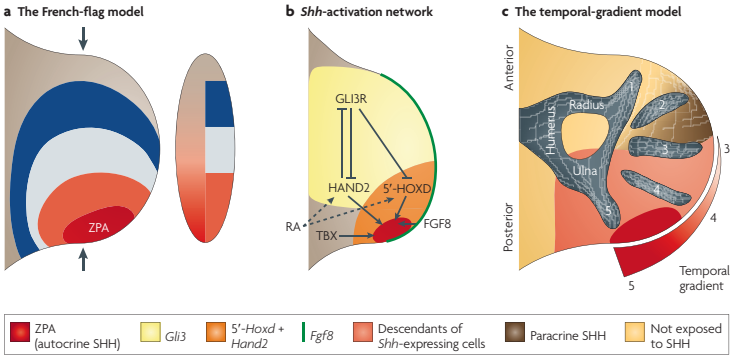

(A) ***The French-flag model*** (Wolpert, 1969) can explain the results of manipulating the chicken limb bud organizer (zone of polarizing activity (ZPA), which is located in the posterior limb bud mesenchyme). This model proposes that the ZPA secretes a morphogen that diffuses across the limb bud to generate a spatial gradient. The identities of the three digits (likened to the colours of the French flag), are specified by threshold levels of the morphogen.

(B) the gene network that restricts the activation and maintenance of sonic hedgehog (Shh) expression to the posterior limb bud mesenchyme.

(C) ***The temporal gradient model*** states that the specification of anteroposterior identities occurs by spatial and temporal gradient of SHH signalling (Ahn et al., 2001; Harfe et al., 2004). As cells cease to express Shh, they exit the ZPA. The expanding population of cells derived from Shh-expressing cells (Shh descendants) displaces non-ZPA cells (which are specified by long-range SHH signalling) towards the anterior. Shh descendants give rise to the ulna, digit 4 and digit 5, and contribute to digit 3. Cells that give rise to digit 2 and parts of digit 3 are specified by long-range SHH signalling. The humerus, radius and digit 1 are specified in a SHH-independent manner. 5′-HOXD, 5′-located homeobox D; FGF8, fibroblast growth factor 8; GLI3R, repressor form of GLI3; HAND2, heart and neural crest derivatives 2; RA, retinoic acid; TBX, T-box. Adapted from Zeller et al., 2009.

The classical hypothesis proposed by Wolpert claims that a gradient of a hypothetical ZPA morphogen within the limb bud establishes the AP axis (Wolpert, 1969). Later studies demonstrated that ZPA-derived Shh signalling is both necessary and sufficient to maintain these ZPA functions (Riddle, 1993).

The initiation and position of a *shh* expressing domain at the posterior limb bud margin is under the control of many transcription factors including *dHand*, *5'-Hox*, *tbx*, *Alx4*, *Twist*, *Gli3* and *fgf8* genes as well as RA signalling from the flank (Stratford et al., 1997; Chiang et al., 2001; Niederreither et al., 2002; Wang et al., 2004). Besides that, the prospective ZPA region seems to be linked with the expression of several Hox genes, namely *hoxb8* whose expression appears to be correlated with forelimb ZPA establishment and Shh induction. Indeed, RA may induce Shh expression through *hoxb8* (Capdevila and Izpisua Belmonte, 2001).
Once induced, early limb bud is pre-patterned by mutual genetic antagonism between anteriorly expressed Gli3 and the posteriorly expressed dHAND. This mechanism seems to be prior to *shh* expression, establishing its localization (te Welscher et al., 2002). Shh negatively regulates Gli3 transcription and post-translational processing, and is under negative regulation by Gli3 (and Alx4) in the anterior margin of the limb bud, creating a Gli3Repressor-Gli3 gradient along the AP axis of the limb. This could account for the determination of digit number and identity (McGlinn et al., 2005).

The crosstalk between the ZPA and the AER was found to be crucial in the complex process of limb formation. Key components of this mesenchymal-ectodermal interaction are *shh*, limb specific FGFs, BMPs and BMP antagonists like *gremlin* (Zuniga et al., 1999; Scherz et al., 2004). The study of targeted mutations of limb specific FGF and BMP/ BMP antagonist genes revealed the existence of self-regulatory loops controlling the appropriate initiation and termination of this signalling in the coordination of limb development (Khokha et al., 2003; Mariani and Martin, 2003; Verheyden et al., 2005; Benazet and Zeller, 2009).

BOX3 - Interlinked feedback loops define a self-regulatory limb signalling

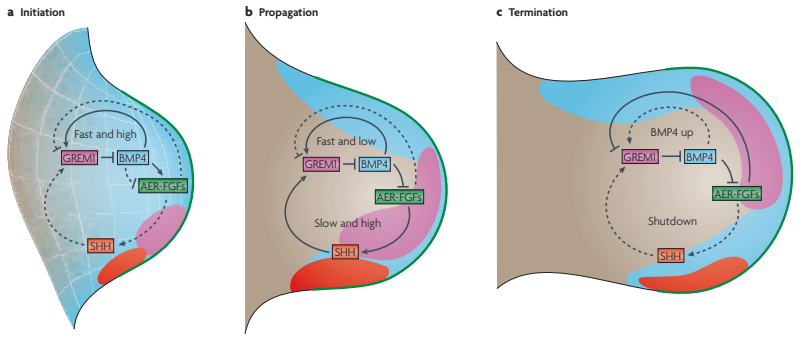

The mesenchymal bone morphogenetic protein (BMP4; light blue), sonic hedgehog (SHH; red), gremlin 1 (GREM1; purple) and apical ectodermal ridge-derived fibroblast growth factor (AER-FGF; green) expression domains during mouse limb organogenesis are indicated schematically. The interlinked signalling feedback loops (Benazet and Zeller, 2009) that operate at each stage are shown as solid lines. Broken lines indicate inactive loops. From Zeller et al., 2009.

(A) Initiation phase: BMP4 upregulates Grem1 expression in a fast initiator loop (~2 h loop time). Shh expression and signalling are activated independently of GREM1 and AER-FGFs.

(B) Propagation phase: the establishment of loops that control the distal progression of limb bud development. SHH predominantly upregulates Grem1 expression. GREM1 reinforces AER-FGF and zone of polarizing activity-derived SHH (ZPA-SHH) signalling by an epithelial–mesenchymal feedback loop (with a loop time of ~12 h). The activity of the fast BMP4–Grem1 initiator module is low. However, this low BMP activity controls the length of the AER (not shown).

(C) Termination phase: the widening gap between ZPA-SHH signalling and the Grem1 expression domain, together with the onset of AER-FGF-mediated inhibition of Grem1, terminates the signalling system. As a consequence, BMP4 activity is likely to increase again.

I.5 Axes coordination during limb development

Limb patronization and growth along the three axes must be a well coordinated and interrelated process: (a) the positive loop of SHH and FGFs is maintained due to an interaction between the AER and the ZPA; (b) SHH synthesis is stimulated both by FGF4 (involved in PD axis patterning) and WNT7a (a DV organizer); (c) SHH

creates a gradient of Gli3 activator and repressor form, allowing the establishment of a DV identity; (d) BMPs are both responsible for shutting down the signalling from the AER and for simultaneously inhibiting the WNT7a signal along the D-V axis. While BMP signalling eliminates growth and patterning along all the three axes, *Gremlin* works against BMP to preserve the AER and the WNT7a pathway (Capdevila and Izpisua Belmonte, 2001; Tickle, 2002a; Gilbert, 2003; Niswander, 2003; Panman and Zeller, 2003).

In summary, to allow the proper development and outgrowth of the limb, the crosstalk between these 3 axes is a crucial process.

I.5.1 Proposed models for axes coordination during limb development

Over the years, a few models have been proposed to explain separate aspects of the complex limb development (Tabin and Wolpert, 2007; Towers and Tickle, 2009b; Zeller et al., 2009). However, there is strong evidence for an obviously integrated, three-dimensional function of all currently known pathways in the orchestration of the limb patterning.

In an attempt to collate all the available knowledge, Zeller *et al*. (2009) suggested an integrative patterning design for the limb morpho- and organogenesis. During the first phase of limb bud initiation, opposing mesenchymal signals of Gli3, Hand2, 5'-Hox, Bmps, Fgfs and RA pre-pattern the nascent limb bud and support the establishment of the two major signalling centres in the developing limb, the AER and the ZPA. Activation of the AER-FGFs and ZPA-Shh signalling creates morphogen gradients across the limb bud and leads to early specification of the two main limb axes, PD and AP.

At this stage cell identities are not yet determined. How the cell fates are specified is not yet known but transcriptional regulators like *Hoxa*, *Hoxd* and *Tbx* genes are probably involved. At that time the BMP activity decreases and the ectoderm-mesenchyme feedback loop mediated by Shh, Gremlin and Fgf is initiated to promote subsequent proliferation, determination and differentiation. The expansion

of the progenitor cell pools is under the control of the self-terminating *Shh-Grem1*-FGF signalling, ectodermal Wnts (e-Wnts) and persistent low levels of Bmps. When core mesenchymal cells escape the control of the above signals due to the progressing proliferation, they start to express *Sox9* and undergo chondrogenic differentiation. Proximal to this differentiation front, the PD and AP identities are completely determined thus allowing the initiation of the differentiation process.

Therefore, the differentiation of digit patterns occurs the last. At the end of this phase, the Bmp activity again increases as a consequence of Shh-Grem1-Fgf self-termination. The digit identities are later determined with the involvement of *Bmp*, *5'-Hox* and *Sall* genes but, unfortunately, no specific regulators of individual digits are currently known (Zeller *et al*., 2009).

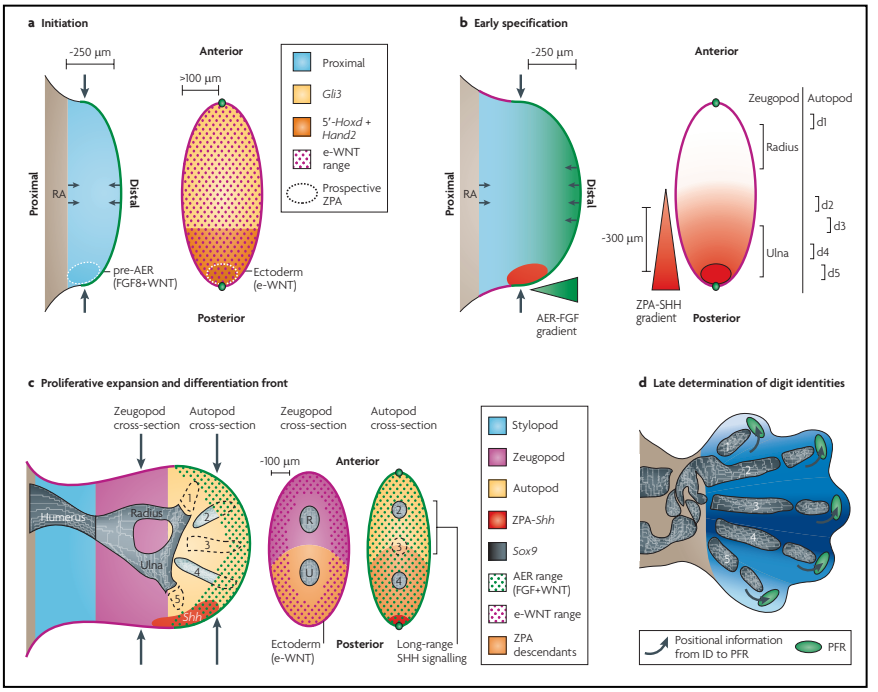

Figure 5. Integrative model proposed by Zeller et al., 2009 for limb bud development. Summary in the text.

II Developmental dynamics of the AER

During limb development, the apical ectodermal ridge (AER) is the organizing centre that controls proximo-distal outgrowth. This thickening of ectodermal cells at the most distal part of the limb bud (Fig. 6A,B) is responsible for maintaining the underlying mesenchymal cells in an undifferentiated and proliferative state (the progress zone, PZ). The importance and requirement of the AER is a conserved feature in the process of vertebrate limb development (reviewed in Fernandez-Teran and Ros, 2008).

In *Gallus gallus*, the AER consists of a strip of pseudostratified columnar epithelium, covered by the overlying periderm (Fig. 6C), which runs along the distal dorso-ventral border of the limb bud (Fernandez-Teran and Ros, 2008). It starts as a flatten structure but becomes anatomically distinguishable at stage 18HH when the distal ectodermal cells acquire a columnar shape, making them easily distinguishable from the rest of the cuboidal ectoderm. During the period of its maximum height, a groove is visible at the base of the AER (Todt and Fallon, 1984).

Classical experiments have shown that surgical removal of the AER results in cell death in the mesenchyme and abrogates limb outgrowth (Saunders J. W., 1948; Summerbell, 1974; Niswander, 2003; Fernandez-Teran and Ros, 2008; Towers and Tickle, 2009a). The importance and necessity of the AER in limb outgrowth is a conserved feature of vertebrate development as illustrated in mice, chick and zebrafish, and even though they serve overall the same function, they present strikingly different structures (Tickle, 2002b; Mercader, 2007; Fernandez-Teran and Ros, 2008).

Although extensive studies have been done, the molecular and genetic mechanisms that control initiation and maintenance of the AER in these model organisms still need to be studied.

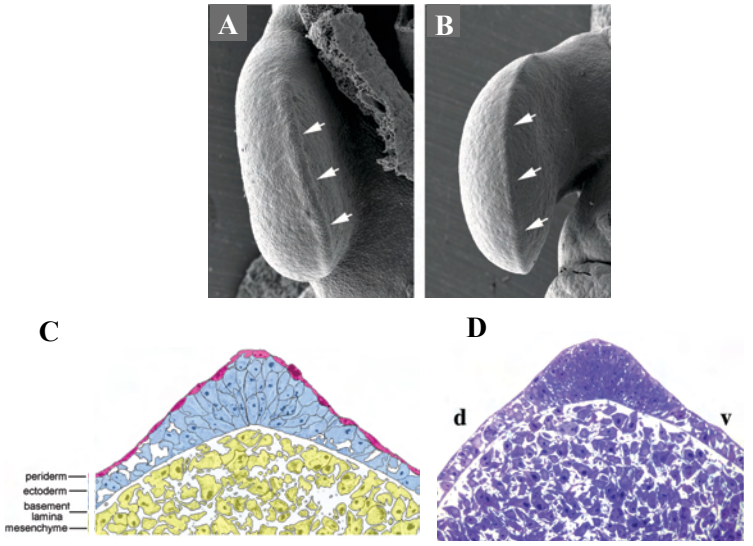

Figure 6. Morphology of the Apical Ectodermal Ridge (AER).**(A, B)** Scanning electron microscopy micrographs of the structures and distinct morphology of the AER over time; **(C)** Schematic representation of an stage 20HH AER; **(D)** Semithin section through the distal tip of a stage 20HH limb bud. Note the pseudostratified epithelium. Adapted from Fernandez-Teran and Ros, 2008, and Towers and Tickle, 2009.

The formation of the AER can be divided into two processes. First, the induction (Fig. 7A) by the mesodermal factor FGF10 of AER-precursor cells in the surface ectoderm that will migrate toward the dorsal-ventral boundary and form the AER at a specific position. These cells start to express *fgf8*, a member of the FGF superfamily that acts as an essential signalling molecule involved in vertebrate limb outgrowth (Lewandoski et al., 2000; Boulet et al., 2004; Fernandez-Teran and Ros, 2008). Second, the maturation of the AER (Fig. 7B), resulting in the formation of the characteristic, thickened structure, maintained by a FGF8/FGF10 positive feedback loop (Carrington and Fallon, 1984; Ohuchi et al., 1997; Lewandoski et al., 2000; Altabef and Tickle, 2002; Boulet et al., 2004; Fernandez-Teran and Ros, 2008).

At this stage, a fluid cell-cell communication aiming to coordinate signalling from the three axes is essential to allow an accurate patterning. *Gremlin*, a BMP antagonist, plays an important role mediating the positive feedback loop between the

FGFs in the AER and SHH in the ZPA (Ganan et al., 1996; Merino et al., 1999; Zuniga et al., 1999; Scherz et al., 2004).

The mature AER is maintained through a tuned balance between proliferation and cell death for additional 2 to 3 days, while mesenchymal skeletal progenitors continue to proliferate and differentiate until a fully patterned limb emerges (Fernandez-Teran and Ros, 2008). This equilibrium is genetically controlled but little is known about the molecules involved in this process.

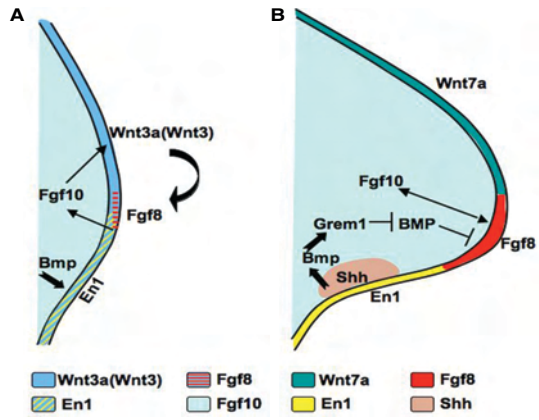

Figure 7. Regulatory cascades involved in AER induction (A) and maintenance (B). From Fernandez-Teran and Ros, 2008.

The AER then regresses via programmed cell death and eventually flattens to a simple cuboidal epithelium, becoming indistinguishable from the dorsal or ventral ectoderm. This regression is under the control of BMP signalling since *Noggin*, a potent antagonist of BMPs, is known to lead to an abnormal AER persistence, when overexpressed in chicken and in mice (Pizette and Niswander, 1999; Guha et al., 2002).

BMPs also have an important role later during limb development, controlling apoptosis in the interdigital areas, by regulating, among other functions, AER-FGFs that act as survival factors for the interdigit mesenchyme (Pajni-Underwood et al., 2007; Fernandez-Teran and Ros, 2008).

III FGF signalling pathway regulation

FGFs are very important molecules during embryonic development, being involved in numerous cell processes such as cell proliferation, differentiation, cell survival and motility (Capdevila and Izpisua Belmonte, 2001; Tickle, 2002a).
During limb development FGFs are key molecules during limb induction, outgrowth and promoting both cell survival and apoptosis (Capdevila and Izpisua Belmonte, 2001; Montero et al., 2001; Zeller et al., 2009). The intracellular response to FGF stimuli is mediated by FGF receptors (FGFRs), which trigger several intracellular pathways, namely the Ras-MAPK/ERK and the PI3K pathways, which we describe briefly.

III.1 Ras-MAPK/ERK pathway

The Ras-MAPK is the most common pathway induced by FGFs (Fig. 8, blue). Binding of Grb2 to phosphorylated FRS2 activates the pathway and the subsequent formation of a Grb2/SOS complex leads to the activation of Ras by GTP exchange. Once active, Ras interacts with several effector proteins, including Raf and Rac leading to the activation of the different MAPK cascades (Bottcher et al., 2004; Thisse and Thisse, 2005). Once activated, these kinases are translocated to the nucleus where they phosphorylate target transcription factors, such as c-*myc*, AP1, and members of the Ets family of transcription factors (like *erm* and *pea3*), and, this way, they control gene expression (Sharrocks, 2001; Lee and McCubrey, 2002; Thisse and Thisse, 2005).

The ERK1/2 Ras-MAPK pathway is implicated in FGF-required developmental processes like sclerotome specification (Brent and Tabin, 2004), neural induction and limb development (Eblaghie et al., 2003), differentiation of the retina (Lovicu and McAvoy, 2001; McCabe et al., 2006), and isthmic organizer function (Suzuki-Hirano et al., 2010).
The co-localization of activated forms of ERK (pERK) with FGF-expressing regions

during early embryonic development has been widely (Corson et al., 2003; Eblaghie et al., 2003; Kawakami et al., 2003; Lunn et al., 2007).

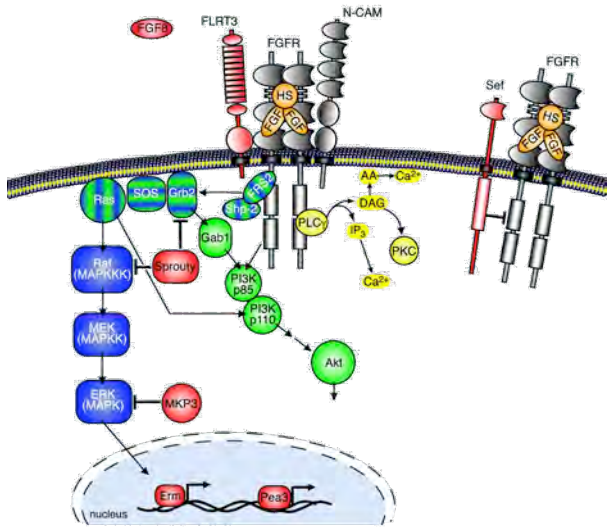

Figure 8. Intracellular signalling pathways activated through FGFRs. Formation of a ternary FGF-heparin-FGFR complex leads to receptor autophosphorylation and activation of intracellular signalling cascades, including the Ras/MAPK pathway (shown in *blue*), PI3 kinase/Akt pathway (shown in *green*), and the PLCγ/Ca^{2+} pathway (shown in *yellow*).

III.2 PI3 kinase/Akt pathway

Upon ligand binding, FGFRs can activate PI3 kinase/Akt pathway by three different mechanisms. First, Gab1 can bind indirectly to FRS2 via Grb2, resulting in tyrosine phosphorylation and activation of the PI3-kinase/Akt pathway through p85. Second, the PI3 kinase-regulatory subunit p85 can bind to a phosphorylated tyrosine residue of the FGFR, as showed in *Xenopus* cell extracts. Alternatively, activated Ras can induce membrane localization and activation of the p110 catalytic subunit of PI3 kinase (Fig. 8, green)(Bottcher et al., 2004).

While activaction of MAPK cascade promotes neural proliferation, differentiation and apoptosis, activaction of PI3K pathway promotes cell survival (Powers et al., 2000; Ong et al., 2001; Kawakami et al., 2003)

III.3 Modulators of FGF signalling

Due to the wide range of biological roles exert by FGFs and to the variety and complexity of the pathways activated, FGF signalling must be tightly regulated (Xu et al., 1998; Sun et al., 2002; Thisse and Thisse, 2005). A growing number of proteins have been identified as specific regulators of FGFR-mediated signalling. These molecules affect the FGF signalling cascade at different levels (Fig. 9) and most of them belong to the FGF synexpression group, a set of genes that share complex spatio-temporal expression patterns and have a functional relationship (Niehrs and Pollet, 1999). *Sprouty, spred, sef*, *shisa* and *mkp3* are known as negative modulators of FGF signalling, whereas *erm, er81* and *pea3* promote FGF signalling (Raible and Brand, 2001; Zhang et al., 2001; Furthauer et al., 2002; Dikic and Giordano, 2003; Kawakami et al., 2003; Tsang and Dawid, 2004; Sivak et al., 2005; Furushima et al., 2007).

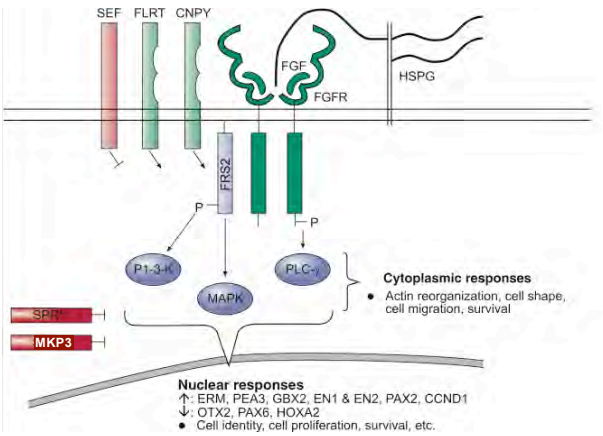

Figure 9. Fibroblast growth factor (FGF) signalling pathways and their regulators. FGF, FGFR and heparan sulphate form a ternary complex resulting in FGFR dimerization and transphosphorylation. This leads into an increase in FGFR kinase activity and phosphorylation of intercellular substrates, including a docking protein FRS2. Three major signalling pathways include PI-3 kinase pathway (PI-3-K), mitogen-activated protein kinase (MAPK) pathway and phospholipase C gamma pathway (PLC-c). These pathways regulate cell-type specific responses both in the cytoplasm and nucleus. Some positive (FLRT and CNPY) and negative [SEF, SPRY and MKP3] regulators of the FGF signalling pathways are indicated. HSPG, heparan sulphate proteoglycans. Adapted from Partanen et al., 2007.

III.3.1 Negative regulators: *sef, sprouty* and *mkp3*

Sef, named for "similar expression to FGFs", encodes a single-pass transmembrane protein that negatively modulates FGF signalling. *Sef* is a member of the FGF synexpression group in zebrafish and mouse, expressed in the characteristic pattern of FGF8 and regulated by FGF signalling (Furthauer et al., 2002; Lin et al., 2002; Tsang et al., 2002). Overexpression studies in zebrafish embryos show that *Sef* inhibits FGF signalling via interaction with FGFR1 and FGFR4a and that it functions at the level or downstream of MAPK kinase. Interfering with *Sef* function by antisense morpholino oligonucleotide (MO) injection induces phenotypic changes reminiscent of embryos dorsalized by ectopic expression of *Fgf8* (Furthauer et al., 2002; Tsang et al., 2002)

The feedback inhibitor *Sprouty* was identified in *Drosophila* as a negative regulator of FGF signalling during tracheal development (Hacohen et al., 1998). Four mammalian *Sprouty* proteins (Spry1 to 4) and three Spreds (Sprouty-related EVH1 domain proteins) that share a highly conserved cysteine-rich domain at the carboxy terminus have been identified. This domain is critical to target them to the plasma membrane and to inhibit the MAPK pathway (Lim et al., 2002). Sprouty proteins interfere with FGF signalling through several mechanisms, depending on the cellular context and/or stimulation. Moreover, different Sprouty proteins exhibit different activities and have different interaction partners, including, but not limited, Grb2 and Raf1 (Christofori, 2003). *Sprouty2* and *Sprouty4* are members of the FGF8 synexpression group and are regulated by FGF signalling (Minowada et al., 1999; Chambers and Mason, 2000; Furthauer et al., 2001).
Gain- and loss-of-function experiments confirm the function of Sprouty proteins as intracellular antagonists of FGF signalling. Among other studies, overexpressing *Sprouty* during chick limb development causes a reduction in limb bud outgrowth consistent with reduced FGF signalling (Minowada et al., 1999).

It is well established that receptor tyrosine kinases (RTK) signalling is controlled by protein tyrosine phosphatase (PTPs), which act as positive or negative regulators on RTK signalling (Van Vactor et al., 1998). The dual-specificity PTP MAPK phosphatase 3 (MKP3, also called Pyst1 or DUSP6) exclusively antagonizes the MAPK pathway via ERK1/2 inactivation. MKP3 belongs to the MKP (MAPK phosphatase) subfamily, the largest group of phosphatases specialized in the regulation of MAPKs. In vertebrates, its expression is very similar to that of the FGF8 synexpression group, and it is regulated by FGF8 (Eblaghie et al., 2003; Kawakami et al., 2003).

Kawakami *et al.* propose that in the developing chick limb *MKP3* is induced in the mesenchyme by FGF8 through the PI3K-Akt pathway. The role of MKP3 in the mesenchyme would be to antagonize the Ras-MAPK pathway and prevent cell death. Thus, MKP3 would have an anti-apoptotic function in the mesenchyme. Conversely, intact Ras-MAPK signalling would be necessary for the integrity of the AER (Kawakami et al., 2003). Manipulation of MKP3 activity by short interfering RNA inhibition or its overexpression disrupts limb morphology and outgrowth (Eblaghie et al., 2003; Kawakami et al., 2003).

III.3.2 Positive regulators: *flrt3*

An emerging theme is the regulation of FGF signalling by transmembrane modulators.

FLRT proteins comprise a small family of fibronectin type III domain (FNIII) and leucine-rich repeats (LRR) are single-pass transmembrane glycoproteins in vertebrates (Fig. 10)(Lacy et al., 1999). FLRT3, the best-characterized member of the family, can physically interact with FGF receptors and modulate FGF-ERK signalling (Bottcher et al., 2004).

Initially identified in human genome, this family comprises 3 genes: *flrt1*, *flrt2*, e *flrt3*. h*flrt3* shares 55% similarity with h*flrt1*, and 41% with h*flrt2*. H*flrt1* and h*flrt2* are identical in 41% of their amino acid sequence (Lacy et al., 1999).

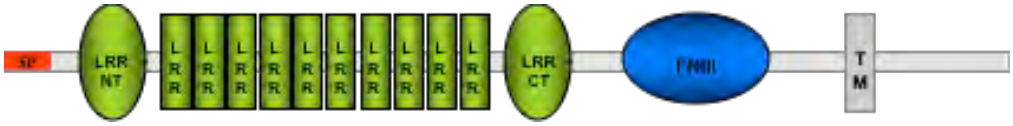

Figure 10. Schematic representation of x*flrt3*. **SP**, signal peptide; **LRRNT**, N-terminal Leucine rich repeat cysteine flank; **LRR**, Leucine-rich repeats; **LRRCT**, C-terminal Leucine rich repeat cysteine flank; **FNIII**, fibronectin domain type III; **TM**, transmembrane domain. Adaptado de (Bottcher et al., 2004).

In opposition to MKPs and Sprouties, FLRTs have uniquely been identified in vertebrates. FLRT3 coincides in both chick and frog with *Fgf8* expression sites during development, including the limb bud and the midbrain-hindbrain boundary (MHB)(Bottcher et al., 2004; Smith and Tickle, 2006).

In *Xenopus, flrt3* was identified as a gene with a similar expression pattern to FGF signalling molecules, particularly at the MHB (Bottcher et al., 2004).
Studies in frog demonstrated that FLRT3 expression is FGF-dependent and that this protein works as positive modulator of FGF signalling. XFLRT3 binds to FGFR1 and FGFR4a and its intracellular carboxy-terminal region is involved in MEK/ERK signalling cascade, as opposed to MKP3, as described before (Bottcher et al., 2004).
In addition, FLRT3 induces homotypic cell sorting in cultured cells and in *Xenopus* embryos. FGF signalling is dependent on the cytoplasmic tail, whereas FGF receptor binding is mediated by the FNIII domain of FLRT3 (Bottcher et al., 2004). The extracellular LRR domains are dispensable for FGF signal activation (Bottcher et al., 2004), but are essential for the FLRT3-mediated cell sorting activity (Karaulanov et al., 2006).

In the mouse, *flrt3* mRNA was also found in regions known to express FGF signalling components and in areas affected by FGF signalling (Haines et al., 2006). As an example, *Flrt3* activity at the midbrain/hindbrain boundary in mouse correlates with the role of FGFs in the formation of and signalling from the isthmus (Carl and Wittbrodt, 1999; Trokovic et al., 2003).

FLRT3 was also identified as a target gene of Nodal signalling, inhibiting cadherin adhesion in *Xenopus* early development through interaction with the Rho family GTPase Rnd1 (Ogata et al., 2007). In the mouse, *flrt3* knockout embryos display defects in ventral closure, headfold fusion and definitive endoderm migration (Maretto et al., 2008), as well as disorganization of the basement membrane which leads to rupture of the anterior visceral endoderm (Egea et al., 2008), suggesting that cell adhesion is affected upon *flrt3* ablation. Furthermore, FLRT3 has been implicated in neurite outgrowth (Robinson et al., 2004; Tsuji et al., 2004).

FLRT3 appears to integrate two different activities: the LRR domains promote homotypic cell sorting/adhesion (Karaulanov et al., 2006), while its intracellular tail confers cell deadhesion via Rnd1 (Ogata et al., 2007) and Unc5 (Karaulanov et al., 2009).
During morphogenesis such duality in functions may be crucial, because the same FLRT3 protein can both loosen adhesion, such as in gastrulating cells (Ogata et al., 2007), allowing them to move, and simultaneously keep homotypic cell groups together, preventing tissue disintegration.

IV The AER as a model for the study of epithelial renewal

Embryonic stem cells (ESCs) have been gaining notoriety as invaluable tools for research and a promising resource for cell replacement therapies, since they were first discovered in late 80's. These cells present the unique property of self-renewal and the ability to generate differentiated progeny in all embryonic lineages both *in vitro* and *in vivo*, having been extensively studied for the molecular characteristics that permit them to achieve and maintain their pluripotency.

A large number of organisms are able to regenerate body parts. It has been recognized also for many years that there are cells in adult mammalian tissues that are involved in maintaining the homeostasis in tissues that are constantly replacing their cell populations, like skin, blood, hair and gut epithelium (Bryant et al., 2002).

In contrast to ESCs, somatic stem cells (SSCs) are maintained by self-renewal and differentiate into function-specific cells in order to replace dead and injured cells in various tissues (reviewed in Naveiras and Daley, 2006; Teo and Vallier, 2010).

Oct4, along with transcriptional co-regulators *Nanog* and *Sox*2, is critical to maintain an undifferentiated and pluripotent state of human and mouse embryonic stem cells as well as early embryonic cells (Nichols et al., 1998; Pesce and Scholer, 2001; Avilion et al., 2003; Chambers et al., 2003; Mitsui et al., 2003; Loh et al., 2006; Niwa, 2007). They positively regulate genes responsible for the ES cell phenotype whilst repressing transcription of genes required for inducing differentiation through a gene dosage effect (Stefanovic and Puceat, 2007). In 2007, Lavial and colleagues, prove it to be also required for chicken embryonic stem cells pluripotency maintenance and continued proliferation, establishing that mechanisms by which genes like *oct4* regulate pluripotency and self-renewal are not exclusive to mammals (Lavial et al., 2007).

In a major breakthrough in regenerative medicine, somatic mammalian cells (mouse fibroblasts) were epigenetically reprogrammed to a pluripotent state (iPS, induced pluripotent stem cells) through the exogenous expression of the transcription factors *Oct4*, *Sox2*, *Klf4*, and c-*Myc.* Unexpectedly, *Nanog* was expendable (Takahashi and Yamanaka, 2006). Although the combinations needed to, *in vitro*, induce pluripotency in different cell types may vary, *Oct4* has been an obligatory component of the cocktail, suggesting a pivotal role for *Oct4* in maintaining the self-renewal and pluripotent state of those cells.

Self-renewal process is generally describe as a parallel cellular event of proliferation, differentiation and apoptosis, and known to be controlled by intrinsic genetic pathways that are subject to regulation by extrinsic signals from the microenvironment in which those cells reside (Zhang and Li, 2005; Haegebarth and Clevers, 2009), and that shares many features with epithelial renewal as we prove in this thesis.

The AER's importance in vertebrate limb development has been extensively demonstrated. This specialized ectoderm rim along the distal edge of the limb bud controls proximal-distal growth by maintaining PZ cells in an undifferentiated and proliferative state.

AER is an epithelial transient structure maintained by a fine-tuned balance between cell proliferation and cell death. As we thoroughly described, AER is sustained throughout development by a coordinated network of signalling pathways during limb development.

To date, little was known on the behaviour of AER cells and the dynamic of cell renewal at the most distal tip of the limb during development.

IV.1.1 The stemness marker, *Oct4*

Oct4, a transcription factor that contains a POU-specific domain and a POU homeodomain (Fig. 11) and belongs to the class V POU homeodomain family of transcription factors, was recently identified in chicken, exhibiting high similarity with other members of the family (Lavial et al., 2007). This molecule is a key factor in maintaining the undifferentiated state (self-renewal) and pluripotency of human and mouse embryonic stem (ES) cells as well as early embryonic cells (Nichols et al., 1998; Pesce and Scholer, 2001; Niwa, 2007), instructing stem cell fate through a gene dosage effect (Stefanovic and Puceat, 2007).

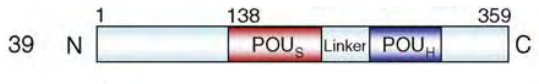

Figure 11. Schematics of human *oct4*. The predicted protein molecular weight in kDa is shown at the left protein. The numbers above the protein show the amino acid position at the start of the DNA binding domain and at the C terminus. DNA binding subdomains (POUS and POUH) are annotated. Adapted from Kang et al., 2009.

In the absence of *oct4*, ES cells lose the capacity to self-renew and subsenquently differentiate into extra-embryonic trophectoderm (Hough et al., 2006; Niwa, 2007).
Moreover, when overexpressed in epithelial tissues, Oct4 blocks progenitor-cell differentiation (Hochedlinger et al., 2005). Besides that, Oct4 is also required for the maintenance of chicken embryonic stem cells (cESC) pluripotency and continued proliferation (Lavial et al., 2007).
In addition to its role in ES cells, *oct4* is also required for the maintenance of the germ cell lineage (Kehler et al., 2004).
In both ESCs and embryonic carcinoma cells, expression of *oct4* is strong and rapidly downregulated during RA-induced differentiation (Pikarsky et al., 1994; Schoorlemmer et al., 1994; Lavial et al., 2007).

AIMS

The necessity of the Apical Ectodermal Ridge (AER) in limb development has long been established. The existence of an intricate network of signals between the AER of the developing limb and the cells that lye underneath is responsible for the correct outgrowth and patterning of the limb along development.

In this thesis, we intended to clarify the role of *flrt3*, a known modulator of FGF signalling during limb development, aiming to:

- Characterize the expression profile of *flrt3* during chick limb development
- Compare the expression pattern of different members of the *flrt* family of genes to analyse possible redundant or differential functions
- Explore the effects of *flrt3* missexpression in the limb patterning and AER formation and maintenance
- Study the involvement of known limb signalling pathways in the regulation of *flrt3* gene expression

We were also interested in characterize and understand the mechanism behind apical ectodermal ridge renewal along development and uncover genes that might be responsible this renewal, such as *oct4*, a known key factor in maintaining an undifferentiated state (self-renewal) and pluripotency of ESCs. Therefore, we specifically aimed to:

- Characterize the expression pattern of *oct4* during chick limb development
- Describe and analyse the profiles of proliferation and cell death at the AER
- Explore the effects of *oct4* overexpression in AER
- Understand the relationship between the genetic cascades responsible for AER activity and *oct4* expression
- Uncover other candidate *oct4* co-regulator genes

RESULTS

CHAPTER I

- *Flrt3* as a key player in Limb Development -

(Part of the results presented in this chapter are unpublished and have been submitted to publication)

Overview

The importance and requirement of the AER is a conserved feature in the process of vertebrate limb development (reviewed in Fernandez-Teran and Ros, 2008). Although extensive studies have been carried out, the molecular mechanisms controlling the initiation and maintenance of the AER are still far from understood.

Maintenance of limb bud outgrowth is due to the action of signals emanating from the AER, namely FGF8, that are able to induce the expression of *fgf10* in the underlying mesenchyme which, in turn, signals back to the AER resulting in the establishment of a reciprocal positive feedback loop responsible for each one's expression (Xu et al., 1998; Lizarraga et al., 1999). It has been also established that Wnt/β-catenin activity, in particular Wnt3a, is required for the induction of *fgf8* expression in the AER (Kawakami et al., 2001; Logan, 2003).

At the intracellular level, FGF activity induces different MAP kinase cascades, including the Ras/ERK pathway in the AER and the PI-3K pathway in the PZ. As a result, during limb bud development, phosphorylated ERK can be detected in the AER but not in the PZ, and FGF8 is responsible for the induction of an ERK inhibitor, *mkp3,* in the PZ, through PI-3 kinase activation. In this context, the activation of ERK in the AER is responsible for its integrity and proper function, and MKP3 antagonism in the distal mesenchyme accounts for cell survival in that area (Eblaghie et al., 2003; Kawakami et al., 2003).

Members of the Fibronectin Leucine-Rich Transmembrane (*flrt*) gene family encode putative single pass transmembrane proteins with conserved domain structure among vertebrates, which include a putative signal peptide, ten leucine-rich repeats (LRR), a type III fibronectin domain, a transmembrane domain, and a short intracellular tail (Lacy et al., 1999; Haines et al., 2006). FLRT3 is the family member that has been more extensively characterized (Bottcher et al., 2004; Haines et al., 2006).

Xenopus flrt3 was identified as a gene with a similar expression pattern to FGF signalling molecules, particularly at the midbrain/hindbrain boundary (Bottcher et al., 2004). It is involved in the activation of ERK by FGFs. Moreover, it has been described that *flrt3* is able to modulate FGF signalling, to interact with the FGF receptor enhancing the activation of the FGF pathway and to be regulated by FGF signalling (Bottcher et al., 2004). In the mouse, *flrt3* mRNA was detected in regions known to express FGF signalling components and in areas affected by FGF signalling (Haines et al., 2006). As an example, *Flrt3* activity at the midbrain/hindbrain boundary in mouse correlates with the role of FGFs in the formation of and signalling from the isthmus (Carl and Wittbrodt, 1999; Trokovic et al., 2003). *Flrt3* knockout embryos exhibit defects in ventral closure, headfold fusion and definitive endoderm migration, as well as rupture of the anterior visceral endoderm caused by disarrangement of the basal membrane, suggesting that cell adhesion is affected upon *flrt3* ablation (Egea et al., 2008; Maretto et al., 2008).

In this chapter, we show that expression of the chicken *flrt3* in the AER co-localizes with FGF expression and ERK activation, supporting the known role of FGFs in limb formation (Lewandoski et al., 2000; Smith and Tickle, 2006). We also show that *flrt3* is an important player during chicken limb development maintaining the integrity and proper activity of the AER during limb bud development under the control of BMP and WNT signalling. Moreover, we draw some parallels of expression with the zebrafish *flrt3* and other *flrt* genes.

I.1 FLRT3 phylogenetic analysis

Flrt3 is the best-characterized member of this family of Fibronectin Leucine-Rich Transmembrane (*flrt*) genes. An open reading frame encoding for 675 amino acids, the largest of the group, was identified and compared with the 648 aminoacids of *Xenopus*, and the 640 of zebrafish, mouse and human. The chicken *flrt3* is highly homologous to FLRT3 from other vertebrates (Fig. 12B), as it shares 85,6% of amino acids with its mouse homologous, and 71,4% with the zebrafish one (Fig. 12C). Homology is especially high in the Leucine-rich repeats (LRR) domains and in the small intracellular portion.

A.

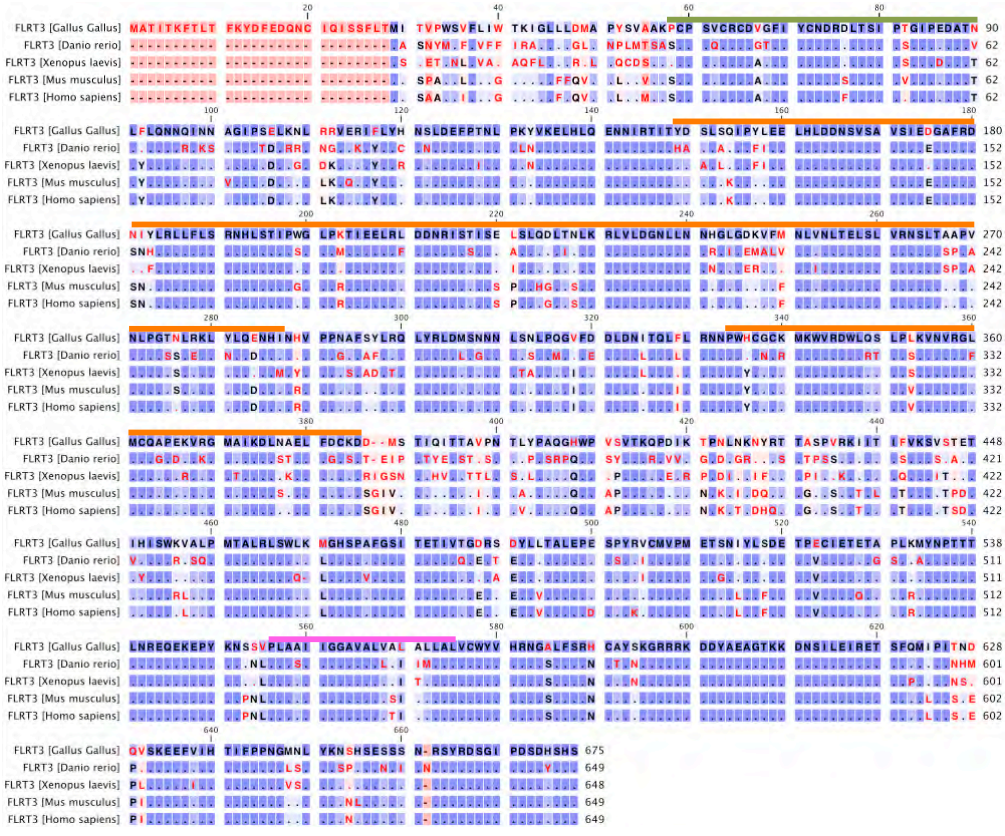

B.

Species	GeneBank Accession Number	**Identity (%)**
Gallus Gallus	XP_426107	Protein
vs. *Homo sapiens*	NP_938205	86,6%
vs. *Mus musculus*	NP_848469	85,6%
vs. *Danio rerio*	XP_687230	71,4%
vs. *Xenopus laevis*	NP_001080928	81,1%

C.

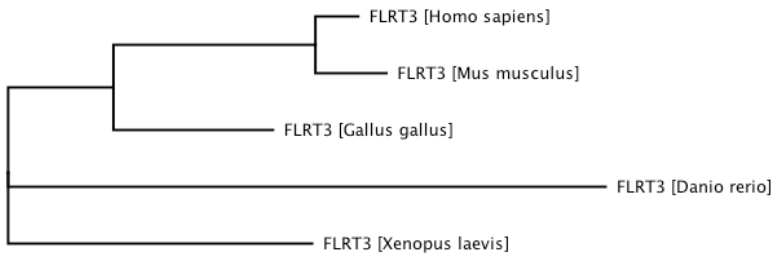

Figure 12. Family relationship, sequence and structural comparison of *flrt3*. A, ClustalW alignment of FLRT3 protein representatives of other major vertebrate groups (human, mouse, *Xenopus laevis* and zebrafish. Amino acids are colour-coded by consensus, from red to blue. Identical residues are indicated by dots, different residues in red. The lines above the sequence indicates regions of interest, as described below **A**. **B**, percentage of protein similarity between chicken *flrt3* and human, mouse, *Xenopus laevis* and zebrafish. **C**, An evolutionary tree showing the phylogenetic distance among FLRT3 proteins.

The divergence between proteins generally matches known evolutionary relationships (Fig. 12C).

I.2 *Danio rerio*'s *flrt3*

zFlrt3 was identified in a large scale analysis of gene expression by whole mount *in situ* hybridization during zebrafish embryogenesis and larva stages using templates provided by the ZFModels (zebrafish model for Human Development and Disease) consortium (Thisse et al., 2004).

We isolated a partial cDNA clone for the zebrafish *flrt3* through RT-PCR. A BLAST search of the GenBank® database showed only one annotation for *flrt3*, and two for

each of the other two *flrt* family members, showing that there was no gene duplication of *flrt3* in *Danio rerio*. The clone obtained was sequenced and blasted against GenBank® database to confirm its identity. The sequence agreed with the latest release of the zebrafish genome project (Zv8).

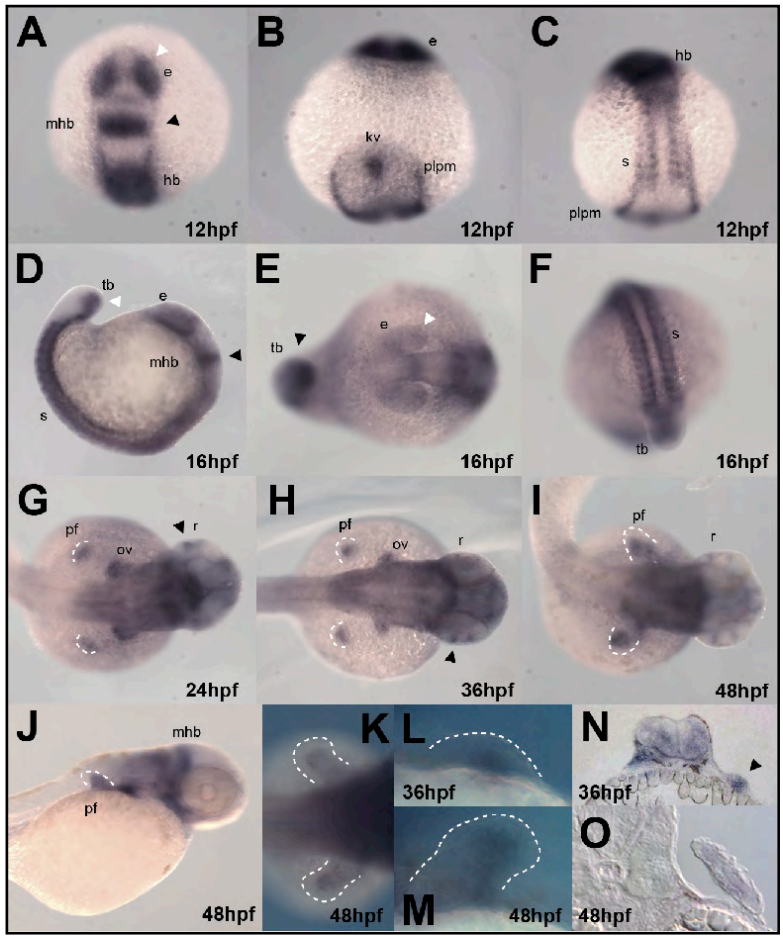

Figure 13. Expression Pattern of *flrt3* in *Danio rerio*. *In situ* hybridisation for z*flrt3*. **A-C**, different perspectives of a zebrafish embryo at 12 hpf; **D-F**, zebrafish embryo at 16 hpf; **G-J**, zebrafish embryo at 24, 36 and 48 hpf, highlighting the pectoral fin along development. **K-M**, close-ups of the developing pectoral fin, note the expression of *flrt3* in the mesenchyme, also observed in **N** and **O**. e, eye; mhb, midbrain-hindbrain boundary; hb, hindbrain; kv, kupffer vesicle; plpm, posterior lateral plate mesoderm; s, somite; tb, tailbud; ov, otic vesicle; r, retina; pf, pectoral fin.

I.2.1 Gene expression pattern of *flrt3* during zebrafish development

To elucidate the expression pattern of *flrt3* during teleost development, we performed whole-mount in situ hybridisation analyses. The earliest signal of *flrt3* was observed at 50% epiboly in the endoderm and in the margin. At 12 hpf (hours post-fertilization) is observed in the developing eye (Fig. 13A, white arrow), midbrain-hindbrain boundary (Fig. 13A, black arrow), hindbrain, along the lateral plate mesoderm, in the somites and the in the kupffer vesicle (Figs. 13B,C). By 16 hpf the staining become more evident in the somites and in the ventral part of the tail bud (Fig. 13D, white arrow). *Flrt3* expression can still be found in the eye, diencephalon-mesencephalon border, midbrain-hindbrain boundary, and hindbrain.
The pectoral fins, at 24 hpf are clearly stained for the presence of *flrt3* transcripts (Fig. 13G, white dashed line), as well as the retina (Figs. 13G, white arrow), dorsal diencephalon, mesencephalon, branchial arches and otic vesicles (Figs. 13G-I).
During Pharyngula period, from 24 hpf to 48 hpf, expression of *flrt3* can be found, like in younger embryos, at known centers of FGF signalling in the developing fin, brain, eye, and ear (Fig. 13G-I). It becomes evident that *flrt3* expression in the pectoral fins is restricted to the mesenchyme (Fig. 13J,K), as it can be observed in the magnification (Figs. 13L-P), complementary pattern observed in the chicken and mice homologues, where *flrt3* is expressed in the AER (Haines et al., 2006; Smith and Tickle, 2006; Tomás et al., 2010). No *flrt3* transcripts can be detected in the pectoral fin 62 plus hpf, suggesting a role for z*flrt3* in the maintenance of the AER.

I.2.2 Immunolocalization of FLRT3 during pectoral fin development

Immunohistochemistry studies were performed in embryos from 12hpf to 72hpf, both wholemount and in sections. Two antibodies against the human FLRT3 are commercially available. We have tested it on zebrafish embryos.
We have identified FLRT3 protein in cells that constitute the dermomyotome, branchial arches, and the developing retina (Fig. 14A-D), correlating with the structures where the *flrt3* mRNA is expressed. However, in the pectoral fin, we have

immunolocalized FLRT3 to the apical fold (Fig. 14E), instead of the mesenchyme, as for the mRNA (Fig. 13M).

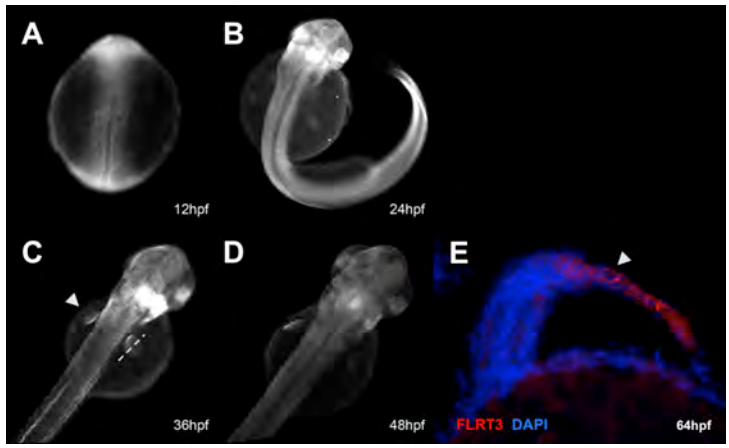

Figure 14. Immunolocalization of *flrt3* in *Danio rerio.* Immunohistochemistry with anti-FLRT3 antibody in wholemount zebrafish embryo (A-D) along development. FLRT3 protein correlates with the *flrt3* expression pattern with the exception of the pectoral fin, here detected at the apical fold. **E,** cross section of 64hpf zebrafish embryos, showing specific membrane staining of apical ectodermal fold (AEF) cells with anti-FLRT3 antibody; FLRT3 (red), nuclei are counterstained with DAPI (blue).

I.3 *Gallus gallus*'s *flrt3*

I.3.1 *Flrt3* expression is restricted to the AER and coincides with that of *fgf8* and pERK activity

In order to determine the role of *flrt3* in the development and patterning of the vertebrate limb, we started by examining the spatial and temporal expression pattern of *flrt3* mRNA by *in situ* hybridisation and protein localisation by immunohistochemistry during chicken limb development.

Chicken *flrt3* is expressed at stage 11HH in the neural ectoderm, at the developing optic placodes and in the neural crest cells around the otic placodes (Fig. 15A, white arrow). *Flrt3* transcripts are also found along the anterior-posterior (AP) axis in the somites (Fig. 15A, black arrow) and at lower levels in the presomitic mesoderm. As the somites differentiate, *flrt3* expression becomes restricted to the region of the

dermomyotome closer to the neural tube (Fig. 15C, arrows). *Flrt3* can also be found in the head at the midbrain-hindbrain boundary, in the optic vesicle (Figs. 15C, E black arrow), in the branchial arches (Figs. 15C, D, E white arrow) and in the tail bud.

During limb bud development, *flrt3* transcripts are first detected in the ectoderm of the prospective limb fields at stage 14HH (Fig. 15B). By stage 16-18HH expression expands over the whole ectoderm of the limb bud (Figs. 15C, 2A) and as the limb bud grows and the limb ectoderm condenses to form the Apical Ectodermal Ridge, *flrt3* expression becomes restricted to the thickened ectoderm of the AER (Figs. 15D, E), co-localizing with *fgf8* and pERK activity (Mahmood et al., 1995; Kawakami et al., 2003)

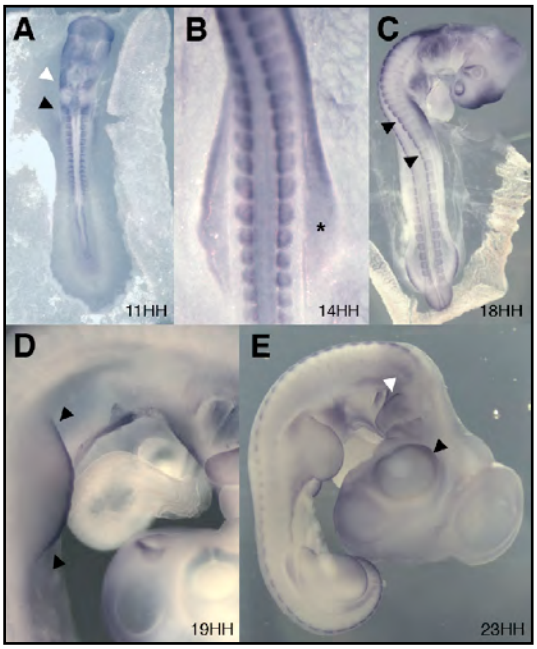

Figure 15. Expression Pattern Pattern of *flrt3* in *Gallus gallus.* *In situ* hybridisation for *flrt3*. **A**, chicken embryo at stage 11HH; arrows indicate localized expression of *flrt3* in the somites (black arrow) and around the otic placodes (white arrow). **B**, chicken embryo at stage 14HH; * indicates localized expression of *flrt3* in the limb field. **C**, chicken embryo at stage 18HH, *flrt3* expression is restricted to the epaxial dermomyotome closer to the neural tube (arrows). At 19 and 23HH (**D** and **E**) *flrt3* is expressed in the apical ectodermal ridge (AER, arrows in **D**), the developing eye (**E**, black arrow) and in the branchial arches (**E**, white arrow).

Flrt3 expression at the AER is maintained during limb bud outgrowth, disappearing as the AER regresses (Figs. 16A-D). The presence of specific AER *flrt3* mRNA transcripts can be observed in a transverse section of a stage 22HH forelimb (Fig. 16F). MKP3, a p-ERK inhibitor, is expressed in a complementary pattern to *flrt3* (Fig. 16E). There is a clear delay in expression along the AP axis. Although *flrt3* expression pattern is identical in both forelimbs and hindlimbs, *flrt3* expression in hindlimbs is delayed.

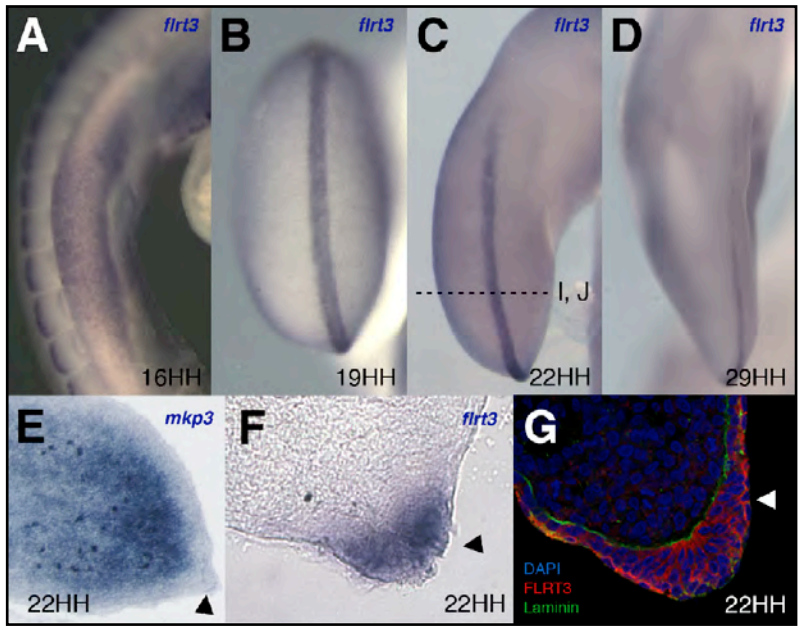

Figure 16. Expression Pattern of *flrt3* in *Gallus gallus.* *In situ* hybridisation for *flrt3*. **A-D**, a series of stages can be observed where condensation of epithelial cells that will form the AER becomes evident due to *flrt3* staining, beyond stage 19HH to stage 29HH *flrt3* expression is restricted to AER. **E**, Transverse section of an *in situ* hybridisation for *mkp3* at stage 22HH limb bud; note the complementary expression pattern to *flrt3*. **F**, Transverse section of an *in situ* hybridisation for *flrt3* at stage 22HH limb bud. **G**, Immunohistochemistry in a stage 22HH cross section, showing specific membrane staining of AER cells with anti-FLRT3 antibody; FLRT3 (red), Laminin (green); nuclei are counterstained with DAPI (blue).

I.3.2 Immunolocalization of FLRT3 during limb development

Immunohistochemistry studies were performed in sections of stage 10HH to 29HH chick embryos. We have identified FLRT3 protein in the membranes of cells that constitute the developing limb, dermomyotome, branchial arches, and the developing retina, correlating with the structures where we previously have described *flrt3* mRNA to be expressed (Figs. 15,16).

During limb bud development FLRT3 is immunolocalized at stage 14-15HH all over the ectoderm and as the ectoderm condenses to form the AER, the FLRT3 protein becomes restricted to the distal ectodermal cells (stage 18HH; Fig. 17A). Finally, it localises to the membranes of AER cells (Fig. 19C) and a small portion of the surrounding ectoderm until it completely disappears with the regression of the structure (Fig. 18).

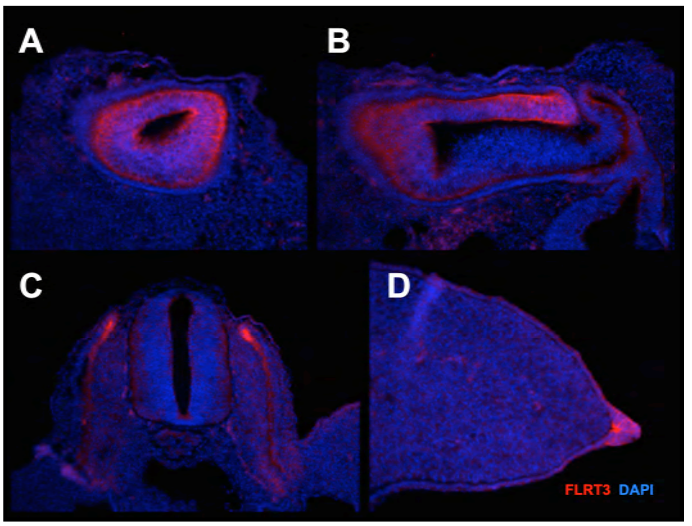

Figure 17. Immunolocalization of FLRT3. Immunohistochemistry with anti-FLRT3 antibody in chicken embryo transverse sections. Chicken embryo at stage 21HH where the FLRT3 protein can be detected at the otic vesicle (**A**), developing eye (**B**), the epaxial dermomyotome closer to the neural tube (**C**), and at the developing limb (**D**). FLRT3 is detected at the most distal part of the limb in the apical ectodermal ridge (AER). FLRT3 (red), nuclei are counterstained with DAPI (blue).

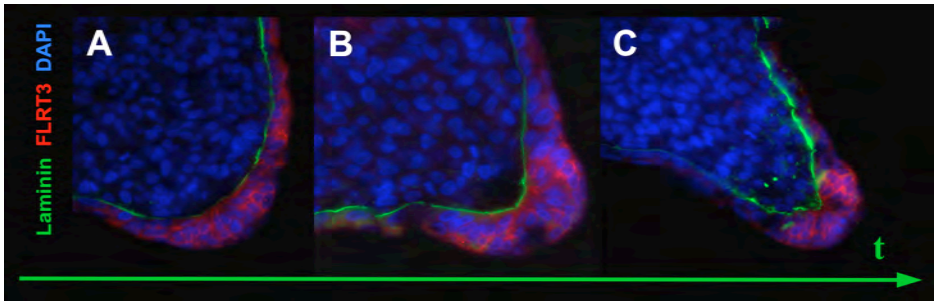

Figure 18. Immunolocalization of FLRT3 at the developing limb. Immunohistochemistry for FLRT3 (red) and Laminin (green) in a serie of tranverse section of the developing AER: A, 18HH; B, 22HH; C, 29HH; nuclei are counterstained with DAPI (blue).

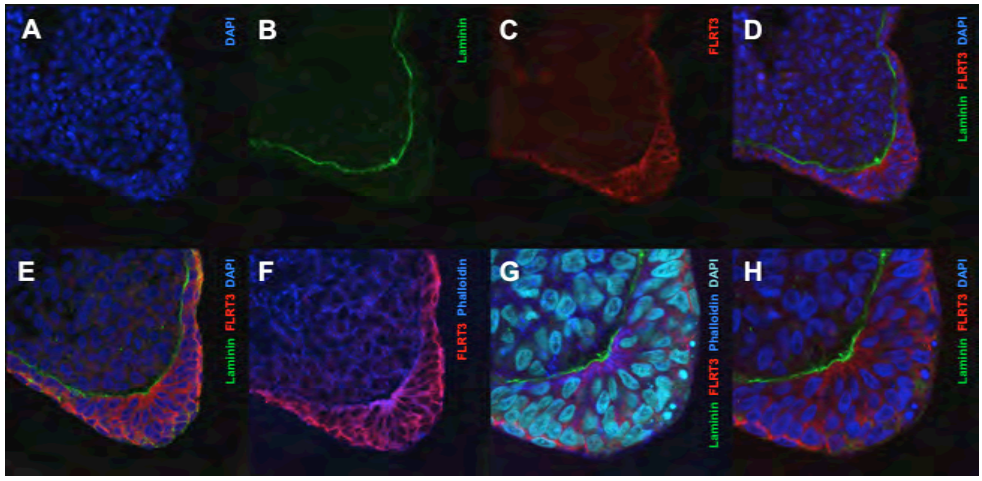

Figure 19. Immunolocalization of FLRT3 at the developing limb. Immunohistochemistry for FLRT3 (red), Laminin (green), and phaloidin(Blue) in a serie of tranverse section of the AER of a stage 22HH chicken embryo. Nuclei are counterstained with DAPI (blue/cyan).

I.3.3 Overexpression of *flrt3* in the limb ectoderm induces ectopic ridges and enlargements of the pre-existent AER

In gain and loss-of-function experiments in Xenopus, FLRT3 was shown to mediate FGF signalling (Bottcher et al., 2004). Considering the key importance of FGF in limb initiation and outgrowth, we investigated the role of *flrt3* in the formation and maintenance of the AER.

A pCAGGS-*flrt3* vector was co-electroporated with pCAGGS-AGFP (control) into the ectoderm of stage 13-14HH chicken limb fields, and expression was examined 24h to 96h post-electroporation. Electroporation with pCAGGS-AGFP alone induced no significant changes in gene expression or limb morphology (Fig. 20).

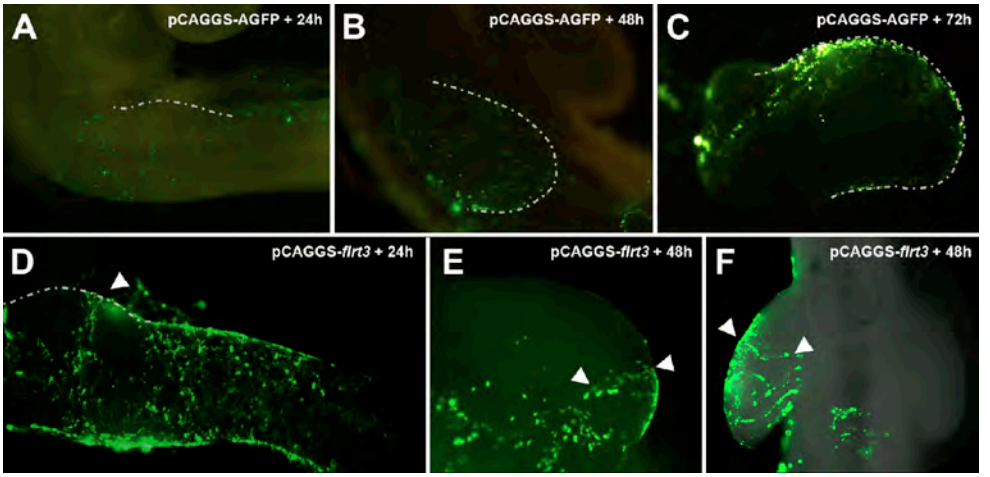

Figure 20. Gain-of-function studies for *flrt3* in *Gallus gallus.* Control of GFP-fluorescence in electroporated embryos, 48h post-manipulation. Embryos were co-electroporated with an expression pCAGGS vector harbouring the full-length chicken *flrt3* and pCAGGS-AGFP.

	Phenotype observed	Nº. limbs	% of limbs	
GFP	Normal	81	93%	
	Abnormal	6	7%	
	Total	87		
Full-length *Flrt3*	Normal	49	47%	
	Enlargements	29	28%	53%
	Projections	7	7%	
	Both	19	18%	
	Total	104		

Table 1 - Phenotypes upon *flrt3* overexpression studies. pCAGGS-AGFP electroporation used as controls.

Phenotypes obtained with overexpression of *flrt3* on limb ectoderm could be mainly classified in two groups (Figs. 22D, C'): enlargements and projections of the AER. Such phenotypes were observed in 53% of pCAGGS-*flrt3* electroporated embryos (n=104) (Table 1).

Limb outgrowth is maintained by a constant crosstalk between different tissues, thus became relevant to analyse the effect of a shift in this fine-tuned molecular balance. Excess of *flrt3* transcripts give rise to enlargements of the pre-existing AER both over the dorso-ventral and anterior-posterior axes of the structure, which is evident from *in situ* hybridisation for the AER marker *fgf8* at 24h and 48h post-electroporation (Figs. 21A, C, C' and B, D, D', respectively). In agreement with the increase in FGF signalling from the AER, *Mkp3* shows an expansion of its expression domain (Figs. 21A, B).

At the non-AER ectoderm, excess of *flrt3* transcripts promote the development of projections from the AER (Figs. 22B, C'). These ectopic ridges appear to be extensions of the pre-existing AER towards the dorsal and ventral sides of the limb bud. Among the different phenotypes obtained we can distinguish main ectopic ridges, closer to the pre-existing AER and approximately the same width (Figs. 21B, 22A), and secondary ectopic ridges, thinner and further apart from the AER (Figs. 22B, C arrows). Although *flrt3*-positive (Fig. 22B) these ridges do not express *fgf8* in its full ectopic-extension (Figs. 21B and 22A, B').

To test if AER expansions induce changes in the dorso-ventral patterning, several *in situ* hybridisations with dorso-ventral markers were performed. In the ventral ectoderm, *en*-1 expression is required to inhibit *lmx-1* expression from the dorsal mesoderm (Johnson and Tabin, 1997). Upon transformation of the ectoderm by excess *flrt3* we observe a deregulation of *en-1* expression (Figs. 21E, F). The genetic interactions involved in AER formation and specification of dorsal pattern are scrambled and the ventral ectodermal boundary is loose on the enlarged AER. The ventral *en-1*-positive ectoderm domain is absent from the enlarged ridge and patches

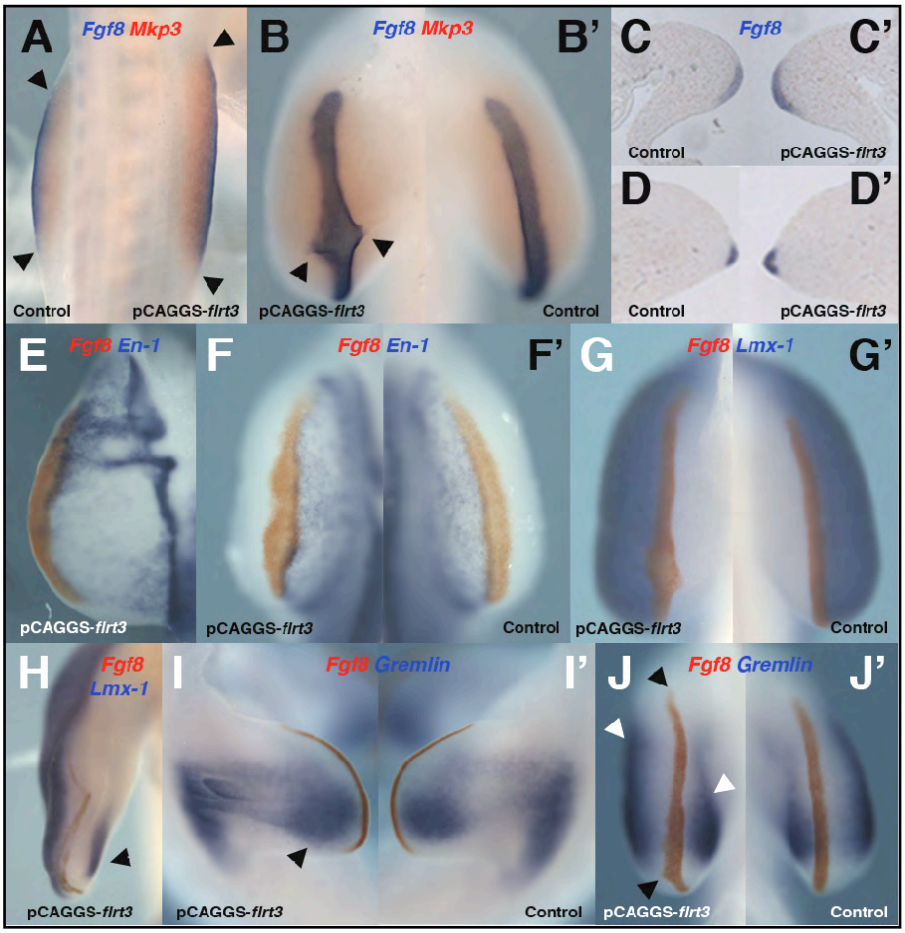

Figure 21. Gain-of-function studies for *flrt3* in *Gallus gallus.* Embryos electroporated with an expression pCAGGS vector harbouring the full-length chicken *flrt3* cDNA: 24h, 48h and 72h after manipulation. A, B, C', D', E, F, G, and H-K are manipulated limbs. B', C, D, F', G', are counterlateral control limbs. **A-B'**, double *in situ* hybridisation for *fgf8* (blue) and *mkp3* (red) expression 24h (A) and 48h (B, B') post-electroporation; note the extended pCAGGS-*flrt3* electroporated limb (**A**, arrows) compared with the control, and the AER enlargement and formation of projections in **B**. **C-D'**, cross sections of wholemount *in situ* hybridisation for *fgf8* expression (blue) showing an enlarged *fgf8*-positive AER, 24h (C, C') and 48h (D, D') after manipulation. **E-F'**, double *in situ* hybridisation for *fgf8* (red) and *en-1* (blue) expression 48h post-electroporation; patches of *en-1* expression are observed in the newly formed boundary upon transformation of the ectoderm with excess *flrt3*. **G-I**, double *in situ* hybridisation for *fgf8* (red) and *lmx-1* (blue) expression 48h (G) and 72h (H) post-electroporation; the dorsal mesenchymal marker *lmx-1* extends its domain of expression towards the areas affected by excess FGF signalling (**E**), generating a invasion of the dorsal territory towards the ventral part (**H**). **I-J'**, dorsal (I, I') and top (J-J') view of a 48h post-electroporation embryo stained for *fgf8* (red) and *gremlin* (blue); note the enlarged *fgf8*-stained AER (J, black arrows) and the extended *gremlin* domain in I and J.

of *en-1* expression are observed in the newly formed boundary (Figs. 21E-F'). In one case, due to the deregulation of *en-1*, the dorsal mesenchymal marker *lmx-1* extends its expression domain towards the areas affected by excess of FGF signalling, generating an invasion of the dorsal territory towards the ventral part (Fig. 21H). Overexpression of *flrt3* leads to deregulation of *en-1* expression (Figs. 21E, F). The genetic interactions involved in AER formation and specification of dorsal pattern are scrambled and the ventral ectodermal boundary is loose on the enlarged AER. The ventral *en-1*-positive ectoderm domain is absent from the enlarged ridge and patches of *en-1* expression are observed in the newly formed boundary (Figs. 21E-F'). In one case, due to the deregulation of *en-1*, the dorsal mesenchymal marker *lmx-1* extends its expression domain towards the areas affected by excess FGF signalling, generating an invasion of the dorsal territory towards the ventral part (Fig. 21H).

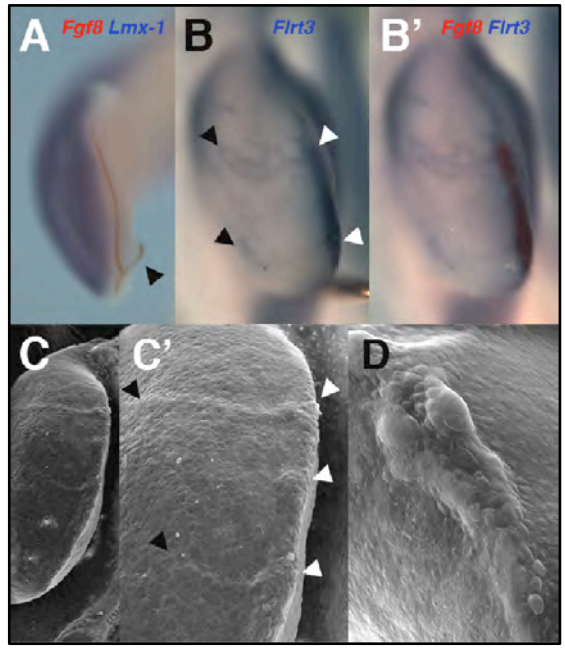

Figure 22. Ectopic ridges are formed upon transformation of the ectoderm with excess *flrt3*. Embryos electroporated with an expression pCAGGS vector harbouring the full-length chicken *flrt3* cDNA: 48h and 72h after manipulation. **A**, double *in situ* hybridisation for *fgf8* (red) and *lmx-1* (blue) expression 72h post-electroporation; ectopic AERs induced after *flrt3*

overexpression are *fgf8*-positive in all its A-P extension but only in the vicinity of the original AER, and maintain their ventral identity. **B-B'**, double *in situ* hybridisation for *flrt3* (blue; B prior to *fgf8* probe developing) and *fgf8* (red) expression 48h post-electroporation; ectopic AERs (B, black arrows) induced after *flrt3* overexpression are *flrt3*-positive in all their extension but only *fgf8*-positive in the vicinity of the original AER (B', arrows). **C-D**, Scanning Electron Micrograph of pCAGGS-*flrt3* electroporated embryos 72h after manipulation; Control in Anex I; **C'** is a detail of the phenotype shown in **C**, zooming on the projections towards the dorsal side of the limb bud and enlargement of the pre-existing AER (**D**).

In order to prove that the excess of FGF signalling and subsequent enlargement of AER territory could be due to a deregulation of the FGF or BMP expression at the AER, we checked if *gremlin*, the main BMP antagonist required for early limb outgrowth and patterning (Merino et al., 1999; Khokha et al., 2003), was upregulated upon *flrt3* overexpression. We have observed an enlargement of *gremlin*'s expression territory towards the posterior part of the limb bud (Fig. 21I), associated with an enlargement of the AER and subsequent *fgf8* upregulation in that area (Fig. 21J).

I.3.4 Silencing of *flrt3* affects the integrity of the AER

Given that ectopic expression of *flrt3* in the limb field of 14HH chicken embryos triggers the onset of signalling cascades that culminate in the induction of ectopic ridges, we tested if removal of the endogenous *flrt3* expression during limb bud development affects normal development.

Silencing of *flrt3* was achieved by co-electroporation into the ectoderm of both pCAGGS-AGFP (control) and a pSUPER plasmid that directs intracellular synthesis of short interfering RNA (siRNA)-like transcripts specifically targeting *flrt3*. Embryos were manipulated at stage 12-16HH, and examined 24h to 96h post-electroporation. As shown before, electroporation of pCAGGS-AGFP alone induced no significant changes in gene expression or limb morphology, and neither did mismatch siRNA (Table 2; Fig. 23).

Upon *flrt3* silencing by electroporation of siRNA, 31% of the embryos presented alterations to normal limb morphology (n=86). A wide range of phenotypes was observed, and the severity correlates with the size of *flrt3*-siRNA+PCAGGS-AGFP

electroporated area. Phenotypes obtained from silencing of *flrt3* vary from small indentations along the AER, shown by discontinued *fgf8* expression (Fig. 24A), to complete disruptions of AER integrity leading to impairment of limb development (Fig. 24G) (Table 2). Residual levels of *flrt3* expression (Figs. 24B, C) appear to be enough to promote initiation and outgrowth of the remaining limb bud (Fig. 24F).

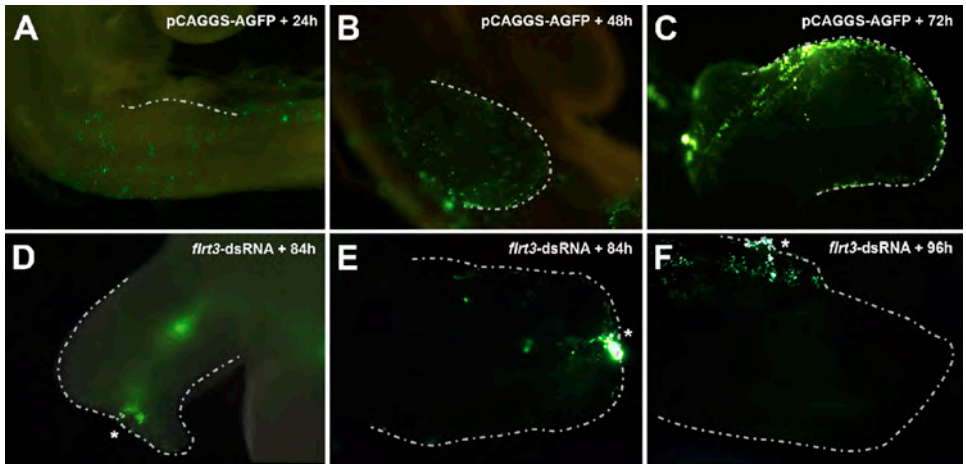

Figure 23. Loss-of-function studies for *flrt3* in *Gallus gallus*. Control of GFP-fluorescence in electroporated embryos.

	Phenotype observed	Nº. limbs	% of limbs	
Mismatch *Flrt3* RNAi	Normal	54	92%	
	Abnormal	5	8%	
	Total	59		
Flrt3 RNAi	Normal	86	69%	
	Slightly square	10	8%	31%
	Indented	20	16%	
	Mild truncation	6	5%	
	Truncation	2	2%	
	Total	124		

Table 2 - Phenotypes upon *flrt3* RNA interference studies. pCAGGS-AGFP (data showed in Table 1) and mismatch *Flrt3* RNAi electroporation used as controls.

The effect of *flrt3* silencing can also be observed in the distal mesenchyme that responds to AER signals through the loss of expression of *msx1* in progress zone cells (Fig. 24D).

Morphological effects of *flrt3* loss-of-function experiments become evident in scanning electron micrographs of a stage 27HH embryo, where the well-defined ridge normally present at the distal margin was discontinuous or completely absent in some places (Fig. 24F). In two cases, a complete lack of the limb was observed with the consequent loss of its skeletal pieces (Fig. 24G).

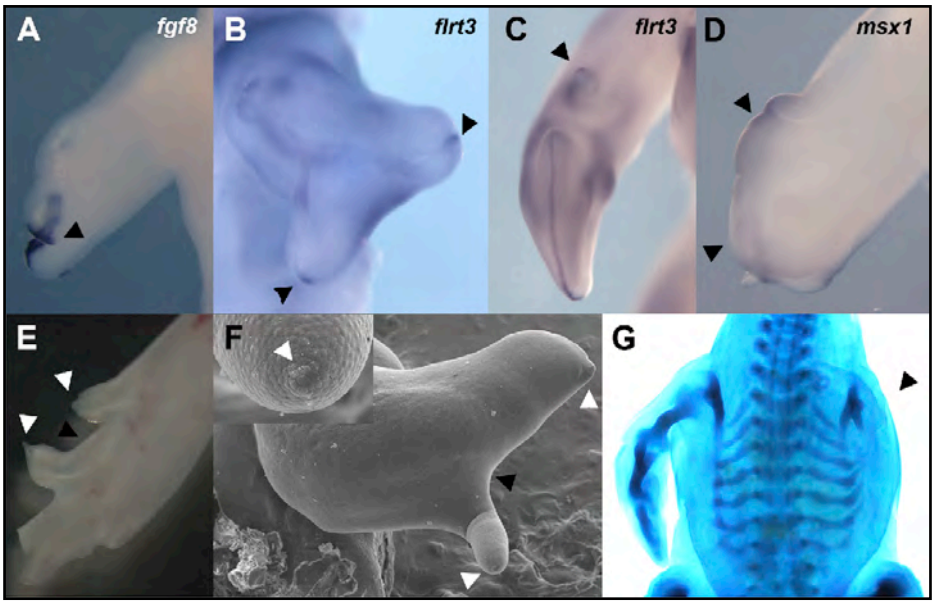

Figure 24. Loss-of-function studies for *flrt3* in *Gallus gallus*. A-C, AER loss of integrity in embryos 72h post-*flrt3*-dsRNA electroporation as shown by *in situ* hybridisation for *fgf8* (**A**) and *flrt3* (**B, C**). **D**, *in situ* hybridisation for the PZ marker *msx1*, also affected by *flrt3* downregulation. **E**, observed phenotype 96h post-electroporation with *flrt3*-dsRNA. **F**, Scanning Electron Micrograph of a *flrt3*-dsRNA electroporated limb; note that a small cluster of isolated AER cells is still able to promote outgrowth of part of the limb (**E, F**, white arrows; close up in **F;** control limb in Annex I - Fig. 44). **I**, complete truncation of the limb in a 72h *flrt3*-dsRNA electroporated embryo stained for cartilage with Alcian green.

I.3.5 *Flrt3* expression is not regulated by FGF activity, although ectopic Wnt3a is able to induce *flrt3*

Studies by Bottcher et al. (2004) suggest that expression of *xflrt3*, the *Xenopus laevis* homologue, is induced by FGF signalling. Spatial and temporal localization of *cflrt3* during normal limb bud development as shown before (Fig. 16) together with results from gain- and loss-of-function studies suggest a key role for *flrt3* in the initiation and maintenance of the AER in *Gallus gallus*.

Therefore, we examined the involvement of key proteins during limb development in the regulation of *flrt3* expression. Beads soaked in several molecules known to be directly related to processes leading to induction, growth and shaping of the limb were applied at the most anterior part of stage 20-21HH limb buds, close to the AER. Control beads soaked in PBS showed no effect on *flrt3* expression (annex I - Fig. 45A).

Several FGF family genes are responsible for AER activity. Of the 17 known FGF genes, 5 are expressed in the distal part of the established limb bud, 4 in the AER (*Fgf2, Fgf4, Fgf8, Fgf9*), and 2 in the mesenchyme underlying it (*Fgf2, Fgf10*). Their role is to provide AER function, either directly or indirectly, controlling proximal-distal outgrowth of the bud maintaining the distal progress zone cells in a proliferative state (Niswander, 1992; Mahmood et al., 1995; Savage and Fallon, 1995; Martin, 1998; Montero et al., 2001; Boulet et al., 2004; Kurose et al., 2004).

We tested if any of these FGFs were able to induce *flrt3* expression. In our model, we have observed that *flrt3* expression is not regulated by FGF activity from the ectoderm such as FGF2, 4 and 19, although FGF8 applied to the anterior part of the AER seems to be inhibiting *flrt3* expression (Figs. 25A).

SU5402 is a commercially available molecule that competes with FGFs for their receptors, therefore inhibiting its activity. SU5402 applied to the anterior distal part of the mesenchyme in close contact to the AER was shown to be responsible for the loss of expression of transcription factors such as *sp8,* 10h post-bead implantation

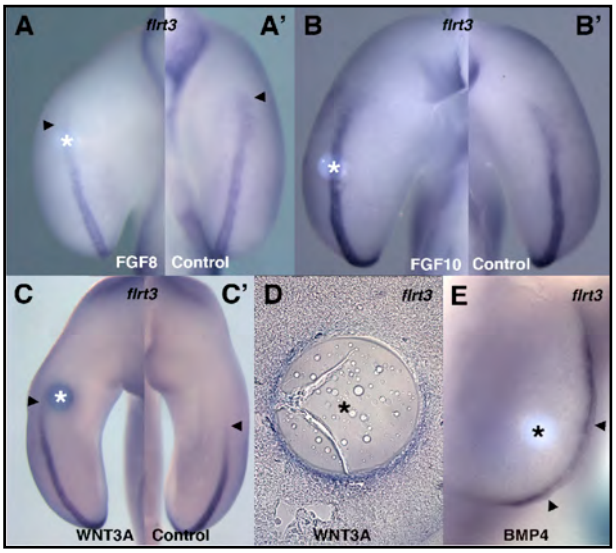

Figure 25. Regulation studies of *flrt3* expression in *Gallus gallus* limb development. B, E and G, are control limbs of A, D and F, respectively. (A and C) Inhibition of *flrt3* expression 10h and 20h, respectively, after treatment with FGF8. (D) Non-altered expression of *flrt3*, 10h after treatment with FGF10. (F) Induction of ectopic expression of *flrt3* by WNT3A, 20h after treatment. (H) Section of F, showing the *flrt3* ectopic expression around the WNT3A bead. (I)

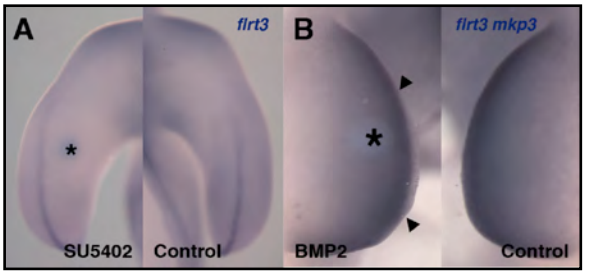

Figure 26. Regulation studies of *flrt3* expression in *Gallus gallus* limb development. A, *In situ* hybridisation showing unaltered expression of *flrt3* 10h after treatment with SU5402. **B**, Double *in situ* hybridisation for *flrt3* and *mkp3* (both in blue); inhibition of *flrt3* expression 5h after treatment with BMP2 beads. Note the gap (arrows) on *flrt3*'s AER expression on the area of influence of BMPs. *, Bead location.

(annex I - Fig. 45C,D) where transcription factors like *sp8* are already induced (Kawakami et al., 2004). No induction or enlargement of *flrt3* expression was observed in the distal epithelium (Fig. 26A).

In order to show if FGF activity from the progress zone is directly responsible for *flrt3* induction in the AER we applied FGF10 beads to the developing limb. Embryos were fixed 5h and 10h post-implantation to assure a time window where there is no induction of other signalling molecules on the AER such as *wnt3a* and *fgf8*, but where transcription factors like *sp8* are already induced (Kawakami et al., 2004). We found no alteration on *flrt3* expression in the manipulated limbs as compared to the control ones on the same embryo (Figs. 25B, B').

Because *wnt3a* is a known inducer of *fgf8* expression and because the establishment of the ridge (Barrow et al., 2003), and FGF activity do not seem to be involved on *flrt3* induction, we further looked if *wnt3a* was directly inducing *flrt3*. Limbs treated with WNT3A show an elongation of the *flrt3* expression domain in the apical ectoderm (Figs. 25C; compare arrows). Moreover, WNT3A is able to induce ectopically the expression of *flrt3* in the mesenchyme around the bead (Fig. 25D).

I.3.6 BMPs specifically inhibit *flrt3* in the AER

Bone Morphogenic Proteins (BMPs), as well as FGFs and WNTs, are key signalling molecules involved in limb development. Several BMP-family members such as *bmp2*, *bmp4* and *bmp7* are expressed in the AER (Geetha-Loganathan et al., 2006), being their main roles the establishment of the dorso-ventral axis, induction of apoptosis and maintenance of the integrity of the ridge.

To study the BMP role in the control of *flrt3*, avoiding the initiation of activation of apoptotic genes by cells, embryos were sacrificed within 6h post-bead implantation. As a control, we performed in the same experimental limb *in situ* hybridisation for *mkp3* and for *flrt3*. Results show no alteration on *mkp3* expression 3h and 5h upon bead implantation (Fig. 26B), however a closer look at the AER shows a gap on *flrt3* expression on the area of influence of BMPs both 3h and 5h post-implantation (Fig. 25E). These results support a role for BMP activity in *flrt3* inhibition.

I.4 *Gallus gallus's flrt2*

In chicken, apart from *flrt3*, there is just one other family member identified, *flrt2*. We have previously shown (Tomás, 2006)(MSc thesis, unpublished data) that c*flrt2* is also present during chicken limb development, however, outside the AER and at later stages of development.

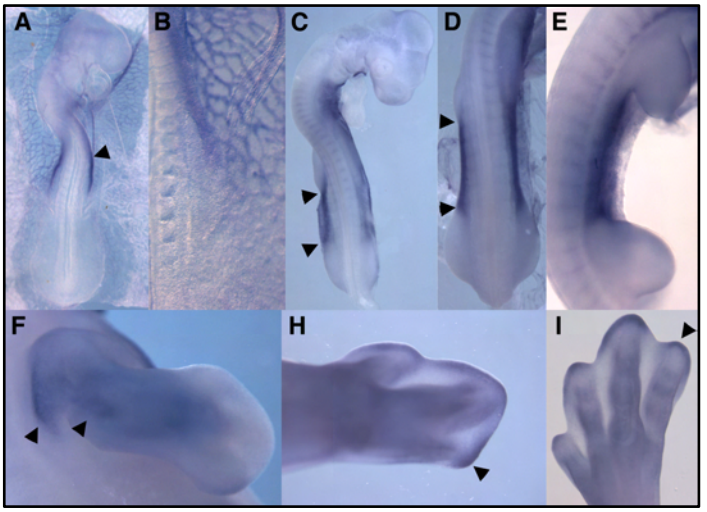

Figure 27. Expression pattern of *flrt2* in Gallus Gallus. A, **B**, *flrt2* transcripts are detected acompaning the formation of blood vessels. **A**, *flrt2* is detected at stage 14HH in the anterior limb field. **C**-**E**, *flrt2* is expressed in the flank, between the limbs, through stages 16 HH, 18 HH e 23 HH, respectively. **F**, at stage 27, *flrt2* can be detected at the insertion point of the forelimb in the flank and at its distal mesenchyme. **H**, **I**, *flrt2* expression at the most distal part of the forming fingers of the wing (H) and leg (I, 32HH). From Tomás, 2006.

Initially (14HH) expressed in the lateral plate mesoderm, at stage 18HH c*flrt2* expression is detected in the flank, between the forelimb and the hindlimb, and ventrally until the border with the amnion (Fig. 27C-E), being completely absent from the limb field until stage 25HH. At this stage *flrt2*-positive cells are observed invading the limb bud mesenchyme, (Fig. 27F) and by 27HH, they are clearly observed in the central limb mesenchyme. At stage 29HH, *flrt2* transcripts are detected at the most distal tip of the forming digits (Fig. 27 I).

CHAPTER II

- *Oct4* sustains Apical Ectodermal Ridge renewal -

(Part of the results presented in this chapter are unpublished and included in a manuscript in preparation)

Overview

Signalling centres are groups of cells located at the primordia of tissues and organs that pattern these structures for proper morphogenesis. Formation and maintenance of signalling centres is tighly regulated, both spatially and temporally, being the vertebrate limb a paradigm in the study of these centres (Capdevila and Izpisua Belmonte, 2001; Niswander, 2003).

The apical ectodermal ridge (AER), a thickening of the limb epithelium at its distal tip, controls proximal-distal growth by maintaining cells in the underlying mesenchyme in an undifferentiated and proliferative state, the called progress zone (PZ) (Bueno et al., 1996; Capdevila and Izpisua Belmonte, 2001). In *Gallus gallus*, it consists of a strip of pseudostratified columnar epithelium, covered by the overlying periderm, which runs along the distal dorso-ventral border of the limb bud. It starts as a flatten structure but becomes anatomically distinguishable at stage 18HH when the distal ectodermal cells acquire a columnar shape, making them easily distinguishable from the rest of the cuboidal ectoderm (Todt and Fallon, 1984).

The formation of the AER can be divided into two processes. First, the induction of AER-precursor cells in the surface ectoderm that will migrate toward the dorsal-ventral boundary and form the AER. Second, the maturation of the AER, resulting in the formation of the characteristic, thickened structure, maintained by a FGF8/FGF10 positive feedback loop (Carrington and Fallon, 1984; Ohuchi et al., 1997; Lewandoski et al., 2000; Altabef and Tickle, 2002; Boulet et al., 2004; Fernandez-Teran and Ros, 2008).

The mature AER is maintained through a tuned balance between proliferation and cell death for an additional 2 to 3 days, while mesenchymal skeletal progenitors continue to proliferate and differentiate until a fully patterned limb emerges. This equilibrium is genetically controlled but little is known about the molecules involved

in this process. The AER then regresses via programmed cell death and eventually flattens to a simple cuboidal epithelium.

In addition to FGFs, ectodermal Wnt/ß-catenin and BMP signalling are essential for induction and maintenance of *Fgf8* expression in AER (Kawakami et al., 2001; Pizette et al., 2001; Barrow et al., 2003; Soshnikova et al., 2003). Retinoic Acid (RA) signalling plays also an important role as it is required for limb bud initiation and then later acts as a proximalizing morphogenetic signal during AER formation (Mercader et al., 2000; Mic et al., 2004; Zhao et al., 2009).

Oct4 is a key factor in maintaining an undifferentiated state (self-renewal) and pluripotency of human and mouse embryonic stem (ES) cells as well as early embryonic cells (Nichols et al., 1998; Pesce and Scholer, 2001; Niwa, 2007), instructing stem cell fate through a gene dosage effect (Stefanovic and Puceat, 2007). *Oct4* was recently identified in chicken and shown to be required for the maintenance of chicken embryonic stem cells (cESC) pluripotency and continued proliferation (Lavial et al., 2007), proving that the mechanisms by which genes like *oct4* regulate pluripotency and self-renewal are not exclusive to mammals.

Most of the studies aiming to assess *oct4* role in self-renewal and control of pluripotency are performed in *in vitro* models and therefore lack the morphologic and molecular context in which cells exist in an organ, either embryonic or adult.

In this chapter we integrate *oct4* in a somatic cell morphological context during chicken embryonic limb development. We here show evidences that *oct4* controls the proliferative balance within the AER cells, that overexpression of *oct4* in the limb ectoderm disrupts the ratio cell death/ proliferation and that this activity is under the control of the canonical Wnt pathway. We also describe a special localization and behaviour of proliferating cells in the AER that could be a response to *oct4* activity in the developing vertebrate limb.

II.1 *Oct4* is expressed during limb development

Previous studies (Lavial et al., 2007; Rodriguez-Leon et al., 2008) have shown that chicken *oct4*, a gene known to be required to establish and maintain an undifferentiated state (self-renewal) and pluripotency of the cell population necessary for embryogenesis in mouse and human, is expressed in early embryos before gastrulation and thereafter in germ cells (Fig. 28A,C,E).

To ascertain whether *oct4* might be responsible for maintaining AER cells in constant renewal during the development and patterning of the vertebrate limb, we have cloned c*Oct4* and examined its spatial and temporal expression during chicken limb development by *in situ* hybridisation. We have tested different Proteinase K digestion times in the *in situ* hybridisation protocol and, overall, *oct4* expression domains were maintained.

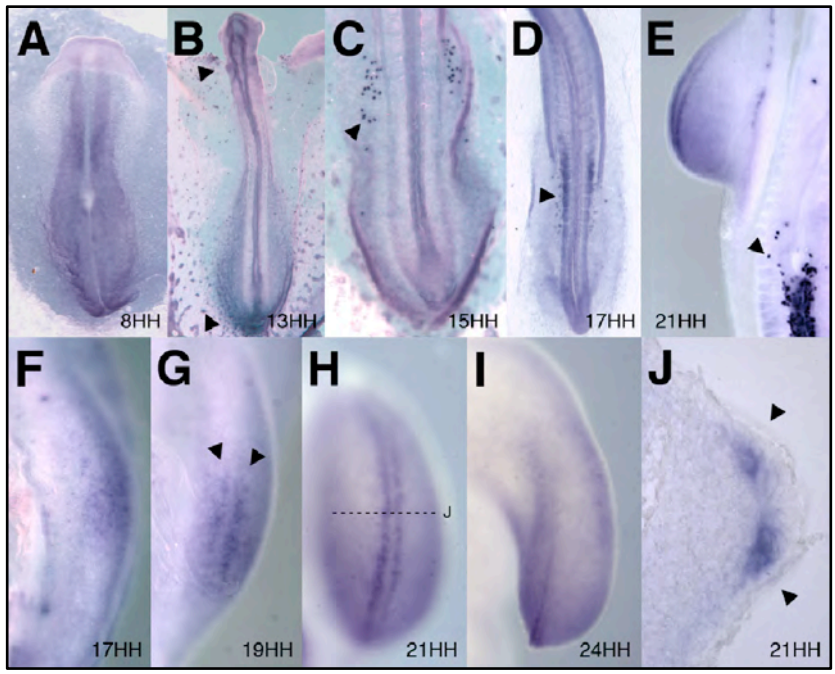

Figure 28. Expression Pattern of *oct4* in *Gallus gallus.* Whole-mount *in situ* hybridisation to *cOct4* transcripts. (**A**) Chicken embryo at stage 8HH; *oct4* transcripts can be found in the neural plate and the forming neural tube. (**B**) Chicken embryo at stage 13HH. Localized

expression of *oct4* can be observed around the otic placodes, at the lateral plate mesoderm, spinal chord and in the blood islands (arrow). (**C-E**) Chicken embryo at stage 15HH, 17HH and 21HH; *oct4* expression is observed at the primordial germ cells (PGCs; **C**, arrow) and gonads primordia (**E**, arrow). At 17HH (**D**) is clear the expression of *oct4* in the limb field and at 21HH (**E**) *oct4* is expressed in the distal limb ectoderm and at the AER, in a two-stripe pattern (**G**, arrows) along the anterior-posterior axis. From F to J, a series of stages can be observed where the condensation of epithelial cells that will form the AER (**G**, **H**) becomes evident due to *oct4* staining. At stage 24HH (**I**) *oct4* transcripts can still be found at the AER, however beyond stage 25HH we cannot detect *oct4* expression in the limb. (**J**) Transverse section of a stage 21HH limb bud (**H**), showing *oct4* expression in a baso-lateral, two-stripe pattern.

We have found expression of *oct4* in neural plate at stage 8HH (Fig. 28A). By stage 13HH *oct4* expression can be found in the developing neural tube, otic vesicles, blood islands, tail bud (Fig. 28B, D), and in the primordial germ cells (PGCs; Fig. 28C, arrow). *Oct4* transcripts were also found in the developing limb (Fig. 28C-E).
To elucidate the role of a stemness gene in a somatic cell context, we have focused our study in the stages of limb development from its initiation until AER regression.
We found *oct4* transcripts in the prospective limb field in a salt-and-pepper pattern (Fig. 28C, D) although in lower levels than those in the germ cells (Fig. 28C-E'). As the limb bud grows and the ectoderm condenses to form the AER at its distal tip, *oct4* expression can be observed in the ectoderm and in the forming AER in a "two stripes" pattern running along the anterior-posterior axis of the limb (Fig. 28F-I), dorsally and ventrally to the AER. This basolateral, two-stripe pattern can be clearly observed in a transverse section of a stage 21HH chicken limb bud (Fig. 28I).
Oct4 transcripts are no longer found at later stages when the AER starts to regress, suggesting a role for *oct4* in the maintenance of AER during limb development.

II.2 Cell dynamics in the AER

These characteristic domains of expression in two twin stripes in the most distal part of the limb bud and along its anterior-posterior axis have also been described for other genes, such as *cyp26* (Swindell et al., 1999) and *cux1* (Tavares et al., 2000), although *cux1* is expressed in both the dorsal and ventral limb ectodermal cells

bordering the AER, but excluded from the last. Notwithstanding, the behaviour of the cells that constitute the AER during limb development has ever been described.

In order to characterize the behaviour of AER cells and the dynamic of cell renewal at the most distal tip of the limb during development, we have studied at the developing AER (from stage 20HH to 30HH) the pattern of apoptosis by TUNEL assays, and proliferation through detection of BrdU incorporation and imunostaining against the phosphorylated form of the mitotic marker Histone H3.

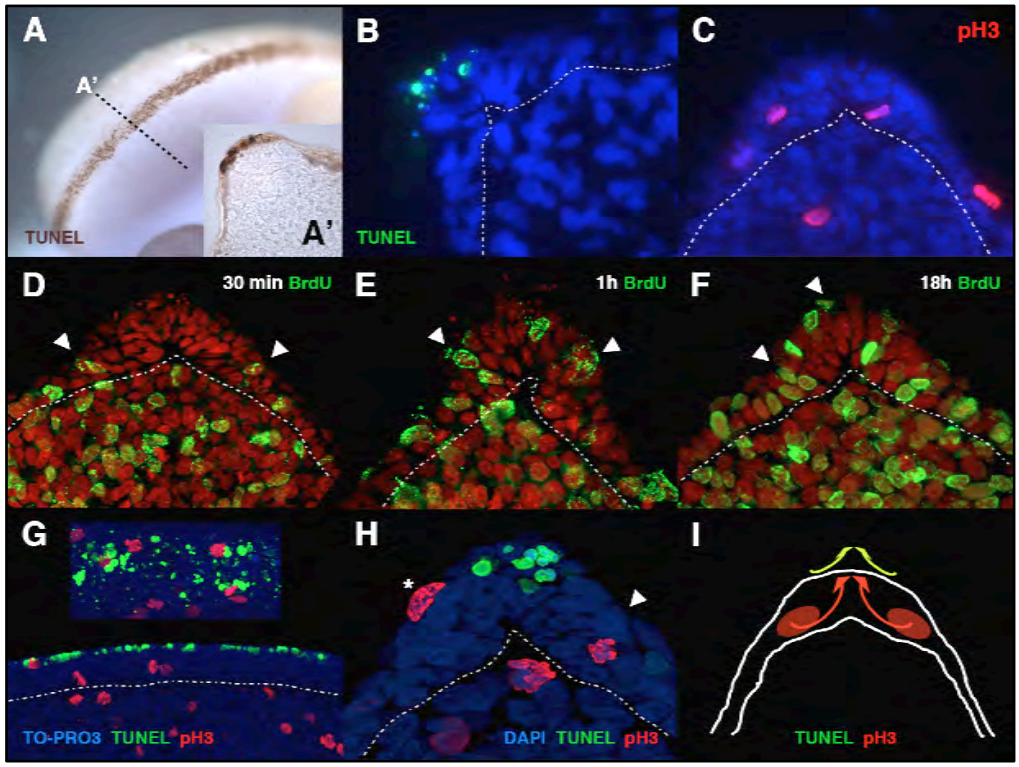

Figure 29. Cell Dynamic at the Apical Ectodermal Ridge. (**A-B**) stage 24HH limb bud stained with TUNEL (brown and green; DAPI nuclear staining in blue). In the transverse sections A' and B, cell death can be observed at the tip of the AER. (**C**) Immunostaining against phospho-Histone H3 (pH3; red) marks the proliferating cells located on the basis, both on the ventral and dorsal sides of the AER. D-F, Different BrdU pulses (30 min, 1 hour, and 18 hours) were given to stage 20-21HH developing embryos, in order to be able to infer about cell movement in the AER. BrdU staining in green; Propidium Iodide counterstaining in red. AER cells of embryos sacrificed 30 (**D**) and 45 minutes after the BrdU incorporation showed the same pattern as the p-Histone H3 (C), with stained cells in the lower 1/3 of the

AER, on both sides of the groove on the base of the AER. AER cells of embryos that have been exposed to BrdU during 1h show BrdU positive cells at a more central and apical position (**E**). From 5 hours onwards (**F**, 18 hours) BrdU stained cells are often observed at all levels of the AER. G-H, confocal imaging of a stage 22HH limb bud processed for TUNEL (green) and immunostaining against phospho-Histone H3 (red). DAPI nuclear counterstain in blue. (**G**) Top and sagital view of the limb bud showing phospho-Histone H3 (red) staining at both sides of the strip of cells undergoing apoptosis, close to the base of the AER. (**H**) Transverse section. It is also possible to find periectoderm cells undergoing mitosis (**H**, *). (**I**) We propose a model in which in the developing AER there are two pools of cells at the base of the structure (**H**, arrow; **I**, in red) that are responsible for the renewal of the AER, and that, as cells loose contact to the extracellular matrix and dye at the tip of the AER (**H**, **I**, in green), a new batch of cells are dividing at the base and moving towards the top. These areas of proliferation at the base of the AER and running through the anterior-posterior axis of the limb (**G**) coincide with *oct4* expressing areas.

We used TUNEL assay to describe the pattern of cell death in the AER. We have observed that cells are dying on the most distal and central part of the ridge along the anterior-posterior axis of the limb bud (Fig. 29A-B). This pattern is constant throughout the limb bud development, until the AER completely regresses at stage 32HH.

Immunolocalization of Phospho-Histone H3 (pH3), which marks nuclei in cells undergoing mitosis, is observed in the proliferating cells located on the AER basis, both on the ventral and dorsal sides of the AER (Fig. 29C). These observations were coherent throughout limb bud development in which the proliferation rate obviously diminishing with the regression of the AER. No cells undergoing mitosis were found on the central apical part of the AER.

To confirm this proliferation pattern we gave different BrdU pulses (30 and 45 minutes, 1h, 5h, 7h, 18h, 24h) to stage 20-21HH developing embryos, after which we fixed the limbs. Since all cells that have divided in that period of time have incorporated BrdU, at the end we detect the number of cells that have divided in that period of time and their offspring, thus being able to indirectly infer cell movement in the AER.

The AER cells of the embryos sacrificed 30 and 45 minutes after BrdU incorporation showed the same pattern as pH3 (Fig. 29D), in which cells in the lower 1/3 of the

AER, on both sides of the groove on the base of the AER are found to be BrdU-positive. AER cells of embryos that have been exposed to BrdU for 1 hour show BrdU positive cells at a more central and apical position (Fig. 29E). In some cases is possible to spot stained cells on the tip of the AER. From 5 hours onward BrdU stained cells are often observed at all levels of the AER (Fig. 29F).

Therefore, we can describe the existence of two pools of cells at the base of the AER that are responsible for the renewal of this structure, and that a batch of cells are dividing at the base and moving towards the top as cells loose contact to the extracellular matrix, dying at the tip of the AER (Fig. 29G-I).

These areas of proliferation at the base of the AER and running through the anterior-posterior axis of the limb coincide with *oct4* expressing areas (Fig. 28J).

II.3 *Oct4* overexpression expands the AER and enlarges the limb mesenchyme

Being *oct4* a key factor in maintaining an undifferentiated state (self-renewal) and pluripotency of human and mouse embryonic stem (ES) cells as well as early embryonic cells (Nichols et al., 1998; Pesce and Scholer, 2001; Niwa, 2007), and since *oct4* is expressed in one of the most important organizing centres of the vertebrate limb, the AER, we performed gain-of-function experiments for *oct4* in order to explore its role in the formation and maintenance of the ridge.

A pCAGGS-*oct4* vector was co-electroporated with pCAGGS-AGFP into the ectoderm of stage 13-14HH chicken limb fields, and examined 24 to 96 hours post-electroporation (Fig. 31A). Apart from very few abnormal embryos presenting phenotypes structurally different from the *oct4*-induced limb-restricted ones, no significant changes in gene expression or limb morphology were observed in single pCAGGS-AGFP electroporations (Fig. 30).

Phenotypes derived from *oct4* overexpression were observed in 61% of the electroporated embryos (n=94; Table 3). We have observed an enlargement of the limb mesenchyme of the experimental limb 24 and 48 h post-electroporation when compared with the control one, as well as an expansion of the AER, shown here by

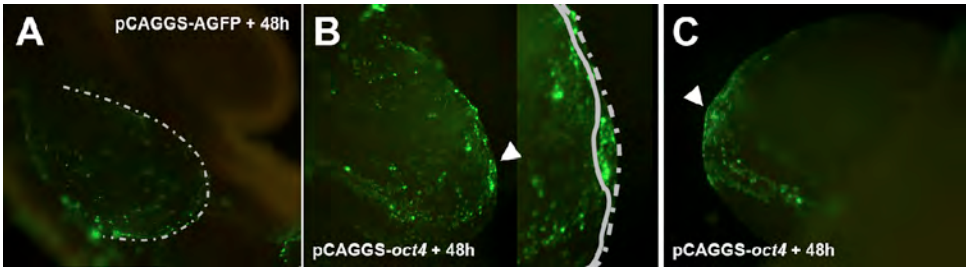

Figure 30. Gain-of-function studies for *oct4* in *Gallus gallus.* Control of GFP-fluorescence in electroporated embryos, 48h post-manipulation. Embryos were co-electroporated with an expression pCAGGS vector harbouring the full-length chicken *oct4* and pCAGGS-AGFP.

	Phenotype observed	Nº. of limbs	% of limbs
AGFP	Normal	81	93%
	Abnormal	6	7%
	Total	87	
Oct4	Normal	37	39%
	Enlargements	57	61%
	Total	94	

Table 3 - Phenotypes upon *oct4* overexpression. Embryos were electroporated with an expression pCAGGS vector harbouring the full-length chicken *oct4*. pCAGGS-AGFP was used as control.

the AER marker *fgf8* (Fig. 31C,C' and Fig. 31B,B',D, and D', respectively), both along the anterior-posterior (A-P) and the dorso-ventral (D-V) axis.

At the ventral ectoderm *en*-1 is required to inhibit *lmx1* on the dorsal mesoderm and create a ventral ectodermal boundary. We accessed if the D-V territories were affected upon transformation of the ectoderm by excess of *oct4* transcripts. The ventral ectoderm appears to be deregulated in key points where an enlargement of the AER is evident, locally misplacing the dorso-ventral boundary (Figs. 31G,H). Consequently, an enlargement of the limb mesenchyme is also observed, as stained with the dorsal mesenchymal territory of *lmx1* (Fig. 31F,F'). The chondrogenic marker *Sox9* has its expression enhanced in *oct4*-electroporated limbs (Fig. 31I). Moreover, in *oct4*-overexpressing limbs it is possible to observe the development of extra skeletal pieces (Fig. 31J').

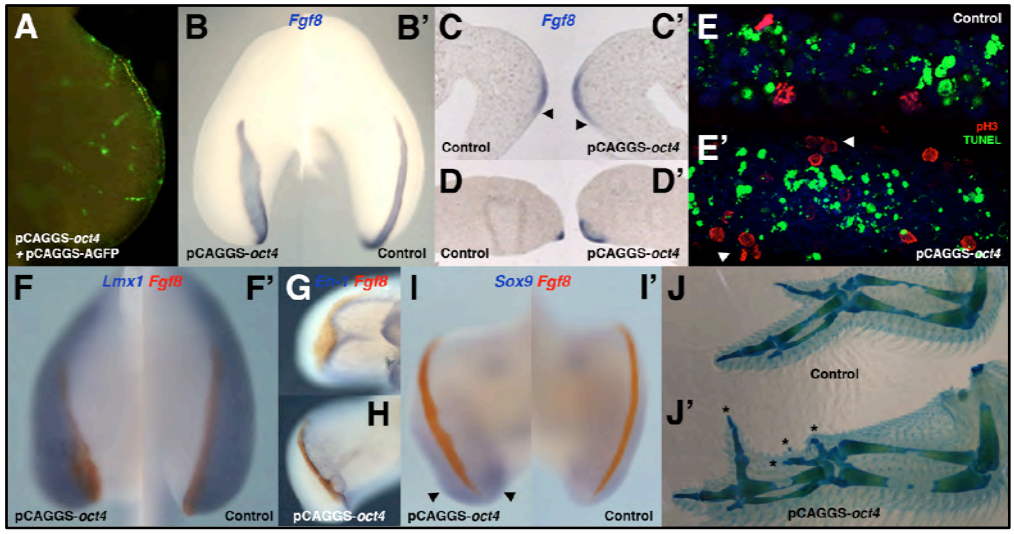

Figure 31. Gain-of-function studies for *oct4* in *Gallus gallus.* Embryos electroporated with an expression pCAGGS vector harbouring the full-length chicken *oct4*, 24 hours (C, C'), 48 hours (A, B, B', C-H), 72 hours (I, I') and 96 hours (J, J') after manipulation. (**A**) *oct4* electroporated limb showing GFP-positive AER cells. (**B**), *in situ* hybridisation for *fgf8* expression (blue) show an enlargement of the AER of the *oct4*-electroporated limb when comparing to the control one (**B'**). (**C-D'**) Transverse sections of whole-mount *fgf8 in situ* hybridisations. C and D, controls. C' and D', experimental limbs. (**E-E'**, arrows), the proliferating rate at the AER is increased in *oct4*-electroporated limbs. F-H, the limb territories are altered upon *oct4* electroporation: double *in situ* hybridisation for *fgf8* (red) and *lmx1* (**F-F'**, blue, dorsal mesenchymal marker) or *en-1* (**G,H)**, blue, ventral ectodermal marker). The ventral ectoderm appears to be deregulated in key points where an enlargement of the AER is evident, locally disrupting the dorso-ventral boundary. (**I-I'**) Double *in situ* hybridisation for *fgf8* (red) and *sox9* (blue), showing an enlargement of the AER; the *sox9*-positive domain of the *oct4*-electroporated limb (**I**, arrows) is enlarged when comparing to the control one (**I'**). (**J, J'**) Alcian green cartilage staining of 96 hours post-electroporation limbs. The experimental limb (bottom) presents extra skeletal pieces (*).

II.4 AER cell dynamics upon *oct4* overexpression is altered

A fine tuned balance between proliferation and apoptosis sustains the correct shaping and outgrowth of the limb. We analysed whether the expansion of the AER and consequent enlargement of the limb upon *oct4* overexpression was due to an alteration on the cell balance towards an increase of the proliferation rate or a decrease on the cell death ratio.

We performed TUNEL assays in *oct4*-overexpressed limbs and compared them with their counter-lateral control ones. The apoptotic pattern is not altered in the AER, 48h and 72h post-electroporation (Fig. 32).

In order to access the proliferation rate, we performed immunohistochemistry assays against phospho-Histone H3 and observed an increase of the proliferation rate at the AER, and consequently on the mesechyme, induced by *oct4*'s increased levels, as can be seen in Fig. 33.

In an AER's top view (Fig. 31E') we can observe an overall increase in cell proliferation when comparing the *oct4*-electroporated limb with its counter-lateral control (Fig. 31E).

Hence, we can state that the enlargement of the limb bud and the expansion of the AER structure is the product of an increase of proliferation as a response to the increase of *oct4* activity in the developing limb.

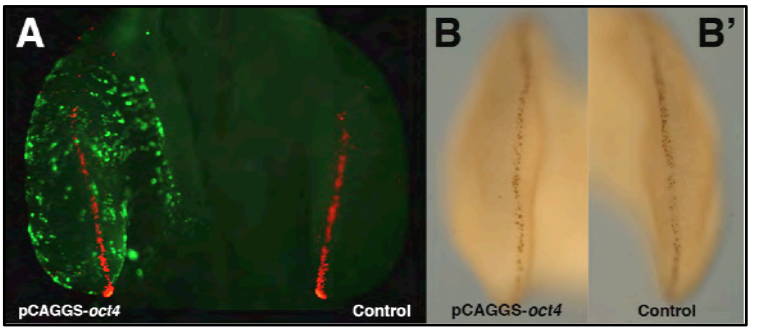

Figure 32. Cell death remains unaltered upon *oct4* electroporation of chicken limb ectoderm. Embryos co-electroporated with pCAGGS-*cOct4* and pCAGGS-AGFP, 48 (**A**) and 72 (**B, B'**) hours after manipulation. pCAGGS-AGFP was used as control of the electroporated area and is showed in green in A. TUNEL assay (red in A, brown in B) shows no significant alteration on cell death in the limbs that undergone electroporation with full-length *oct4* (A, left limb; B), comparing with the counterlateral control ones (A, right limb; B').

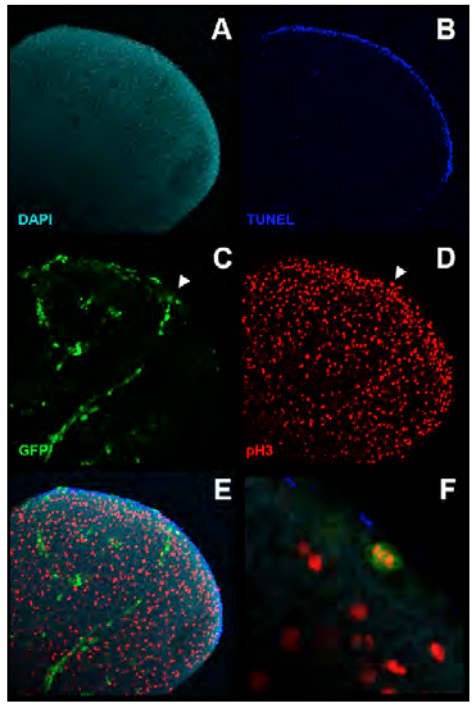

Figure 33. Gain-of-function studies for *oct4* in *Gallus gallus.* Wholemount detection of Apoptosis (TUNEL) and proliferation (phospho-Histone H3) in a *oct4*-electroporated limb, 48h post-manipulation. Embryos were co-electroporated with an expression pCAGGS vector harbouring the full-length chicken *oct4* and pCAGGS-AGFP.

II.5 FGF signalling is needed to maintain *oct4* expression

It has been established that FGFs play an important role in induction, initiation and maintenance of AER activity and structure (reviewed in Capdevila and Izpisua Belmonte, 2001) and moreover, data from ESCs studies have shown that FGF signalling is required for maintaining the self-renewal activity (Eiselleova et al., 2009; Gotoh, 2009)

Our data from *oct4* expression pattern and the altered AER cell dynamics upon *oct4* overexpression in the limb ectoderm suggest a commitment of *oct4* in the maintenance of the cell balance in the AER.

In order to access the involvement of key proteins during limb development in the regulation of *oct4* expression we implanted beads soaked in different molecules

known to be directly related to processes that lead to the induction, growth and shaping of the limb. These molecules were applied at the most anterior part of stage 20-21HH limb buds, close to the AER. Control beads soaked in PBS and DMSO showed no effect on *oct4* expression.

We examined if FGFs are able to induce *oct4* expression. When applied in the flank, FGF8 beads are capable of ectopically induce *oct4* expression in a salt-an-pepper fashion (Fig. 34A), 20h post-bead implantation. Complementary, SU5402, a commercially available molecule that competes with FGFs for their receptors therefore inhibiting its activity, applied to the anterior distal part of the mesenchyme in close contact to the AER promotes *oct4* downregulation (Fig. 34B).

To prove if FGF activity from the progress zone could be directly responsible for *oct4* induction we applied FGF10 beads to the developing limb. The embryos were fixed 10h post-implantation to assure a time window where there is still no induction of other signalling molecules on the AER such as *wnt3a* and *fgf8*, but there is presence of transcription factors such as sp8 (Kawakami et al., 2004). No alteration on *oct4* expression was observed in the manipulated limbs compared to the control ones on the same embryo (Fig. 34C).

We have previously described FLRT3 as being necessary but not sufficient for proper AER formation and maintenance and also its ability to produce *fgf8*-positive enlargements and projections of the pre-existing AER when overexpressed in the limb ectoderm.

To assess if FGF signalling enhancement by FLRT3 is able to upregulate *oct4*, we have electroporated the full-length chicken *flrt3* cDNA. We have observed enhanced *oct4* expression in the AER (Fig. 35A). Also, *oct4* transcripts were detected in the ectopic ridge-like structures produced by *flrt3* overexpression in the limb ectoderm (Fig. 35B).

Likewise, *oct4* is able to ectopically induce sprinkled expression of *flrt3* in the non-AER ectoderm when overexpressed, as well as in the enlarged AER (Fig. 35C, arrows).

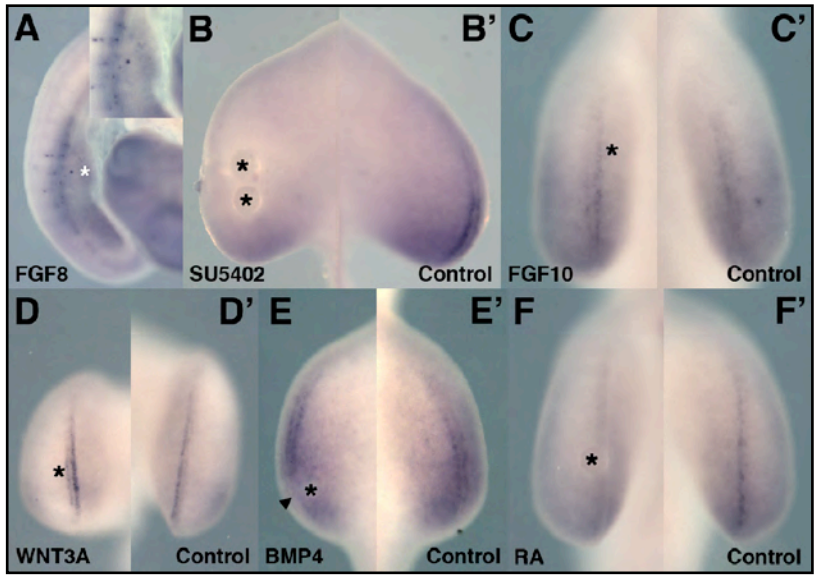

Figure 34. Regulation studies of *oct4* expression in *Gallus gallus* limb development. B, E, G and I, are control limbs of A, D, F and H, respectively. (**A**) Induction of *oct4* expression in the flank of a stage 11HH embryo by FGF8, 10 hours after treatment. (**B**) Inhibition of *oct4* expression, 20 hours after treatment with FGF inhibitor SU5402. (**C**) Unaltered expression of *oct4*, 10h after treatment with FGF10. (**D**) WNT3A-soaked beads enhanced *oct4* expression on the pre-existent ridge, 20h after treatment. (**E**) Inhibition of *oct4* expression, 3 hours after treatment with BMP4. (**F**) Inhibition of *oct4* expression, 10 hours after treatment with Retinoic acid. *, Bead location.

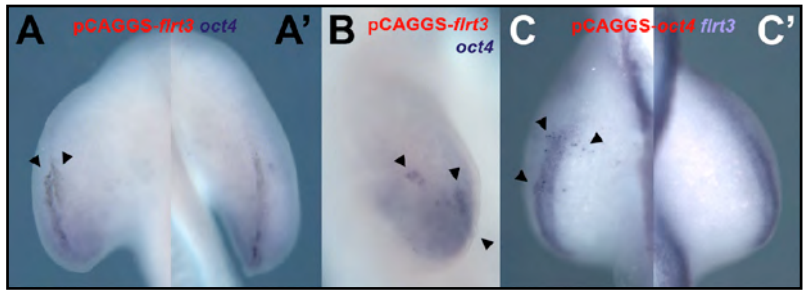

Figure 35. (A-B) *Oct4* upregulation in ectopic ridge-like upon electroporation of chicken limb ectoderm with a pCAGGS vector harbouring the full-length chicken *flrt3*. **(C-C')** *Flrt3* is ectopically expressed in the ectoderm as a result of pCAGGS-*oct4* electroporation.

II.6 The canonical WNT, WNT3A, controls *oct4* expression in the AER

Similar to FGF, WNT signalling has an important role on AER initiation and development since WNT3A is known to be responsible for *fgf8* induction and the establishment of the ridge (Barrow et al., 2003). Besides that, WNT signalling is a common pathway for maintenance of the undifferentiated state in both mouse and human ESCs (Sato et al., 2004; Katoh, 2007).

We wanted to clarify if the enhanced oct4 expression promoted by AER FGF activity was achieved via *wnt3a*, and if WNT3A was able to directly induce *oct4* expression. WNT3A treated limbs show an elongation of the *oct4* expression in the apical ectoderm. Moreover, WNT3A is able to locally enhance the expression of *oct4* in the preexistent AER, 22 hours post bead implantation (Fig. 34D). We can, therefore, conclude that *oct4* expression is being directly controlled by WNT canonical pathway most probably through ß-catenin.

II.7 BMPs negatively control *oct4* expression prior to induction of cell death

Bone Morphogenic Proteins (BMPs), such as FGFs and WNTs, are key signalling molecules involved in limb development, establishing the dorso-ventral axis, inducing apoptosis and maintaining the integrity of the ridge (Geetha-Loganathan et al., 2006). Although with different functions in different stem cell compartments, accumulated evidence indicate that BMPs play an important role in the regulation of stem cell properties (Chen et al., 1998; Ying et al., 2003; Zhang et al., 2003; He et al., 2004; Bai et al., 2010).

To study the BMP role in the control of *oct4* and to avoid the early activation of apoptotic genes, embryos were sacrificed before 6 hours post bead implantation.

The results show a gap on AER's *oct4* expression on the area of influence of BMPs both 3 and 5 hours post bead implantation (Fig. 34E, arrow), supporting a role for BMP activity in *oct4* inhibition.

II.8 RA activity controls *oct4* expression but cannot induce an ectopic AER

Retinoic acid (RA) promotes proximalization of limb cells (Mercader et al., 2000) and massive excess of RA produces ectopic or extra limbs in mouse embryos and frog tail regeneration (Mohanty-Hejmadi et al., 1992; Niederreither et al., 1996). Moreover, RA controls interdigital cell death through BMP signalling (Rodriguez-Leon et al., 1999)

To ascertain whether RA is able to control AER's *oct4* expression like in ES cells, where RA-induced differentiation is known to rapidly downregulate oct4 expression (Lavial et al., 2007), we applied RA-soaked beads to the developing limb and sacrificed the embryos 10h and 20 hours post bead implantation.

Our data show a strong inhibition of *oct4* expression in the manipulated limb (Fig. 34F) when comparing to the control one (Fig. 34F').

II.9 Other candidate genes for *oct4* co-regulation during AER renewal

The expression of regulatory networks and related signalling pathways that are responsible for the molecular mechanisms of pluripotent cell fate decisions of ESC are intricate.

Oct4, along with *sox2* and *nanog* are master transcription factors for maintenance of the undifferentiated state and self-renewal (Chew et al., 2005; Loh et al., 2006; Lavial et al., 2007; Wei et al., 2009). In mouse, they form a regulatory circuitry with co-regulators, such as ß-catenin, *Stat3*, *Myc*, *Klfs*, and *Sall4* to control the expression of pluripotency-related genes including themselves (Li, 2010).

Our purpose was to identify candidate genes for *oct4* co-regulators in the renewal of Apical Ectodermal Ridge cells, and therefore unravel a bit more of the coordinated molecular mechanisms responsible for the cell decision between maintaining itself as a progenitor and differentiate.

We analyzed several candidate genes. Some of them as *sox2* and *nanog* (Canon et al., 2006), were, surprisingly, not expressed during limb development.

II.9.1 Retinoic acid metabolic enzymes, *cyp26* and *raldh2*

We have observed that RA-soaked beads have a strong inhibitory effect over *oct4* expression at the AER. Moreover, RA is known to induce interdigital cell death in later stages of limb development (Rodriguez-Leon et al., 1999) and to act as differentiating signal (Weston et al., 2000; Stavridis et al., 2010).

Due to the differentiation effect of RA during limb development we have looked into the expression patterns of RA synthesizing, *raldh2*, and degrading, *cyp26*, enzymes at the distal tip of the limb, in order to try to find a pattern for *cyp26* and *raldh2* that could fit our data so far.

We observed, as described (Swindell et al., 1999), expression of *cyp26* in a similar pattern as *oct4*, in two basal twin stripes along the A-P axis of the AER (Fig.36A, B, arrows). Moreover, we have found a never before described, *raldh2* expression at the tip of the AER (Fig. 36 C, D).

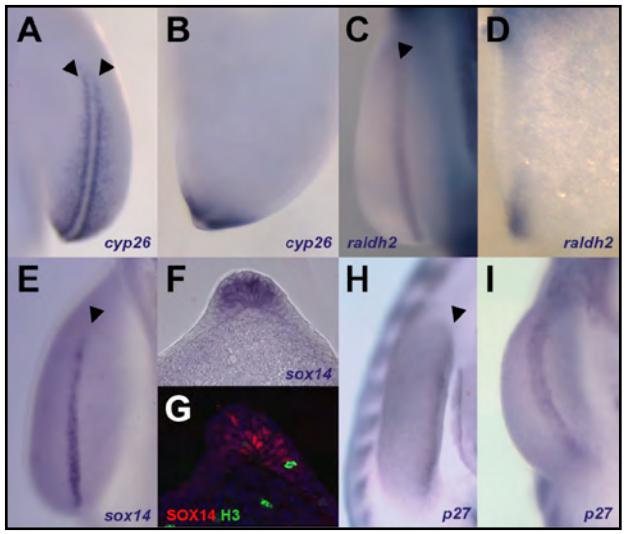

Figure 36. Candidate genes involved in *oct4* regulation and self-renewal of the AER cells. Whole-mount *in situ* hybridisation to stage 21HH embryos with *cyp26* (**A**, **B**), *raldh2* (**C**, **D**), *sox14* (**E**-**F**), and *p27* in stage 19HH (**H**) and 20HH (**I**) embryos. (**F**) Transverse section of **E**. (**G**) Immunohistochemistry against SOX14.

II.9.2 *Sox14*

Upon evidence of *sox2* lack of expression in the limb, we searched for a different Sox family member that might accomplish *oct4* gene regulation in AER cells.

From the SOX family genes we tested, *sox14*, a sub-group B2 SOX family gene described as a negative transcription regulator and a onset of neural differentiation in *Xenopus laevis* (Hartenstein, 1993; Uchikawa et al., 1999; Popovic and Stevanovic, 2009) shares 93% of identity with *Sox2* within the High mobility Group (HMG) box domain, and 28% outside of the HMG box domain (Fig. 37).

Sox14 has come to our attention due its expression pattern (Fig. 36E, F) and imunolocalization (Fig. 36G) in the AER, at its most distal tip, in a complementary pattern to *oct4*, suggesting that it might be involved in the committement of AER cells to differentiate.

We have gather tools, by cloning its full-length cDNA into a pCAGGS expression vector and producing RCAS virus (annex III.5) that drive *sox14* expression, to pursue studies on this subject at the lab.

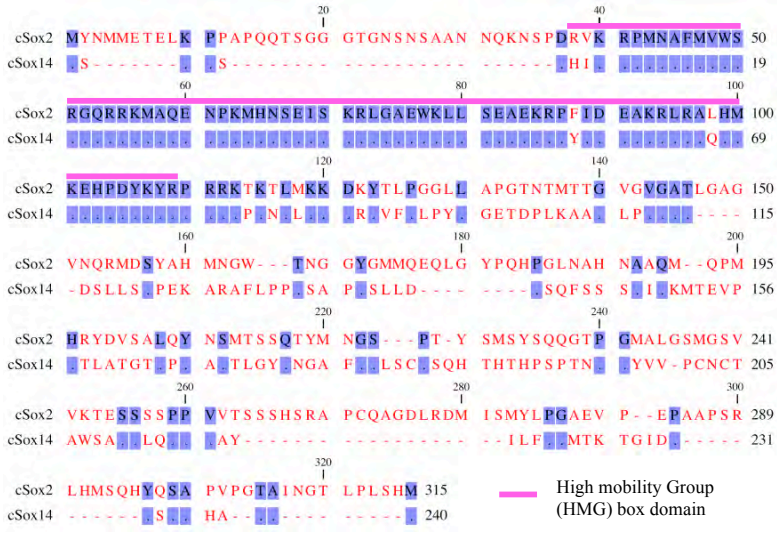

Figure 37. Comparative analysis of the amino acid sequences of chicken *sox2* and *sox14*. ClustalW alignment of SOX2 and SOX14 proteins. Amino acids are color-coded by consensus, from red to blue. Identical residues are indicated by dots, different residues in red. The pink line above the sequence indicates the region of the HMG box domain.

II.9.3 *p27*^{Kip1}

Cell cycle genes are an obvious choice on a search for cell fate decision-taking genes. p27^{Kip1}, belongs to the Cip/Kip family of cyclin dependent kinase (Cdk) inhibitor proteins, it binds to and prevents the activation of Cyclin E/CDK2 or Cyclin D/CDK4 complexes, and thus controls G1-to-S phase transition of the cell cycle. CDKs and their inhibitors are shown both in the context of proliferation regulators and as contributors to the apoptotic machinery (Maddika et al., 2007; Mitsuhashi and Takahashi, 2009). Also, in mouse, p27 in known to play a key role in regulation of osteoblast differentiation by controlling proliferation-related events in bone cells (Drissi et al., 1999).

We have found *p27* expression in the limb, at the AER in a single, most distal strip of stained cells (Fig. 36H, I), outside the AER proliferating areas we described before, suggesting a possible role for *p27* in getting these cells to exit the cycle at G1.

As for *sox14*, we have gather tools, by cloning its full-length cDNA into a pCAGGS expression vector and producing RCAS virus that drive *p27*^{kip1} expression, to pursue studies on this subject at the lab.

II.9.4 *Lgr5*

The Wnt signalling pathway plays a key role in the maintenance and activation of proliferation of stem cell niches (Haegebarth and Clevers, 2009). Recently, *lgr5*, a Wnt target gene, was identified as a stem cell marker in colon and small intestine, a system that share similarities with our findings on proliferation and cell death patterns in the AER (Barker et al., 2007). Moreover, we described a role for Wnt signalling in the positive regulation of *oct4.* Therefore, we decided to check if, as for the small intestine, *lgr5*-positive cells co-localized with proliferating areas in the AER during limb development.

cLgr5 transcripts can be found in the neural tube of stage 17HH chicken embryos, and in the fore and hindlimb fields (Fig. 38). As the limb develops and the ectodermal cells condensate at the most distal part of the limb forming the AER,

lgr5-positive cells get restricted to two twin stripes of expression at the base of the AER (Fig. 38C). At stage 24HH, *lgr5* starts to invade the wing and footplate and begins to disappear from the AER. By stage 29HH it is absent from the structure. As the digits become defined, *lgr5* gradually disappears from the interdigital space and surrounds the phalanges (Fig. 38F-I).

Our results suggest that *Lgr5* is a good candidate gene as a positive co-regulator of AER cells renewal, along with *oct4*.

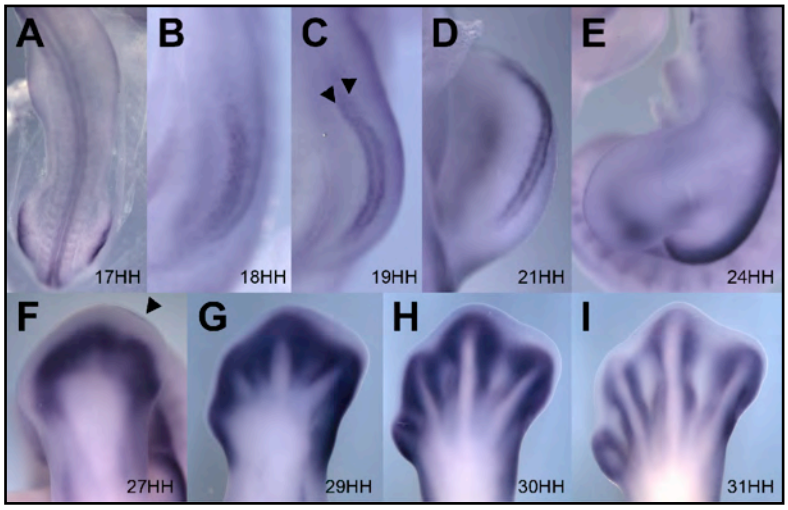

Figure 38. Expression Pattern of *lgr5* in *Gallus gallus*. Whole-mount *in situ* hybridisation to *cLgr5* transcripts. (**A**) Chicken embryo at stage 17HH; *lgr5* transcripts can be found in the neural tube, and in the limb field. (**B-D**) Chicken embryo at stage 18HH, 19HH and 21HH; as the ridge gets defined, *lgr5* expression gets restricted to two twin stripes of expression on the AER. At stage 24HH (**E**), *lgr5* starts to invade the footplate and begins to disappear from the AER. By stage 29HH (**G**) it is absent from the structure. (**F-I**) Chicken embryo at stage 27HH, 29HH, 30HH and 31HH; *lgr5* can be detected in the footplate around the developing digits.

DISCUSSION

I *Flrt3* and vertebrate limb development

The coordinated and intricate network of signalling pathways is a consequence of the interaction between the organizing centres that constitute the developing vertebrate limb and is responsible for the outgrowth and patterning of the limb in its three axis: anterior-posterior (AP), proximo-distal (PD) and dorso-ventral (DV).

These interactions are mediated by several families of signalling molecules such as WNTs, BMPs and FGFs and the integration of this information results in the final and proper positioning of the tissues that will form the limb reviewed in (Capdevila and Izpisua Belmonte, 2001).

FGFs are very important molecules during embryonic development, being involved in numerous cell processes such as cell proliferation, differentiation, cell survival and motility (Capdevila and Izpisua Belmonte, 2001; Tickle, 2002a). FGF8 signals from the AER to the underlying mesenchyme promoting the survival of the mesoderm while sensitizing the mesodermal tissue for the pro-apoptotic effects of BMPs (Montero et al., 2001). The intracellular response to FGF8 stimuli is mediated by FGF receptors (FGFRs), which trigger several signalling pathways, namely the Ras-MAPK/ERK and the PI3K pathways.

Due to the wide range of FGFs' biological roles, and due to the variety and complexity of signalling pathways activated, FGF signalling must be tightly regulated (Xu et al., 1998; Sun et al., 2002; Thisse and Thisse, 2005). A growing number of proteins have been identified as specific regulators of FGFR-mediated FGF signalling. These molecules affect the FGF signalling cascade at different levels. Most belong to the FGF synexpression group, a set of genes that share complex spatio-temporal expression patterns and have a functional relationship. *Sprouty, spred, sef*, *shisa* and *mkp3* are known negative modulators of FGF signalling, whereas *erm, er81* and *pea3* promote FGF signalling (Raible and Brand, 2001; Zhang et al., 2001; Furthauer et al., 2002; Dikic and Giordano, 2003;

Kawakami et al., 2003; Tsang and Dawid, 2004; Sivak et al., 2005; Furushima et al., 2007).

I.1 *Flrt3* is essential for AER integrity and activity

Flrt3 has been described in *Xenopus laevis* as a FGF signalling positive modulator, activating the MEK/ERK signalling cascade, as opposed to MKP3, an inhibitor of the cascade through specific ERK1/2 dephosphorylation (Bottcher et al., 2004).
Our results support not only that *flrt3* is expressed in areas with FGF activity, as previously reported in *Xenopus laevis* (Bottcher et al., 2004), but also that it is confined to places where ERK is phosphorylated, such as the AER (Kawakami et al., 2003). In the limb mesenchyme, where MKP3, the ERK inhibitor, is expressed, we found no expression of *flrt3*, suggesting that *flrt3* expression is excluded from areas where ERK is not activated. In fact, when we overexpress *flrt3* in the limb ectoderm we observe an increase of *mkp3* expression in the mesenchyme as a result of the enlarged AER, and subsequent enhancement of FGF signalling. A similar phenotype was obtained when FGF-soaked beads were applied in the limb bud (Eblaghie et al., 2003; Kawakami et al., 2003).

In chicken, ectopic expression of *mkp3* results in the disruption of limb outgrowth, a phenotype characteristic of FGF signalling blockage (Eblaghie et al., 2003; Kawakami et al., 2003; Bottcher et al., 2004). When a constitutive active form of *mkp3* is overexpressed, cells at the AER are unable to translocate active ERK to the nucleus, resulting in truncations and indentations of the manipulated limbs (Kawakami et al., 2003), which mimics the effects of ridge removal or pharmacological inhibition of FGF or Ras/MAPK signalling. We observe identical phenotypes by silencing the expression of *flrt3* using RNAi technology. Not only AER markers are affected by *flrt3* silencing. The impairment of FGF signalling from the AER to the mesenchyme underneath provides also another evidence that ERK phosphorylation is essential for AER integrity and activity. The importance of *flrt3* signalling from the ridge to the correct progress of the limb outgrowth becomes clear

by observing how a small cluster of isolated AER cells is still able to promote outgrowth of part of the limb (Fig. 24F). The wide range of phenotypes observed is most probably due to the variability in the efficiency of both siRNA interference and electroporation. Notwithstanding, they all converge into the disruption of the AER integrity and consequent impairment of limb outgrowth.

I.2 *Flrt3 is* necessary but not sufficient for proper AER formation and maintenance

Different studies have shown that *en-1* plays a role during migration and compaction of AER cells restricting the expression of *r-fng* and *wnt-7a* to the dorsal ectoderm (Loomis et al., 1998), while Wnt/ß-catenin signalling is required to maintain the AER after AER initiation and maturation (Kengaku et al., 1998; Barrow et al., 2003). *Wnt*-7a instructs the dorsal mesoderm to adopt dorsal characteristics, such as *lmx-1* expression, which in turn specifies dorsal pattern. Thus, *en-1* has a dual function in AER positioning and dorsal specification and hence acts to coordinate the two processes (Johnson and Tabin, 1997).

Overexpression of *flrt3* in the limb ectoderm produces *fgf8*-positive enlargements and projections of the pre-existing AER. The enlarged regions of the AER show also a broadening of the *fgf8* expression domain and a local inhibition of *en-1* expression (Fig 21F). *Flrt3*-electroporated limbs present a clear deregulation of the *en-1* ventral ectoderm territory. There is evidence that in mice lacking *en-1,* the correct positioning of the AER depends on correct *en-1* expression (Loomis, 1996; Loomis et al., 1998), and that homozygous mice for a null allele of *en-1* present both DV and PD axes defects. The same phenotype is observed upon removal of *bmp2* and *bmp4* from the AER (Maatouk et al., 2009). In these mice, such as in *flrt3*-overexpressed chicken limbs, the AER is significantly broadened and *fgf8* expression is expanded, suggesting that the *en-1* domain may be affected by loss of BMP signalling from the AER.

Ectopic AERs induced upon *flrt3* overexpression are *fgf8*-positive only in the vicinity of the original AER (Figs. 21B arrows, 22B, B'). The proximity to the pre-existent

AER seems to be a key factor, suggesting that the cells that compose the ectopic structure are not completely committed to AER fate, denoting the presence of AER-like structures and emphasizing the importance of distinguishing between AER structure and function.

Therefore, *flrt3* seems to be necessary but not sufficient for proper AER formation and maintenance. This is supported by our observation that overexpression of *flrt3* in the flank between the forelimb and the hindlimb does not induce ectopic AERs, although the region has ectodermic competence for AER induction, as shown with FGF bead implantation in the flank (Cohn et al., 1995; Mahmood et al., 1995; Mima et al., 1995; Crossley et al., 1996; Vogel et al., 1996; Yonei-Tamura et al., 1999)

I.3 Limb territorial borders are shiffted but identities are not altered upon *Flrt3* overexpression in the limb ectoderm

Our results also show that the projections from the pre-existing AER are not altered in their positional identity. *Lmx-1,* an established dorsal mesoderm identity marker is absent from both sides of ventrally-derived outgrowths. The same happens with *en-1* absence on dorsal outgrowths, suggesting a double-dorsal identity of those ectopic AERs.

BMP signalling, besides being essential for AER induction, is also necessary and sufficient to regulate *en-1* expression in the ventral ectoderm. Therefore, the loss of BMP signalling from the limb bud ectoderm results in failure of AER formation and bi-dorsal limbs (Ahn et al., 2001; Pizette et al., 2001; Soshnikova et al., 2003). This might explain the partial bi-dorsal identity in one of our *flrt3* electroporated limbs, probably through *gremlin*, a BMP signalling inhibitor known to promote a decrease in cell death and to expand the AER domain. In mice lacking ectodermal BMP signalling, there is a failure in AER maturation and a subsequent loss of *en-1* and *msx2* in the AER. This promotes the expansion of the AER and the expression of FGF genes at high levels, decreasing *gremlin* in the distal mesenchyme and affecting the FGF/BMP loop (Maatouk et al., 2009).

The formation of perpendicular, connected or not, ridges after *flrt3* overexpression, is explained by Loomis' Zipper Hypothesis for the AER Maturation (Loomis et al., 1998). They propose a model that compares the final phase of AER constriction to the closing of a zipper, being the dorsal and ventral AER domains the two halves of the zipper. The zipping would occur with the dorsal half remaining relatively fixed and the ventral half being pulled towards it in a posterior-to-anterior fashion. Upon deregulation of *en-1*, the cells in the middle of the broadened AER are pulled towards the dorsal and ventral AER borders. In some cases distinct secondary AERs are formed due to the self-zipping of the ectopic rim. This theory support the range of phenotypes observed upon *flrt3* overexpression.

I.4 *Flrt3* expression: the effect of FGF and WNT signalling

Studies on xenopus and mice show that *flrt3* expression can be induced by activation of FGF signalling (Bottcher et al., 2004; Haines et al., 2006). However, unpublished data from zebrafish *flrt3* by Fürthauer M., Thisse, B. and Thisse, C (2005), suggest that in zebrafish FLRT3 may be involved in directing cell movements but do not appear to be related to the FGF pathway, since neither gain nor loss of FGF signalling appears to directly affect FLRT3 expression (Furthauer et al., 2002). In addition, *flrt3* expression is not increased in stem cells treated with FGFs and its antagonist (SU5402) (Mallo, M., personal communication). In our hands, no signs of *flrt3* induction by FGFs were obtained. Moreover, FGF8 appears to have a negative effect on *flrt3*. In fact, the FGF antagonist SU5402 does not reduce *flrt3* transcripts' level, as expected. Instead, it has no effect over *flrt3* expression. Taking into account the unpublished data on zebrafish and stem cells, we hypothesize that the FGF signalling pathway exerts a negative effect on *flrt3* expression, however an inhibition of the pathway is not enough to activate *flrt3* expression.

We have obtained ectopic *flrt3* induction around the WNT3A bead (Fig. 25D) in a short time window, suggesting a direct activation of *flrt3* by WNT3A. *Wnt3a* signals through ß-catenin, being expressed in AER precursors and in the established AER

(Kengaku et al., 1998; Kawakami et al., 2001). In fact, injection of RCAS dominant-active β-catenin into chick limb buds induces the appearance of ectopic ridge-like spikes (Capdevila et al., 1998; Kawakami et al., 2004). Therefore, we propose a direct induction of *flrt3* by *wnt3a*, even before it activates *fgf8* expression.

I.5 *Flrt3* regulate AER's BMP signalling through *gremlin*

As already referred, BMPs are expressed in the AER and since they assure the correct balance between apoptosis and survival of the AER cells, are responsible for the integrity of the structure. BMP soaked beads applied into the developing limb promoted the inhibition of *flrt3* expression (Fig. 25E), but *mkp3* expression in the mesenchyme is not affected, suggesting that *flrt3* expression in the AER could be maintained by the activity of the BMP antagonist *gremlin* (Capdevila et al., 1999; Merino et al., 1999; Zuniga et al., 1999). Our results suggest that upon *flrt3* overexpression, an increase of *gremlin* expression (Fig. 21J) and the subsequent loss of AER's BMP signalling affects cell death equilibrium at the AER resulting in a broadened AER. When *gremlin* expression disappears, BMP activity induces the regression of the AER and downregulation of *flrt3*.

I.6 Proposed model for *flrt3* action in chick limb development

In summary, *flrt3* is a key player during chicken limb development. Gain and loss-of-function studies show that *flrt3* is necessary but not sufficient for proper AER formation and maintenance.

We favour a model (Fig. 39) in which FGF10 from the mesenchyme signals to the AER through *Wnt3a*, inducing FGF8 activity. Wnt3a would induce Flrt3 expression, and FGF signalling, together with *flrt3* in the ectoderm, would activate ERK, maintaining, this way, AER integrity. Simultaneously, FGF8 signals to the underlying mesenchyme via PI3K, inducing expression of *mkp3* and, thus, promoting the survival of progress zone cells.

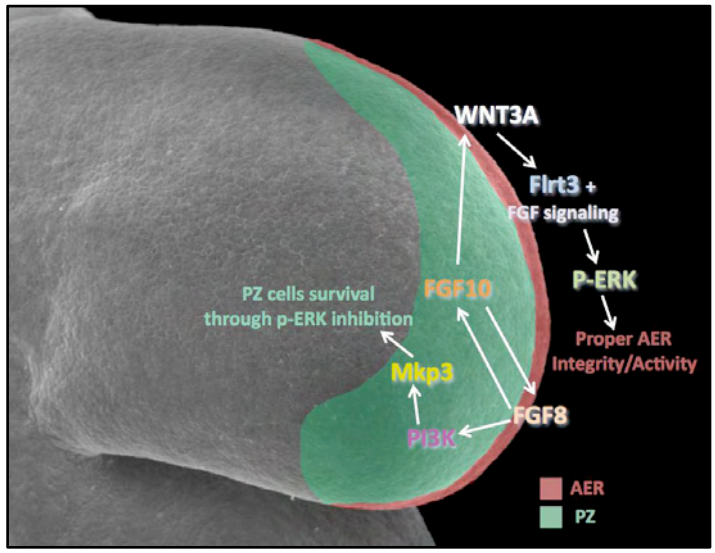

Figure 39. Proposed model for *flrt3* role in chick limb bud development. FGF signalling from the AER maintains *fgf10* expression in the PZ and induces PI3K signalling which is responsible for *Mkp3* activation. MKP3 would promote cell survival by inhibiting ERK activation. FGF activity from the PZ induces *wnt3a* and *fgf8* at the AER. *Wnt3a* would be responsible for inducing *flrt3* expression and this, together with FGF signalling, would activate ERK to maintain AER integrity and activity.

I.7 *Flrt3* in zebrafish fin development

Pectoral and pelvic fins are homologous to the tetrapod fore and hindlimb, respectively.

As Mercader explains, in a recent review that compares fin and limb development (Mercader et al., 2000), although the genetic network that prompts paired fin development seems to be similar to the developmental program of the tetrapod limb, there are evidences for some differences. It is probable that different solutions evolved to solve the distinct problems arising from the different morphological constraints. It may also be that although genes are considerably conserved between species, their regulatory regions diverged during evolution, producing alterations in the expression domains of "limb genes". This could subsequently have led to changes in the gene regulatory network triggering limb outgrowth (Mercader et al., 2000).

The paired fins arise from mesenchymal proliferations that form fin buds in the ventrolateral body wall. While the buds are growing, the apical epidermis produces an apical fold, which circumferences the buds in an anteroposterior direction. It is subsequently transformed into the fin fold as it is populated by migrating mesenchymal cells (Grandel and Schulte-Merker, 1998).

According to our gene expression results (Fig. 13), we detect *flrt3* at known FGF signalling centers, such as the developing brain, eye, ear and fin. It becomes evident that *flrt3* expression in the pectoral fins is restricted to the mesenchyme at 36hpf, when the apical thickening condenses and forms the apical fold, in a complementary pattern observed in the chicken and mice homologues, where *flrt3* is expressed in the AER (Haines et al., 2006; Smith and Tickle, 2006; Tomás et al., 2010).

Moreover, we have located FLRT3 protein (Fig. 14)in cells that constitute the dermomyotome, branchial arches, and the developing retina, correlating with the structures where the *flrt3* mRNA is expressed. However, in the pectoral fin, we have immunolocalized FLRT3 to the apical fold, instead of the mesenchyme, as for the mRNA. This might be due to the unspecific ability of the antibody to recognize the zebrafish FLRT3, but rather be recognizing another zebrafish *flrt* family gene, since the antibody was raised against the human protein and there are significant differences between the aminoacid sequences of both species (Fig. 12A)). Other members of the family should be studied to further understand *flrt* gene family role in zebrafish fin development.

II *Flrt3* in other FGF signalling centers

We have shown that *flrt3* expression in both zebrafish and chick (also in Smith and Tickle, 2006), coincide with regions known to express FGF signalling components or to be regulated by FGF signalling during development, including the limb bud, the dermomyotome, the otic and optic placodes/ vesicles, and the midbrain-hindbrain boundary. This feature is observed also in frog (Bottcher et al., 2004) and mouse (Haines et al., 2006; Gong et al., 2009). In fact, sustained domains of MAPK/ERK activation by FGF signalling were identified during mouse embryonic development in the ectoplacental cone, extra-embryonic ectoderm, limb buds, branchial arches, frontonasal process, forebrain, midbrain-hindbrain boundary, tailbud, foregut and liver. Transient activation was seen in neural crest, peripheral nervous system, nascent blood vessels, and anlagen of the eye, ear and heart (Corson et al., 2003).

At the dermomyotome the temporal pattern of *flrt3* expression and evidences from cell-cell interaction studies (Haines et al., 2006; Karaulanov et al., 2006; Karaulanov et al., 2009) suggest that *flrt3* might be involved in the detachment of muscle precursor cells. In that structure, cells that have an epithelial morphology transforms into a less adhesive myoblast morphology allowing their migration from the demomyotome to their final destination. The signals that regulate the timing of the epithelio-mesenchymal transition (EMT) of the central dermomyotome remain unknown, however it has been shown to depend on the triggering of MAPK/ERK pathway (Delfini et al., 2009).

The midbrain-hindbrain boundary (MHB), also known as the Isthmic Organizer (IsO), is the best-characterized signalling center within the CNS. Located at the level of the isthmus (Marin and Puelles, 1994; Liu and Joyner, 2001), the IsO secretes signalling molecules from the WNT (mainly Wnt1) and the FGF (FGF8, FGF17, FGF18) families (Liu and Joyner, 2001; Mason, 2007). FGFs, FGF8 in particular, are

considered the principal molecules that exert patterning functions while WNT signals are typically associated with proliferative control (Raible and Brand, 2004).
We observed *Flrt3* expression in the anterior part of the neural tube at the MHB in a restricted manner. This expression correlates with FGF expression and the role for FGFs in the formation, patterning and signalling from the isthmus (Carl and Wittbrodt, 1999; Trokovic et al., 2003; Mason, 2007).

Also, *flrt3* is expressed at the retina of the developing eye. Early development of the lens and retina depends upon reciprocal inductive interactions between the embryonic surface ectoderm and the underlying neuroepithelium of the optic vesicle. FGF signalling has been implicated in this signal exchange, via MAPK/ERK(Gotoh et al., 2004). Moreover, retinal regeneration studies proved a role for FGF2 in stimulating Pax6 expression during induction of transdifferentiation of the RPE through FGFR/MEK/ERK signalling cascade (Spence et al., 2007).

A conclusion that can be extracted from the overall analysis of *flrt3* expression is that its expression is dynamic throughout the FGF signalling centers, and like in limb development, promotes cell-cell communication and ERK-mediated patterning.

III *Flrt2*

Contrarily to *flrt3, flrt2*, the only other gene from *flrt* family indentified in *Gallus gallus*, does not seem to be associated to the FGF signal transduction in the developing limb.

During AER induction and limb outgrowth, the peek of FGF activity in the limb bud, *flrt2* expression is not found in the limb, but in the embryo flank (Fig. 27D). Only at stage 25HH, a small zone of *flrt2* expression starts to become evident in the limb's central mesenchyme, whilst the flank *flrt2* expression begins to get fainter.

This pattern is similar to that of *raldh2*, responsible for Retinoic acid (RA) synthesis from retinal, overlaping at the flank and proximal mesenchyme. RA is a potent morphogen, with a prominent role in limb initiation, by the positioning of the ZPA through induction of *hoxb8* (Stratford et al., 1996; Berggren et al., 1999; Berggren et al., 2001). Recently, RA signalling was shown not to be required for limb expression of *Shh* and *Meis2*, acting outside the limb field in the body axis during forelimb induction, but unnecessary at later stages when hindlimb budding and patterning occurs (Zhao et al., 2009).

Although apparently not necessary for the P-D patterning of the limb, RA has an important role in the formation of the limb cartilage, being pivotal for the initial induction and condensation of prechondrogenic tissues (Weston et al., 2000; Berggren et al., 2001), condrocyte proliferation and maturation, regulation of longitudinal bone growth (Koyama et al., 1999; De Luca et al., 2000) and control of interdigital cell death by promoting BMP gene expression and simultaneously repressing the chondrogenic potential of BMPs (Rodriguez-Leon et al., 1999).

In later stages, *flrt2* is detected in the tip and around the digits, in the precartilaginous condensations, suggesting a possible role for *flrt2*, along with RA in the control of chondrogenic differentiation. This is supported by *flrt2* colocalization with *raldh2*, in the flank and limb proximal mesoderm, although further studies must be done for both genes in order to one be able to sustain this hypothesis.

IV AER cell dynamics

The importance Apical Ectodermal Ridge in vertebrate limb development has been extensively demonstrated. Classical experiments of AER removal have shown that progressive late structure surgical ablations result in progressive loss of distal elements of the limb, which can be partially rescued by exogenous application of FGFs (Saunders J. W., 1948; Summerbell, 1974).

This specialized ectoderm ridge along the distal edge of the limb bud has been known to control proximal-distal growth by maintaining PZ cells in an undifferentiated and proliferative state. However, one lacks the knowledge on how do AER cells behave and how is the dynamic of cell renewal at the most distal tip of the limb in order to maintain the organizing centre structure, and function, during development. We have characterized this process during chick limb development.

Immunolocalization of phospho-Histone H3 and different BrdU-pulse assays enable us to describe a niche of proliferating cells located at the base of the AER (Fig. 29C,I), both on the ventral and dorsal sides of the AER along all its length. Also we have indirectly inferred cell movement within the structure and determine the half-live of those cells. Our results suggest that a BrdU-positive cell that has incorporated BrdU while dividing itself in the AER proliferating region at the base of the structure took around 45 minutes, from their proliferating niche at the AER's base, to reach the tip of the ridge.

There, a constant pattern was also observed throughout the limb bud development. AER cells dye on the most distal and central part of the ridge along the anterior-posterior axis of the limb bud (Fig. 29B,I), most probably through a process of Anoikis (apoptosis following loss of cell anchorage), as described for other systems such as normal skin, the involuting mammary gland, epithelial tissues of the colon, and in the first cavitation step of embryogenesis (reviewed in Zhan et al., 2004; Chiarugi and Giannoni, 2008).

Throughout limb development, the structure of this organizing centre must be maintained through a genetically controlled fine-tuned balance between proliferation and cell death, self-renewal and differentiation.

IV.1 Other epithelial cell renewal systems: the small intestine

Ever since embryonic stem cells (ESCs) were first isolated in the early 1980s, they have gained notoriety as invaluable tools for research and a promising resource for cell replacement therapies. These cells present the unique property of self-renewal and the ability to generate differentiated progeny in all embryonic lineages both *in vitro* and *in vivo*. They have been, and continue to be, extensively studied for the molecular characteristics that permit them to achieve and maintain their pluripotency. Somatic stem cells (SSCs) are maintained by self-renewal and, in contrast to ESCs, differentiate into function-specific cells in order to replace dead and injured cells in various tissues. They have been identified in numerous tissues in the adult mammal namely the central nervous system, epidermis, mammary gland, muscle, bone marrow, gonads and intestine epithelium (reviewed in Naveiras and Daley, 2006; Teo and Vallier, 2010).

The intestinal epithelium contains a rapidly proliferating and perpetually differentiating epithelium, being its principal functional unit the crypt–villus axis. In mouse, stem cells located in the crypts give rise to proliferating progenitor or transit amplifying (TA) cells that undergo approximately 4 to 5 rounds of rapid cell division, move out of the crypt and terminally differentiate into enterocytes, goblet cells, and enteroendocrine cells. These differentiated cells continue to move up the villus flanks to die upon reaching the villus tip after 2 to 3 days (Marshman et al., 2002; Shaker and Rubin, 2010).

Although we could not characterize the rounds of division for the AER cells, this portrays a very similar system of epithelial cell renewal to the one we describe in the chicken AER (Fig. 29I): they proliferate in the base of the structure, migrate toward the tip, and dye.

V *Oct4* in AER development and renewal

Oct4, along with the transcriptional co-regulators *sox2* and *nanog,* is critical for the maintenance of the undifferentiated state and self-renewal state of human and mouse embryonic stem cells as well as early embryonic cells (Nichols et al., 1998; Pesce and Scholer, 2001; Avilion et al., 2003; Chambers et al., 2003; Mitsui et al., 2003; Chew et al., 2005; Loh et al., 2006; Lavial et al., 2007; Niwa, 2007; Wei et al., 2009), being an obligatory component of the cocktail needed to, *in vitro*, induce pluripotency in different somatic cell types (Takahashi and Yamanaka, 2006; Yu et al., 2007; Aasen et al., 2008; Aoi et al., 2008). In mouse, they form a regulatory circuitry with co-regulators, such as ß-catenin, *Stat3*, *Myc*, *Klfs*, and *Sall4* to control the expression of pluripotency-related genes including themselves (Li, 2010).
In 2007, Lavial and colleagues, showed that it was also required for chicken embryonic stem cells pluripotency maintenance and continued proliferation, establishing that mechanisms by which genes like *oct4* regulate pluripotency and self-renewal are not exclusive to mammals.

We have found *oct4* expression during limb development, although in lower levels than those observed in the PGCs (primordial germ cells). Initially spawned over the limb ectoderm, as the ectoderm condenses to form the AER at its distal tip, *oct4* expression can be observed in the ectoderm and in the forming AER (Fig. 28H) in a "two stripes" pattern running along the anterior-posterior axis of the limb, that corresponds to areas of cell proliferation. At later stages when a decrease in proliferation rate accompanies the regression of the structure and the commitment towards the cartilage differentiation pathway, *oct4* is no longer expressed, suggesting a role for *oct4* in the maintenance of the ridge during limb development.
In mouse ES cells, RNAi-mediated suppression of *oct4* have been shown to cause a decrease in proliferation and induction of differentiation even in the presence of serum and LIF (leukemia inhibitory factor), inhibitors of ES cell differentiation (Velkey and O'Shea, 2003; Hough et al., 2006). Moreover, ectopic activation of *oct4*

in the intestine or skin results in rapid expansion of progenitor cells and invasive tumour formation indicating that *oct4* can also act as a powerful oncogene in somatic cells (Hochedlinger et al., 2005).

These findings support our evidence that *oct4* controls the proliferative balance within AER cells. The AER cell's response to *oct4* overexpression results in the alteration of the AER's cell dynamics favoring a local increase of proliferating cells and producing an expansion of the AER (Fig. 31B, E'). As a result of that event, an enlargement of the limb mesenchyme and increased number of chondrogenic precursors occur, as seen by an increased *sox9* expression, and consequently by the formation of extra skeletal pieces on *oct4*-electroporated limbs (Fig. 31J').

V.1 RA and BMPs negativelly regulate *oct4*

The self-renewal process is generally described as a parallel cellular event of proliferation, differentiation and apoptosis, and is known to be controlled by intrinsic genetic pathways that are regulated by extrinsic signals from the microenvironment in which those cells reside (Zhang and Li, 2005; Haegebarth and Clevers, 2009).

Along with their known roles in AER induction, maintenance and regression during limb development, several extrinsic signals such as RA, BMP, FGF and WNT support self-renewal and pluripotency of ES cells by regulating "pluripotent genes". Giving its critical role in maintaining pluripotency, *oct4* activity must be tightly regulated.

The retinoic acid (RA) effect on limb bud initiation has long been established, however, its role on proximo-distal limb patterning is far from consensual. Although prior studies stated that RA promoted proximalization of limb cells and endogenous RA signalling is required to maintain the proximal *Meis* domain in the limb (Mercader et al., 2000; Mic et al., 2004), Zhao and colleagues show that, in mice, RA signalling is not required for limb expression of *Shh* and *Meis2*. Moreover, they say that RA action is required outside the limb field in the body axis during forelimb

induction, but that RA is unnecessary at later stages when hindlimb budding and patterning occurs (Zhao et al., 2009).

As we mentioned before, Retinoic Acid is synthesized in the proximal mesenchyme, mainly by RALDH2, and spreads into the distal limb bud, where it is degraded by CYP26 (Okamoto et al., 1990; Yashiro et al., 2004). Moreover, RA has a key role in chicken interdigital BMP-mediated cell death, activating *msx* genes in the interdigital space, and repressing the chondrogenic effect of BMPs (Rodriguez-Leon et al., 1999).

In the mouse and chick embryonic axis, RA promotes differentiation by inhibiting expression of *fgf8* as cells leave the tailbud (Wilson et al., 2009), a step that may be analogous to the RA-mediated downregulation of *fgf4* in ES cells (Stavridis et al., 2010). In both ESCs and embryonic carcinoma cells, expression of *oct4* is strong and rapidly downregulated during RA-induced differentiation (Pikarsky et al., 1994; Schoorlemmer et al., 1994; Lavial et al., 2007). We obtained similar effects on AER *oct4* expression with RA bead implantation (Fig 34F), supporting the data from ESCs.

The existence of complementary domains of retinoic acid production (by *raldh2*) and degradation (by *cyp26*), and the fact that *cyp26* expression on the AER (Swindell et al., 1999) is coincident with *oct4*'s, strengthens our model for *oct4* function in the AER cells and RA signalling involvement in keeping these particular niche of cells self-renewing.

BMP family members *bmp2*, *bmp4* and *bmp7* are expressed in the AER (Geetha-Loganathan et al., 2006) and are the main source of BMP signalling in the limb. Their main roles are to establish the dorso-ventral axis, to induce apoptosis and to maintain the integrity of the ridge (Pizette and Niswander, 1999; Geetha-Loganathan et al., 2006). *Bmp5* is expressed at the distal mesenchyme being accountable for the induction of apoptosis in the undifferentiated mesoderm and growth in the prechondrogenic mesenchyme (Zuzarte-Luis et al., 2004).

Studies indicate that, although with different functions in different stem cell compartments (Chen et al., 1998; Ying et al., 2003; Zhang et al., 2003; He et al.,

2004; Bai et al., 2010), BMPs play an important role in the regulation of stem cell properties. Among others, in intestinal stem cells, BMP signalling is responsible for the inhibition of stem cell self-renewal through suppression of WNT-β-catenin signalling (He et al., 2004).

Our results shown that *oct4* AER expression is downregulated in the area of influence of the BMP-soaked bead (Fig. 34E), supporting a role for BMP activity in the negative regulation of *oct4* expression, as it happens with RA, and supporting the data from SC systems for both molecules.

V.2 *Oct4* is upregulated through exogenous application of FGFs and WNT3A

Several FGF family genes are responsible for AER activity. Of the 17 known FGF genes, 5 are expressed in the distal part of the established limb bud, 4 in the AER (*Fgf2, Fgf4, Fgf8, Fgf19*), and 2 in the mesenchyme underlying it (*Fgf2, Fgf10*). Their role is to provide AER function, either directly or indirectly, controlling proximal-distal outgrowth of the bud maintaining the distal progress zone cells in a proliferative state (Niswander, 1992; Mahmood et al., 1995; Savage and Fallon, 1995; Martin, 1998; Montero et al., 2001; Boulet et al., 2004; Kurose et al., 2004) .Moreover, data from ESCs studies have shown that FGF signalling is required for maintaining the self-renewal activity (Eiselleova et al., 2009; Gotoh, 2009). The transcriptional program responsible for the pluripotency of human ESCs is believed to be co-maintained by exogenous FGF2, which activates FGF receptors and stimulates the mitogen-activated protein kinase (MAPK) pathway (Eiselleova et al., 2009; Gotoh, 2009).

Evidences have been pointing to the Wnt signalling pathway as a major signalling pathway during embryonic development and a key regulator of self-renewal homeostasis in several adult tissues, such as in the adult epithelial stem cells of the skin and intestine (Korinek et al., 1998; Haegebarth and Clevers, 2009). These studies support our data from FGF and WNT3A bead implantation, where an

upregulation of AER's *oct4* expression with these factors can be observed (Fig. 34D).

Also, enhancing FGF signalling through *flrt3* overexpression in the limb ectoderm, has proved to be effective in inducing *oct4* expression on ectopic ridge-like structures produced (Fig. 35B), supporting our results from regulatory studies upon bead implantation. Moreover, *oct4* is expressed in a salt-and-peper fashion in ectopic limbs induced in the flank between the forelimb and the hindlimb by FGF8 bead implantation in the flank (Fig. 34A), supporting a role for *oct4* in the maintenance of the ridge during early limb development.

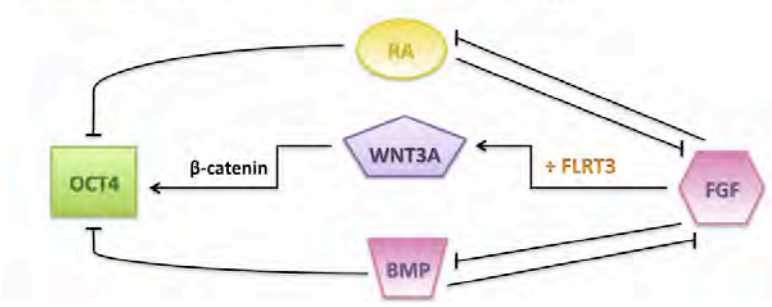

Figure 40. Schematic representation of *oct4* regulation in *Gallus gallus*'s early limb development.

VI *Oct4* co-regulators of AER renewal

An interesting fact is that, although favouring AER cell's self-renewal, *oct4* it is not sufficient, by itself, to induce the formation of ectopic ridge-like structures in the non-AER ectoderm nor in the flank between the forelimb and the hindlimb, even though the region has ectodermic competence for AER induction as shown with FGF bead implantation in the flank (Cohn et al., 1995; Mahmood et al., 1995; Mima et al., 1995; Crossley et al., 1996; Vogel et al., 1996; Yonei-Tamura et al., 1999).

Additional factors must be necessary to "reprogram" non-AER cells into an AER fate in coordination with *oct4*, therefore emphasizing the unique microenvironment that AER provides.

We can exclude *nanog* from the candidate list for AER cell renewal co-regulator since it has been described as not expressed during limb development (Canon et al., 2006).

VI.1 *Sox14* and *p27*, onsets for AER cell differentiation?

Due to the synergistic interaction between *oct4* and *sox2* in ESCs (Chew et al., 2005; Okumura-Nakanishi et al., 2005), we have looked into its expression in the AER during limb development. However, we could not find *sox2* expression there. When generating iPS (induced pluripotent stem) cells, *sox2* can be replaced by *sox1* or *sox3* (Nakagawa et al., 2008). We then looked for a different Sox partner that might accomplish *oct4* gene activation in AER cells.

The Sox gene family codes for a group of developmental transcription factors that belong to the group of High Mobility Group (HMG) box domain proteins (Uchikawa et al., 1999; Bowles et al., 2000). The Sox group B has been further divided into two subgroups, B1 and B2, based on homology in the C-terminal domains. SoxB1 proteins (SOX1, SOX2, SOX3) have been demonstrated to act as transcription activators whereas the SoxB2 proteins (SOX14, SOX21) act as repressors (Uchikawa et al., 1999).

Sox proteins act in a wide range of developmental processes with the Group B proteins acting in the development of the nervous system. Specifically, SoxB1 proteins are generally thought to be involved in maintaining a neural stem cell or progenitor population (Wegner and Stolt, 2005). Functional analysis of chick *sox21* suggests that it specifically counteracts SoxB1 proteins, and as a consequence, promotes the progression of neurogenesis in the developing CNS (Sandberg et al., 2005). Also *sox14,* it has been described as a mediator of cell death and dendritic and axonal pruning (Osterloh and Freeman, 2009), and as an interneuron differentiation factor (Popovic et al., 2010).

Ours results show that *sox14* is expressed at the central and distal portion of the AER, in an almost complementary pattern to *oct4* (Fig. 36E,F). Immunohisto-chemistry analysis has confirmed (Fig. 36G), that *sox14* it is absent from the proliferation areas of the AER. These results, together with *oct4* expression data, suggest a role for *sox14* in promoting differentiation of the cells that leave the *oct4*-positive proliferating area. Further studies should be done in order to dissect *sox14* role in this process.

The cyclin-dependent kinase (CDK) inhibitor $p27^{Kip1}$ binds to and prevents the activation of Cyclin E/CDK2 or Cyclin D/CDK4 complexes, and thus controls G1-to-S phase transition of the cell cycle. p27 is one of the proteins induced when mES cells enter a differentiation pathway (Savatier et al., 1996; Bryja et al., 2004). Moreover, in *Xenopus laevis* has been shown to be involved in exit from the cell cycle and differentiation of cells into a quiescent state in the nervous system, muscle tissue, heart and retina (Ohnuma et al., 1999; Ohnuma et al., 2002; Vernon et al., 2003; Vernon and Philpott, 2003; Movassagh and Philpott, 2008; Naylor et al., 2009). Also, in mouse, *p27* in known to play a key role in regulation of osteoblast differentiation by controlling proliferation-related events in bone cells (Drissi et al., 1999).

As for *Sox14*, we have found *p27* expression at the AER in a single, most distal strip of stained cells (Fig. 36H, I), outside the AER proliferating areas. Our results,

together with observations that imply p27 as a regulator of proliferation and differentiation in numerous systems, suggest a possible role for *p27* in getting AER cells to exit the cycle at G1 and differentiate, as they move towards the tip of the structure.

We have gather tools, by cloning its full-length cDNA into a pCAGGS expression vector and producing RCAS virus that drive $p27^{kip1}$ expression (as we did for *sox14*), to pursue studies on this subject at the lab, and further understand the mechanism by which *p27* might be regulating AER cells differentiation.

VI.2 *Lgr5*

We have previously discussed (II.1) the similarities between the dynamic we describe here for the epithelium renewal at the most distal tip of the limb during development and the intestinal epithelium: cells proliferate at the base of the structure, migrate towards the tip, and dye (Fig.29 I).

The crypt is a unique cell biological system as proliferation (transit cell lineages), differentiation and cell migration are all distributed linearly along the axis of the crypt (Potten et al., 2009).

The Wnt signalling pathway plays a key role in the maintenance and activation of proliferation of stem cell niches (Haegebarth and Clevers, 2009). The Wnt target gene *lgr5* has been recently identified as a novel stem cell marker of the intestinal epithelium and the hair follicle. The *lgr5* gene encodes an orphan G protein-coupled receptor characterized by a large leucine-rich extracellular domain and seven transmembrane domain (Haegebarth and Clevers, 2009).

In the intestine, *lgr5* is exclusively expressed in cycling crypt base columnar cells (Barker et al., 2007; Snippert et al., 2010). Genetic lineage-tracing experiments revealed that crypt base columnar cells are capable of self-renewal and multipotency, thus representing genuine intestinal stem cells. Expression of *lgr5* in multiple other organs indicates that it may represent a global marker of adult stem cells (Barker et al., 2007; Haegebarth and Clevers, 2009)

We have shown that *lgr5*-positive cells co-localized with proliferating areas in the AER during limb development (Fig. 38C), point to a role for *lgr5* in sustaining, together with *oct4*, the maintenance of a proliferating niche of cells at the base of the AER.

Thus we believe that *Lgr5* is a good candidate gene as a positive co-regulator of AER cells self-renewal, along with *oct4*.

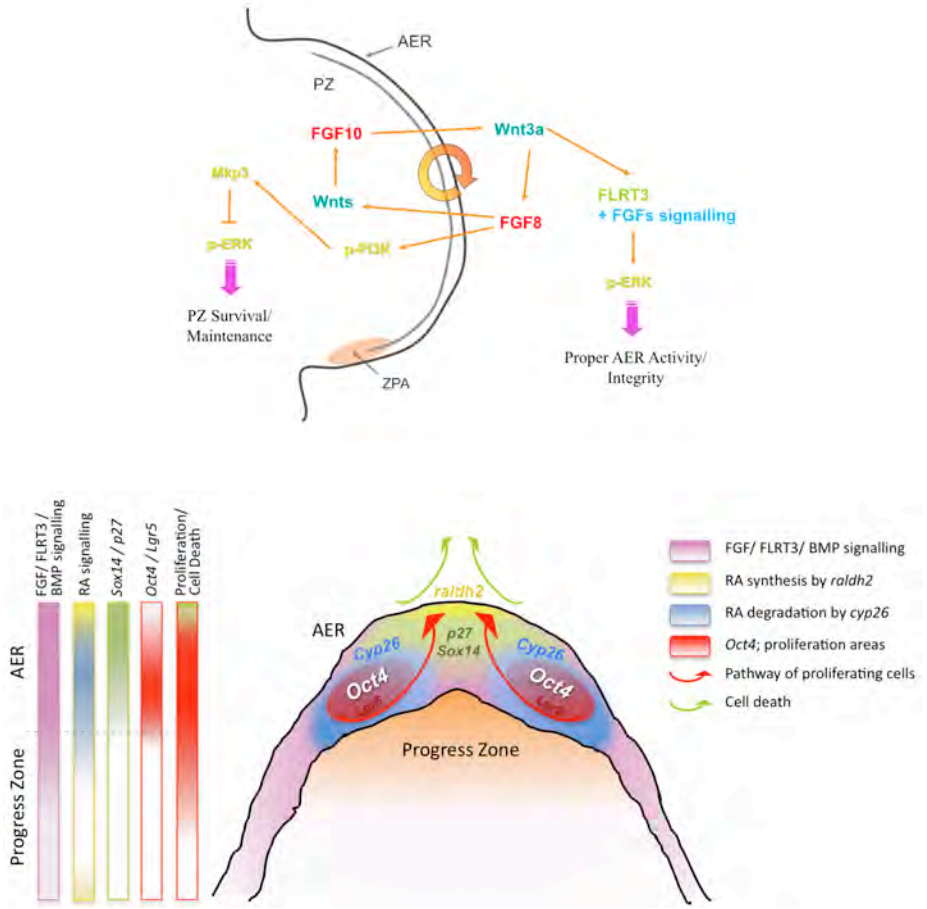

Figure 41. Proposed model for AER activity and renewal in *Gallus gallus* limb development.

VII Proposed model for AER activity and renewal and involved players

In conclusion, *flrt3* is a key player during chicken limb development. Gain and loss-of-function studies show that *flrt3* is necessary but not sufficient for proper AER formation and maintenance.

We propose a model (Fig. 41) in which FGF10 from the mesenchyme signals to the AER through *Wnt3a*, inducing FGF8 activity. In this model, Wnt3a will induce the expression of *flrt3* and FGF signalling, together with *flrt3* in the ectoderm, would activate ERK, maintaining, this way, AER integrity.

AER epithelial cell renewal would be sustained by two multipotent, non-committed, *oct4*-positive, cell populations at the base of the structure and running along the anterior-posterior axis of the limb, in constant proliferation. These cell populations would be nurtured by FGF, FLRT3 and WNT signalling, and protected in their niche from differentiation signals from BMP and RA. These cells possess a very short half-live and as they move towards the AER tip, they loose their stemness-like capability, differentiate, dye and leave the AER by anoikis. At the same time, a new batch of *oct4*-positive cells are dividing at the base and moving towards the top, assuring the AER maintenance.

Simultaneously, at the underlying mesenchyme, FGF8 signals through PI3K, inducing expression of *mkp3* and, thus, promoting survival of progress zone mesenchymal cells.

CONCLUSIONS

- *Flrt3* expression during limb development is restricted to the AER and coincides with that of *fgf8* and pERK activity.
- *Flrt3* is necessary but not sufficient for proper AER formation and maintenance.
- *Flrt3* expression is not regulated by FGF activity, although ectopic *Wnt3a* is able to induce *flrt3*; BMPs specifically inhibit *flrt3* in the AER.
- *Flrt3* regulate AER's BMP signalling through *gremlin.*
- AER renewal is very dynamic: cells proliferate at the base of the structure, both on the ventral and dorsal sides of the AER and all over its length, and as they move towards the AER's tip, they loose their stemness-like capability, differentiate, dye, loose contact to the extracellular matrix and leave the AER by anoikis. At the same time, a new batch of cells are dividing at the base and moving towards the top, assuring the AER maintenance
- At the AER, *oct4* expression coincides with AER proliferation niches
- AER Cell Dynamic upon oct4 overexpression is altered: the recruitment for cells that will contribute for the AER or proliferation within AER cells is increased in *Oct4*-electroporated limbs; cell death is not affected
- FGF signalling is needed to maintain *oct4* expression in the AER
- The canonical WNT, WNT3A, controls oct4 expression in the AER
- BMPs and RA negatively regulate *oct4* expression
- *Cyp26, Sox14, $p27^{Kip1}$, Lgr5* might be candidate genes for *oct4* co-regulators of AER renewal

MATERIALS AND METHODS

I Embryo Models

Most of the experiments carried out in this thesis work were performed in chick embryos. However, zebrafish embryos were used to perform a comparative expression pattern analysis during limb development and therefore used in the corresponding developmental stage range.

All experimental procedures were carried out following protocols approved by the CMRB (Center of Regenerative Medicine in Barcelona) and IGC (Instituto Gulbenkian de Ciência) ethical committees.

I.1 Staging, collection and processing of the biological material

The zebrafish embryos were wildtype AB kept and bred under standard conditions at 28ºC. Embryos were staged and fixed at specific hours post-fertilization (hpf) as described in (Kimmel et al., 1995)

To facilitate visualization of *in situ* hybridisations, 0.2 mM phenylthiourea (PTU) was added to the embryo media at approximately 24hpf to block pigment formation. For the purpose of this work were studied from ~10hpf to 3 1/2 days.

Chicken (Gallus gallus) eggs were supplied by a local farm. Eggs were incubated at 37,5ºC and 40% humidity. Chicken embryos used in this work ranged from stages 10 to stages 31 and were classified according to Hamburger and Hamilton (HH) stage series (Hamburger and Hamilton, 1951; Hamburger and Hamilton, 1992)(See annex II).

Chicken embryos were collected in cold PBS, and depending on the stage of the embryos, embryonic membranes were removed, heads pierced and guts removed (from chicken embryos above stage 20HH).

All embryos used for ISH were fixed overnight (ON) in paraformaldeyde (PFA 4%) in phosphate buffered saline (PBS; pH7.4) at 4ºC. After fixation embryos were

dehydrated in crescent serie of Methanol (MetOH) solutions in PBT, until 100% MetOH and then stored at -20ºC for at least 6 hours prior use.

Embryos used for immunohistochemistry studies were only fixed for 2h in 4%PFA and then stored appropriately, according to the protocols to use.

II Cloning of full-length and dsRNA constructs

II.1.1 Full-length *flrt3*

Full-length *flrt3* (XM_426107) was obtained after a two-step PCR amplification of chicken RNA collected from embryos at stage 14, 21 and 25 HH using High Fidelity PCR Master kit (Roche) and subsequent cloning into an empty modified expression vector, pCAGGS-PL4 (provided by A. Raya). The following primers were used for PCR amplification: PA (FW), 5'-ATGGCAACCATCACAAAATTTACTC-3'; PB (RV), 5'-TCATGAGTGTGAATGATCTGAATCTGG-3'; P1 (FW), 5'-CCA CGGATTAGGAGACAAGG-3'; P2 (RV), 5'-GCTGAGTTATGTTGTCCAGG-3'.

Briefly, PCR products PA+P2 (1239 bp, RI) and P1+PB (1289 bp, RII) sharing a common middle part with a *HindIII* restriction site, were cloned into pGEM®-T easy (Promega) and pCR®II-TOPO® (Invitrogen™), respectively. RII was extracted from pCR®II-TOPO® with *HindIII* and subcloned into RI's pGEM®-T easy. Full-length *flrt3*, RI+RII, was finally excised with *NotI* from and subcloned into an empty modified expression vector, pCAGGS-PL4 (provided by A. Raya).

Successful cloning at all steps was confirmed by DNA sequencing.

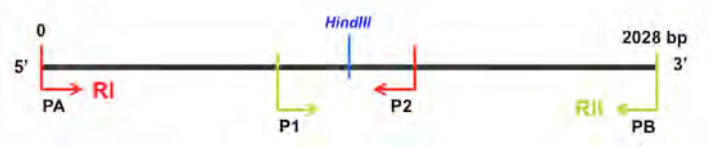

Figure 42. Schematic representation of full-length *flrt3* cloning process.

II.1.2 Full-length *oct4*

Full-length *oct4* (XM_425352) was obtained by PCR amplification as for *flrt3,* and

cloned into pCR®II-TOPO® (Invitrogen™). The following primers were used for PCR amplification: *ClaI*-P1-FW, 5'-ATCGATATGCATGTAAAAGCC-3' and P2-RV, 5'-TTAGTGGCTGCTGTTGTTCATGG-3'. Successful cloning was confirmed by DNA sequencing. Full-length *oct4* was excised with *ClaI/XbaI* and directionally cloned into an empty modified expression vector pCAGGS (provided by A. Raya). Successful sub-cloning was confirmed by DNA sequencing.

II.1.3 dsRNA against *flrt3*

In several organisms, introduction of double-stranded RNA (dsRNA) has proven to be a powerful tool to suppress gene expression through a process known as RNA interference (RNAi) (Sharp, 1999). pSUPER RNAi system (oligoengine™) provides an expression vector that directs intracellular synthesis of short interfering RNAs (siRNA)-like transcripts. The resulting transcript of the recombinant vector is predicted to fold back on itself to form a 19–base pair stem-loop structure, wich is quicky cleaved in the cell to produce a functional siRNA (Brummelkamp et al., 2002).

According to the pSUPER RNAi manufacturer system, a unique 19-nt sequence derived from the mRNA transcript of the gene targeted for suppression was designed (through iRNAi software from Mekentosj Inc.) (Brummelkamp et al., 2002), and the following oligos containing *Bgl*II and *Hind*III sites, as well as the hairpin sequence, were assembled as described by the manufacturer (detailed protocol in annex III):

Forward primer, 5'-GATCCCCTTTCAGGCTACTGCTGCGATTCAAGAGATCG CAGCAGTAGCCTGAAATTTTTGGAAA-3';

Reverse primer, 5'-AGCTTTTCCAAAAATTTCAGGCTACTGCTGCGATCTCTT GAATCGCAGCAGTAGCCTGAAAGGG-3';

43,5% GC content; target sequence: 5'-AATTTCAGGCTACTGCTGCGATT-3'.

Briefly, pSUPER vector was linearized with BglII and HindIII, forward and reverse strands of the oligos containing the siRNA-expressing sequence targeting flrt3 were annealed and cloned into the vector. Competent bacteria were transformed with the

vector, and checked for presence of positive clones. After digestion with EcoRI and HindIII, positive clones will have a fragment approximately 360 bp in length. An empty pSUPER vector has a fragment of 300 bp. The presence of the correct insert was confirmed by DNA sequencing.

A mismatch RNAi (target sequence: 5'-AATTTCAGGCTAGATCTGTGGTT-3') was used as a control.

III Chicken Embryo Manipulation

Experimental manipulations of limb buds were performed always in the right wing leaving the left one as a control. Upon manipulation, eggs were sealed with tape, incubated for different periods of time and treated for further processing.

III.1 Bead implantation

Ion exchange (AG1-X2, Bio-Rad) or heparin acrylic beads (Sigma®) were washed in DMSO and PBS with 0.1% BSA, respectively, and then incubated in the selected molecule. Retinoic acid was absorbed in AG1-X2 microspheres at 50 µg/ml as described previously (Helms et al., 1994). AG1-X2 beads were soaked in the FGF receptor kinase inhibitor SU5402 (Calbiochem), at a final concentration of 2 µg/µl in DMSO. The remaining proteins used in this work were embedded in heparin acrylic beads at the following concentrations: FGF2, FGF8, FGF10 and FGF19 at 1 µg/µl; BMP2, BMP4, WNT3A at 0.1 µg/µl; Beads were implanted into stage 19-21 HH developing chick limb buds as described previously (Montero et al., 2001).

Briefly, eggs were windowed at the desired stages and the right limb bud was exposed. Beads, ranging between 100 and 200µm in diameter, incubated in the different factors (1 hour at room temperature) or in PBS with 0.1% BSA or DMSO (controls) were implanted into the anterior margin mesoderm of the chick wing bud, close to the AER. RA and SU5402 beads were kept protected from the light.

III.2 Electroporation of limb ectoderm

Loss-of-function studies were achieved by co-electroporation of both pCAGGS-AGFP and dsRNA-*flrt3*. Gain-of-function studies were achieved by co-electroporation of both pCAGGS-AGFP and pCAGGS-*flrt3*; pCAGGS-AGFP and pCAGGS-*oct4*. A mix of 0.1% Fast Green (Sigma®), 1 µg/µl of pCAGGS-AGFP and 5 µg/µl of dsRNA-*flrt3* or pCAGGS-*oct4* was prepared.

In both experiments, controls with single electroporation of a GFP expression vector (a kindly gift from A. Tavares), pCAGGS-AGFP were performed.

Eggs were allowed to cool down to room temperature before starting the procedure. Eggshell was swabbed with 70% ethanol and a small window opened (2 cm^2) overlying the embryo. The viteline membrane above the limb field was carefully torn off with fine tweezers and the right-dorsal surface of the lateral plate mesoderm was covered with the DNA or dsRNA mix, using a borosilicate glass capilar (Kwik Fil™-

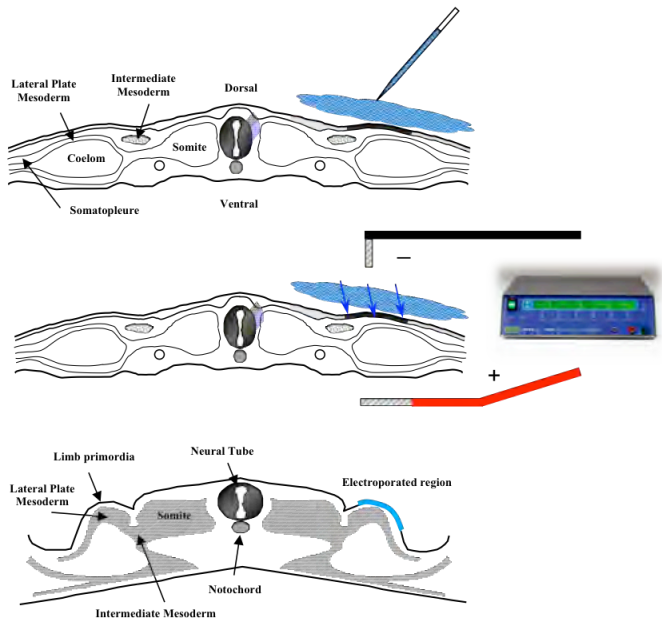

Figure 43. Schematic representation of the electroporation procedure and expected result. Injection and electroporation of RNAi and GFP plasmids. Region of the lateral plate mesoderm expected to be transfected.

WPI) coupled to a mouth pipette. Electrodes were placed in position over and under the prospective limb, in a parallel position to each other and to the neural tube with the negative electrode over the embryo. The DNA will be driven into the surface ectoderm of the prospective limb. Electroporation was performed with an Intracel TSS20 Ovodyne electroporator (Intracel LTD) using 3 pulses of 50 ms length (8 V each) with 60 ms interval. A drop of PBS/0,1% Pen/Strep was applied. Eggs were sealed with clear tape, incubated for the desired period of time and then fixed as previously described.

IV *In situ* hybridisation

IV.1 Probes

Probes for *flrt2*, *flrt3*, *fgf8*, *en*-1, *msx1, lmx-1, lgr5, sox14, p27, cyp26* and *raldh2* were obtained from chicken ESTs as shown in the table below, from Geneservice (Boardman et al., 2002). *Mkp3, gremlin* and *sox9* were obtained as previously described (Merino et al., 1999; Chimal-Monroy et al., 2003; Kawakami et al., 2003).

Probe	Reference	Enzime	Pol. for AS
flrt2	ChEST873n14	NotI	T3
cflrt3	ChEST840j5	NotI	T3
zflrt3	Cloning	SalI	T7
oct4	Cloning	Ecl136II	T3
fgf8	ChEST320b9	NotI	T3
en-1	ChEST92p12	NotI	T3
msx1	ChEST660e20	KpnI	T7
lmx-1	ChEST100c17	NotI	T3
lgr5	ChEST999g16	NotI	T3
sox14	ChEST847i12	NotI	T3
p27	ChEST639l15	NotI	T3
cyp26	ChEST423d23	NotI	T3
raldh2	ChEST819m8	NotI	T3
mkp3	Kawakami et al., 2003	XhoI	T3
gremlin	Merino et al., 1999	NcoI	T7
sox9	Chimal-Monroy et al., 2003	NotI	T3

Table 4 - Probes used: linearization enzyme and polymerase required for transcription of antisense probe

IV.1.1 Cloning of the zebrafish *flrt3* probe

Total RNA was isolated from 24 hpf and 48 hpf embryos using Trizol reagent (Invitrogen) according to manufacturer's instructions. cDNA was synthesised using the 1st Stand cDNA Synthesis Kit for RT-PCR (AMV) (Roche) using Random Primer p(dN)6. An 817 bp fragment generated by PCR amplification of cDNA with primers z*flrt3*fw (5´-GGTTCTGGATGGCAACCTCC-3´) and z*flrt3*rv (5'-CCAGCTTTAGCCAACTGAGC-3') was cloned into pGEM®-T easy (Promega). The sequence was confirmed by nucleotide sequencing.

IV.1.2 Cloning of the chicken *oct4* probe

Full length *oct4* was excised from pCAGGS and subcloned into pBluescript II KS(+) (Stratagene) to be able to produce both sense and antisense probes.

IV.2 Protocols

In situ and double *in situ* hybridization were performed as described (Schulte-Merker et al., 1992; Wilkinson, 1992; Pott and Fuss, 1995; Furthauer et al., 2002; Thisse and Thisse, 2008)(See annex III for detailed protocols used for chicken and zebrafish). Several Proteinase K digestion times were used to access the optimum one for each stage. Specific labelling was controlled using sense RNA probes. Alkaline phosphatase reactions were developed using BM Purple (Roche) substrate.

For chicken double *in situ* hybridisation, both digoxigenin- and fluorescein-labeled probes, synthesized according to standard protocols, were added simultaneously at day one. After developing one of the probes with BM Purple, the reaction was stopped in PBT, the embryos incubated with MABT without levamisole at 70ºC for 1 hour to stop alkaline phosphatase activity and then soaked in pre-antibody blocking for 30 minutes. The antibody against the second probe was then added, and the protocol followed as for the first probe, except for the alkaline phosphatase substrate. INT/BCIP (Roche) was used as manufacturer's description.

V Cryopreservation and sectioning

Chicken embryos were fixed as described above and cryoprotected in 10% sucrose in PBS overnight at 4ºC. Embryos were then embedded in 30% gelatine in the previous solution for 1 h at 37ºC, oriented as desired into cryomolds and snap-frozen at -80ºC. Cryosections of 10-12 µm were placed into pre-coated slides and processed for immunostaining.

Sections of embryos that had undergone *in situ* hybridisation were also performed, at 20-25µm, mounted in Aquatex medium and analysed under a microscope.

VI Immunohistochemistry

Single or double immunohistochemistry for laminin (Sigma; 1:300) and FLRT3 (MAB, R&D Systems; 1:150) was performed using the manufacturer's recommended dilutions, and following standard protocols for immunohistochemistry in sections.

Briefly, tissue sections were dried at room temperature for 30 minutes and gelatine was removed by heat (37ºC) in PBS and then rinsed in TBS. The tissue was permeabilized with 0.5% Triton, 3% heat inactivated goat serum in TBS for 30 min, and incubated with the primary antibody/antibodies. Primary antibodies were incubated overnight at 4ºC, and ALEXA-conjugated (Invitrogen™) secondary antibodies were incubated for 1 h at 37°C. Staining with Propidium Iodide or DAPI for DNA were carried out following standard procedures at a final dilution of 1.5 mM and 1.5 µg/ml, respectively.

Antibody	Specie	Dilution	Brand - Ref.
MAB FLRT3	Mouse	1:150	R&D AF2795
Phospho Histone H3	Rabbit	1:100	Upstate 06-570
Phospho Histone H3	Rat	1:100	Sigma H9908
Laminin	Rabbit	1:300	Sigma L9393

Table 5 - Primary antibodies

VII Proliferation assays

VII.1 Phospho-Histone H3

Chicken embryos were fixed, cryoprotected, and sectioned as described above. Immunohistochemistry for phospho-Histone H3 (Ser10) (UpState #06-570 (rabbit); 1:100 and Sigma H9908 (rat), 1:100) was performed according to the manufacturer's protocols for dilutions, and following standard protocols for immunohistochemistry in sections and whole-mount. Staining with Propidium Iodide or DAPI for DNA was carried out as described above.

VII.2 BrdU incorporation and detection

Eggs were windowed and 100 µl of 5-bromodeoxyuridine (BrdU) solution (100 µg/µl) were pipetted directly on top of stage 20-21HH embryos. Subsequently, eggs were sealed and incubated for 30 minutes, 45 minutes, 1, 5, 7, 18, and 24 hours at 37.5°C. Embryos were fixed and then processed for cryosectioning and imunohistochemistry as previously described. BrdU incorporation was detected using Roche 5-Bromo-2′-Deoxy-Uridine Labelling and Detection Kit I according to the manufacturer's instructions, incorporation some minor changes. Briefly, tissues were treated with Citrate Buffer pH 6 for 10 minutes at 96-99ºC and allowed to cool on $_{dd}H_2O$. They were then washed twice in TBS for five minutes and incubated in 0.5% Triton, 3% heat inactivated goat serum in TBS for 30 min. The anti-BrdU antibody, diluted in its own nucleases-containing buffer, was incubated overnight at 4ºC. Detection of BrdU by a specific antibody conjugated to fluorescein was performed by incubating sections for 1 h at 37°C. An Alexa Fluor® 488 labeled anti-Fluorescein/Oregon Green® goat IgG antibody (Invitrogen™) was used to enhance the green-fluorescent signal. Slides were then washed in TBS, counterstained with Propidium iodide and mounted.

VIII Cell Death assays

In Situ Cell Death Detection Kit POD, TMR red or Fluorescein from Roche Diagnostics, was used according to manufacturer's instructions and standard imunostaining protocols. Whole-mount and in sections' terminal deoxynucleotidyl transferase-mediated deoxyuridinetriphosphate nick end-labeling (TUNEL) assays were performed as previously described (Kanzler et al., 2000).

VIII.1 In sections

After the removal of gelatine from the tissue, the slides were first washed two times in Tris buffered saline (TBS) for 10 minutes before they were permeabilised in TBS plus 0.02% Triton and 0.05% tween-20 for 30 minutes at RT. They were then washed twice in TBS for five minutes, incubated in 10 mM Tris-HCl plus 5 mM EDTA at pH 8 for 5 minutes before proteinase K treatment (20 µg/ml) in the same Tris buffer as before for 15 minutes. Two washes in 5 mM EDTA for five minutes were followed by incubation in the TdT buffer (25 mM Tris-HCl, 200 mM Sodium Cacodylate, 1mM Cobalt Chloride) pH7.75 for 10 minutes to equilibrate for the TUNEL reaction.

For the TUNEL reaction (2 h at 37°C), and according to the experiment, the *In Situ* Cell Death Detection Kit POD, TMR red or Fluorescein from Roche Diagnostics, Barcelona, Spain was used according to manufacturer's instruction with an enhancement step: an anti-fluorescein antibody POD conjugated and 3,3'-Diaminobenzidine (DAB) or an Alexa Fluor® 488 labeled anti-fluorescein/Oregon Green® goat IgG antibody was used, accordingly, to enhance the signal.

For single TUNEL detections, slides were washed in TBS, counterstained with DAPI and mounted. If an imunostaining step should follow, sections were to be washed in Saline- sodium citrate (SSC) plus EDTA buffer twice for 10 minutes to stop the TUNEL reaction, followed by two washes in TBS for 10 minutes.

VIII.2 Wholemount

Limbs were treated as previously described for in situ hybridisation until the post-fixation step. The tissues were then treated with 0.1% Sodium Borohydride, rocking at RT for 30 minutes, prior the incubation in the TUNEL reaction mixture for 2 hours at 37ºC. Depending on the experiment, an anti-fluorescein antibody POD conjugate and 3,3'-Diaminobenzidine (DAB) was used, or an Alexa Fluor® 488 labeled anti-fluorescein/Oregon Green® goat IgG antibody was used to enhance the green-fluorescent signal (Kanzler et al., 2000).

In TUNEL plus Proliferation assays, after TUNEL reaction, tissues were washed in TBS, blocked for 30 minutes in 0.5% Triton, 3% heat inactivated goat serum in TBS, and incubated overnight at 4ºC with anti-phospho-H3 antibody. Samples were washed every other hour in 0.1% Triton, 3% heat inactivated goat serum in TBS, and then incubated overnight with secondary antibody and ribonuclease A (10 µg/ml) if TO-PRO 3 (Molecular Probes, 1:1000) was to be used for nuclear staining.

IX Imaging

Imaging of sections/wholemount embryos were performed with a standard Leica Fluorescent microscope or a Leica SP5A OBS confocal microscope using DPSS (diode-pumped solid-state lasers), argon, blue diode and HeNe lasers, and analysed using LAS AF software from Leica Microsystems and/or ImageJ.

X Alcian green cartilage staining

Chicken embryos were also examined by Alcian green cartilage staining as described (Ganan et al., 1996). Briefly, embryos were sacrificed, fixed in 5% trichloroacetic acid overnight at RT and stained with 0.1% Alcian green for another ON. The embryos were then cleared from alcian green remains in alcohol acid solution (0,1N HCl in 70% Ethanol) and dehydrated with absolute ethanol. Finally, the embryos were cleared in methyl salicylate.

XI Scanning Electron Microscopy

Chicken embryos were fixed in 2.5% glutaraldehyde/cacodylate buffer (0.1 M, pH 7.4) for 4 h at 4°C, washed three times in cacodylate buffer, and subsequently processed for critical point and sputtering following standard procedures. Sputtering of limbs buds was performed for 4 minutes. Imaging was performed in a JEOL JSM 6390LV scanning microscope.

REFERENCES

Aasen, T., Raya, A., Barrero, M. J., Garreta, E., Consiglio, A., Gonzalez, F., Vassena, R., Bilic, J., Pekarik, V., Tiscornia, G. et al. (2008). Efficient and rapid generation of induced pluripotent stem cells from human keratinocytes. *Nat Biotechnol* **26**, 1276-1284.

Ahn, K., Mishina, Y., Hanks, M. C., Behringer, R. R. and Crenshaw, E. B., 3rd. (2001). BMPR-IA signaling is required for the formation of the apical ectodermal ridge and dorsal-ventral patterning of the limb. *Development* **128**, 4449-4461.

Altabef, M. and Tickle, C. (2002). Initiation of dorso-ventral axis during chick limb development. *Mech Dev* **116**, 19-27.

Aoi, T., Yae, K., Nakagawa, M., Ichisaka, T., Okita, K., Takahashi, K., Chiba, T. and Yamanaka, S. (2008). Generation of pluripotent stem cells from adult mouse liver and stomach cells. *Science* **321**, 699-702.

Avilion, A. A., Nicolis, S. K., Pevny, L. H., Perez, L., Vivian, N. and Lovell-Badge, R. (2003). Multipotent cell lineages in early mouse development depend on SOX2 function. *Genes Dev* **17**, 126-140.

Bai, H., Gao, Y., Arzigian, M., Wojchowski, D. M., Wu, W. S. and Wang, Z. Z. (2010). BMP4 regulates vascular progenitor development in human embryonic stem cells through a Smad-dependent pathway. *J Cell Biochem* **109**, 363-374.

Barker, N., van Es, J. H., Kuipers, J., Kujala, P., van den Born, M., Cozijnsen, M., Haegebarth, A., Korving, J., Begthel, H., Peters, P. J. et al. (2007). Identification of stem cells in small intestine and colon by marker gene Lgr5. *Nature* **449**, 1003-1007.

Barrow, J. R., Thomas, K. R., Boussadia-Zahui, O., Moore, R., Kemler, R., Capecchi, M. R. and McMahon, A. P. (2003). Ectodermal Wnt3/beta-catenin signaling is required for the establishment and maintenance of the apical ectodermal ridge. *Genes Dev* **17**, 394-409.

Benazet, J. D. and Zeller, R. (2009). Vertebrate limb development: moving from classical morphogen gradients to an integrated 4-dimensional patterning system. *Cold Spring Harb Perspect Biol* **1**, a001339.

Berggren, K., McCaffery, P., Drager, U. and Forehand, C. J. (1999). Differential distribution of retinoic acid synthesis in the chicken embryo as determined by immunolocalization of the retinoic acid synthetic enzyme, RALDH-2. *Dev Biol* **210**, 288-304.

Berggren, K., Ezerman, E. B., McCaffery, P. and Forehand, C. J. (2001). Expression and regulation of the retinoic acid synthetic enzyme RALDH-2 in the embryonic chicken wing. *Dev Dyn* **222**, 1-16.

Boardman, P. E., Sanz-Ezquerro, J., Overton, I. M., Burt, D. W., Bosch, E., Fong, W. T., Tickle, C., Brown, W. R., Wilson, S. A. and Hubbard, S. J. (2002). A comprehensive collection of chicken cDNAs. *Curr Biol* **12**, 1965-1969.

Bottcher, R. T., Pollet, N., Delius, H. and Niehrs, C. (2004). The transmembrane protein XFLRT3 forms a complex with FGF receptors and promotes FGF signalling. *Nat Cell Biol* **6**, 38-44.

Boulet, A. M., Moon, A. M., Arenkiel, B. R. and Capecchi, M. R. (2004). The roles of Fgf4 and Fgf8 in limb bud initiation and outgrowth. *Dev Biol* **273**, 361-372.

Bowles, J., Schepers, G. and Koopman, P. (2000). Phylogeny of the SOX family of developmental transcription factors based on sequence and structural indicators. *Dev Biol* **227**, 239-255.

Brent, A. E. and Tabin, C. J. (2004). FGF acts directly on the somitic tendon progenitors through the Ets transcription factors Pea3 and Erm to regulate scleraxis expression. *Development* **131**, 3885-3896.

Brummelkamp, T. R., Bernards, R. and Agami, R. (2002). A system for stable expression of short interfering RNAs in mammalian cells. *Science* **296**, 550-553.

Bryant, S. V., Endo, T. and Gardiner, D. M. (2002). Vertebrate limb regeneration and the origin of limb stem cells. *Int J Dev Biol* **46**, 887-896.

Bryja, V., Pachernik, J., Soucek, K., Horvath, V., Dvorak, P. and Hampl, A. (2004). Increased apoptosis in differentiating p27-deficient mouse embryonic stem cells. *Cell Mol Life Sci* **61**, 1384-1400.

Bueno, D., Skinner, J., Abud, H. and Heath, J. K. (1996). Spatial and temporal relationships between Shh, Fgf4, and Fgf8 gene expression at diverse signalling centers during mouse development. *Dev Dyn* **207**, 291-299.

Canon, S., Herranz, C. and Manzanares, M. (2006). Germ cell restricted expression of chick Nanog. *Dev Dyn* **235**, 2889-2894.

Capdevila, J. and Izpisua Belmonte, J. C. (2001). Patterning mechanisms controlling vertebrate limb development. *Annu Rev Cell Dev Biol* **17**, 87-132.

Capdevila, J., Tabin, C. and Johnson, R. L. (1998). Control of dorsoventral somite patterning by Wnt-1 and beta-catenin. *Dev Biol* **193**, 182-194.

Capdevila, J., Tsukui, T., Rodriquez Esteban, C., Zappavigna, V. and Izpisua Belmonte, J. C. (1999). Control of vertebrate limb outgrowth by the proximal factor Meis2 and distal antagonism of BMPs by Gremlin. *Mol Cell* **4**, 839-849.

Carl, M. and Wittbrodt, J. (1999). Graded interference with FGF signalling reveals its dorsoventral asymmetry at the mid-hindbrain boundary. *Development* **126**, 5659-5667.

Carrington, J. L. and Fallon, J. F. (1984). The stages of flank ectoderm capable of responding to ridge induction in the chick embryo. *J Embryol Exp Morphol* **84**, 19-34.

Chambers, D. and Mason, I. (2000). Expression of sprouty2 during early development of the chick embryo is coincident with known sites of FGF signalling. *Mech Dev* **91**, 361-364.

Chambers, I., Colby, D., Robertson, M., Nichols, J., Lee, S., Tweedie, S. and Smith, A. (2003). Functional expression cloning of Nanog, a pluripotency sustaining factor in embryonic stem cells. *Cell* **113**, 643-655.

Chen, D., Ji, X., Harris, M. A., Feng, J. Q., Karsenty, G., Celeste, A. J., Rosen, V., Mundy, G. R. and Harris, S. E. (1998). Differential roles for bone morphogenetic protein (BMP) receptor type IB and IA in differentiation and specification of mesenchymal precursor cells to osteoblast and adipocyte lineages. *J Cell Biol* **142**, 295-305.

Chew, J. L., Loh, Y. H., Zhang, W., Chen, X., Tam, W. L., Yeap, L. S., Li, P., Ang, Y. S., Lim, B., Robson, P. et al. (2005). Reciprocal transcriptional regulation of Pou5f1 and Sox2 via the Oct4/Sox2 complex in embryonic stem cells. *Mol Cell Biol* **25**, 6031-6046.

Chiang, C., Litingtung, Y., Harris, M. P., Simandl, B. K., Li, Y., Beachy, P. A. and Fallon, J. F. (2001). Manifestation of the limb prepattern: limb development in the absence of sonic hedgehog function. *Dev Biol* **236**, 421-435.

Chiarugi, P. and Giannoni, E. (2008). Anoikis: a necessary death program for anchorage-dependent cells. *Biochem Pharmacol* **76**, 1352-1364.

Chimal-Monroy, J., Rodriguez-Leon, J., Montero, J. A., Ganan, Y., Macias, D., Merino, R. and Hurle, J. M. (2003). Analysis of the molecular cascade responsible for mesodermal limb chondrogenesis: Sox genes and BMP signaling. *Dev Biol* **257**, 292-301.

Christofori, G. (2003). Split personalities: the agonistic antagonist Sprouty. *Nat Cell Biol* **5**, 377-379.

Cohn, M. J., Izpisua-Belmonte, J. C., Abud, H., Heath, J. K. and Tickle, C. (1995). Fibroblast growth factors induce additional limb development from the flank of chick embryos. *Cell* **80**, 739-746.

Cohn, M. J., Patel, K., Krumlauf, R., Wilkinson, D. G., Clarke, J. D. and Tickle, C. (1997). Hox9 genes and vertebrate limb specification. *Nature* **387**, 97-101.

Corson, L. B., Yamanaka, Y., Lai, K. M. and Rossant, J. (2003). Spatial and temporal patterns of ERK signaling during mouse embryogenesis. *Development* **130**, 4527-4537.

Crossley, P. H., Minowada, G., MacArthur, C. A. and Martin, G. R. (1996). Roles for FGF8 in the induction, initiation, and maintenance of chick limb development. *Cell* **84**, 127-136.

De Luca, F., Uyeda, J. A., Mericq, V., Mancilla, E. E., Yanovski, J. A., Barnes, K. M., Zile, M. H. and Baron, J. (2000). Retinoic acid is a potent regulator of growth plate chondrogenesis. *Endocrinology* **141**, 346-353.

Delfini, M. C., De La Celle, M., Gros, J., Serralbo, O., Marics, I., Seux, M., Scaal, M. and Marcelle, C. (2009). The timing of emergence of muscle progenitors is controlled by an FGF/ERK/SNAIL1 pathway. *Dev Biol* **333**, 229-237.

Dikic, I. and Giordano, S. (2003). Negative receptor signalling. *Curr Opin Cell Biol* **15**, 128-135.

Drissi, H., Hushka, D., Aslam, F., Nguyen, Q., Buffone, E., Koff, A., van Wijnen, A., Lian, J. B., Stein, J. L. and Stein, G. S. (1999). The cell cycle regulator p27kip1 contributes to growth and differentiation of osteoblasts. *Cancer Res* **59**, 3705-3711.

Dudley, A. T., Ros, M. A. and Tabin, C. J. (2002). A re-examination of proximodistal patterning during vertebrate limb development. *Nature* **418**, 539-544.

Eblaghie, M. C., Lunn, J. S., Dickinson, R. J., Munsterberg, A. E., Sanz-Ezquerro, J. J., Farrell, E. R., Mathers, J., Keyse, S. M., Storey, K. and Tickle, C. (2003). Negative feedback regulation of FGF signaling levels by Pyst1/MKP3 in chick embryos. *Curr Biol* **13**, 1009-1018.

Egea, J., Erlacher, C., Montanez, E., Burtscher, I., Yamagishi, S., Hess, M., Hampel, F., Sanchez, R., Rodriguez-Manzaneque, M. T., Bosl, M. R. et al. (2008). Genetic ablation of FLRT3 reveals a novel morphogenetic function for the anterior visceral endoderm in suppressing mesoderm differentiation. *Genes Dev* **22**, 3349-3362.

Eiselleova, L., Matulka, K., Kriz, V., Kunova, M., Schmidtova, Z., Neradil, J., Tichy, B., Dvorakova, D., Pospisilova, S., Hampl, A. et al. (2009). A complex role for FGF-2 in self-renewal, survival, and adhesion of human embryonic stem cells. *Stem Cells* **27**, 1847-1857.

Fernandez-Teran, M. and Ros, M. A. (2008). The Apical Ectodermal Ridge: morphological aspects and signaling pathways. *Int J Dev Biol* **52**, 857-871.

Furthauer, M., Reifers, F., Brand, M., Thisse, B. and Thisse, C. (2001). sprouty4 acts in vivo as a feedback-induced antagonist of FGF signaling in zebrafish. *Development* **128**, 2175-2186.

Furthauer, M., Lin, W., Ang, S. L., Thisse, B. and Thisse, C. (2002). Sef is a feedback-induced antagonist of Ras/MAPK-mediated FGF signalling. *Nat Cell Biol* **4**, 170-174.

Furushima, K., Yamamoto, A., Nagano, T., Shibata, M., Miyachi, H., Abe, T., Ohshima, N., Kiyonari, H. and Aizawa, S. (2007). Mouse homologues of Shisa antagonistic to Wnt and Fgf signalings. *Dev Biol* **306**, 480-492.

Galloway, J. L., Delgado, I., Ros, M. A. and Tabin, C. J. (2009). A reevaluation of X-irradiation-induced phocomelia and proximodistal limb patterning. *Nature* **460**, 400-404.

Ganan, Y., Macias, D., Duterque-Coquillaud, M., Ros, M. A. and Hurle, J. M. (1996). Role of TGF beta s and BMPs as signals controlling the position of the digits and the areas of interdigital cell death in the developing chick limb autopod. *Development* **122**, 2349-2357.

Geetha-Loganathan, P., Nimmagadda, S., Huang, R., Scaal, M. and Christ, B. (2006). Expression pattern of BMPs during chick limb development. *Anat Embryol (Berl)* **211 Suppl 1**, 87-93.

Gibert, Y., Gajewski, A., Meyer, A. and Begemann, G. (2006). Induction and prepatterning of the zebrafish pectoral fin bud requires axial retinoic acid signaling. *Development* **133**, 2649-2659.

Gibson-Brown, J. J., Agulnik, S. I., Chapman, D. L., Alexiou, M., Garvey, N., Silver, L. M. and Papaioannou, V. E. (1996). Evidence of a role for T-box genes in the evolution of limb morphogenesis and the specification of forelimb/hindlimb identity. *Mech Dev* **56**, 93-101.

Gilbert, S. (2003). Developmental Biology. Sunderland, Massachusetts: Sinauer Associates, Inc.

Gong, S. G., Mai, S., Chung, K. and Wei, K. (2009). Flrt2 and Flrt3 have overlapping and non-overlapping expression during craniofacial development. *Gene Expr Patterns* **9**, 497-502.

Gotoh, N. (2009). Control of stemness by fibroblast growth factor signaling in stem cells and cancer stem cells. *Curr Stem Cell Res Ther* **4**, 9-15.

Gotoh, N., Ito, M., Yamamoto, S., Yoshino, I., Song, N., Wang, Y., Lax, I., Schlessinger, J., Shibuya, M. and Lang, R. A. (2004). Tyrosine phosphorylation sites on FRS2alpha responsible for Shp2 recruitment are critical for induction of lens and retina. *Proc Natl Acad Sci U S A* **101**, 17144-17149.

Grandel, H. and Schulte-Merker, S. (1998). The development of the paired fins in the zebrafish (Danio rerio). *Mech Dev* **79**, 99-120.

Guha, U., Gomes, W. A., Kobayashi, T., Pestell, R. G. and Kessler, J. A. (2002). In vivo evidence that BMP signaling is necessary for apoptosis in the mouse limb. *Dev Biol* **249**, 108-120.

Hacohen, N., Kramer, S., Sutherland, D., Hiromi, Y. and Krasnow, M. A. (1998). sprouty encodes a novel antagonist of FGF signaling that patterns apical branching of the Drosophila airways. *Cell* **92**, 253-263.

Haegebarth, A. and Clevers, H. (2009). Wnt signaling, lgr5, and stem cells in the intestine and skin. *Am J Pathol* **174**, 715-721.

Haines, B. P., Wheldon, L. M., Summerbell, D., Heath, J. K. and Rigby, P. W. (2006). Regulated expression of FLRT genes implies a functional role in the regulation of FGF signalling during mouse development. *Dev Biol* **297**, 14-25.

Hamburger, V. and Hamilton, H. L. (1951). A series of normal stages in the development of the chick embryo. *J. Morphol* **88**, 49-92.

Hamburger, V. and Hamilton, H. L. (1992). A series of normal stages in the development of the chick embryo. 1951. *Dev Dyn* **195**, 231-272.

Harfe, B. D., Scherz, P. J., Nissim, S., Tian, H., McMahon, A. P. and Tabin, C. J. (2004). Evidence for an expansion-based temporal Shh gradient in specifying vertebrate digit identities. *Cell* **118**, 517-528.

Hartenstein, V. (1993). Early pattern of neuronal differentiation in the Xenopus embryonic brainstem and spinal cord. *J Comp Neurol* **328**, 213-231.

He, X. C., Zhang, J., Tong, W. G., Tawfik, O., Ross, J., Scoville, D. H., Tian, Q., Zeng, X., He, X., Wiedemann, L. M. et al. (2004). BMP signaling inhibits intestinal stem cell self-renewal through suppression of Wnt-beta-catenin signaling. *Nat Genet* **36**, 1117-1121.

Helms, J., Thaller, C. and Eichele, G. (1994). Relationship between retinoic acid and sonic hedgehog, two polarizing signals in the chick wing bud. *Development* **120**, 3267-3274.

Hill, T. P., Spater, D., Taketo, M. M., Birchmeier, W. and Hartmann, C. (2005). Canonical Wnt/beta-catenin signaling prevents osteoblasts from differentiating into chondrocytes. *Dev Cell* **8**, 727-738.

Hochedlinger, K., Yamada, Y., Beard, C. and Jaenisch, R. (2005). Ectopic expression of Oct-4 blocks progenitor-cell differentiation and causes dysplasia in epithelial tissues. *Cell* **121**, 465-477.

Hough, S. R., Clements, I., Welch, P. J. and Wiederholt, K. A. (2006). Differentiation of mouse embryonic stem cells after RNA interference-mediated silencing of OCT4 and Nanog. *Stem Cells* **24**, 1467-1475.

Isaac, A., Rodriguez-Esteban, C., Ryan, A., Altabef, M., Tsukui, T., Patel, K., Tickle, C. and Izpisua-Belmonte, J. C. (1998). Tbx genes and limb identity in chick embryo development. *Development* **125**, 1867-1875.

Johnson, R. L. and Tabin, C. J. (1997). Molecular models for vertebrate limb development. *Cell* **90**, 979-990.

Kanzler, B., Foreman, R. K., Labosky, P. A. and Mallo, M. (2000). BMP signaling is essential for development of skeletogenic and neurogenic cranial neural crest. *Development* **127**, 1095-1104.

Karaulanov, E., Bottcher, R. T., Stannek, P., Wu, W., Rau, M., Ogata, S., Cho, K. W. and Niehrs, C. (2009). Unc5B interacts with FLRT3 and Rnd1 to modulate cell adhesion in Xenopus embryos. *PLoS One* **4**, e5742.

Karaulanov, E. E., Bottcher, R. T. and Niehrs, C. (2006). A role for fibronectin-leucine-rich transmembrane cell-surface proteins in homotypic cell adhesion. *EMBO Rep* **7**, 283-290.

Katoh, M. (2007). WNT signaling pathway and stem cell signaling network. *Clin Cancer Res* **13**, 4042-4045.

Kawakami, Y., Capdevila, J., Buscher, D., Itoh, T., Rodriguez Esteban, C. and Izpisua Belmonte, J. C. (2001). WNT signals control FGF-dependent limb initiation and AER induction in the chick embryo. *Cell* **104**, 891-900.

Kawakami, Y., Esteban, C. R., Matsui, T., Rodriguez-Leon, J., Kato, S. and Belmonte, J. C. (2004). Sp8 and Sp9, two closely related buttonhead-like transcription factors, regulate Fgf8 expression and limb outgrowth in vertebrate embryos. *Development* **131**, 4763-4774.

Kawakami, Y., Rodriguez-Leon, J., Koth, C. M., Buscher, D., Itoh, T., Raya, A., Ng, J. K., Esteban, C. R., Takahashi, S., Henrique, D. et al. (2003). MKP3 mediates the cellular response to FGF8 signalling in the vertebrate limb. *Nat Cell Biol* **5**, 513-519.

Kehler, J., Tolkunova, E., Koschorz, B., Pesce, M., Gentile, L., Boiani, M., Lomeli, H., Nagy, A., McLaughlin, K. J., Scholer, H. R. et al. (2004). Oct4 is required for primordial germ cell survival. *EMBO Rep* **5**, 1078-1083.

Kengaku, M., Capdevila, J., Rodriguez-Esteban, C., De La Pena, J., Johnson, R. L., Belmonte, J. C. and Tabin, C. J. (1998). Distinct WNT pathways regulating AER formation and dorsoventral polarity in the chick limb bud. *Science* **280**, 1274-1277.

Khokha, M. K., Hsu, D., Brunet, L. J., Dionne, M. S. and Harland, R. M. (2003). Gremlin is the BMP antagonist required for maintenance of Shh and Fgf signals during limb patterning. *Nat Genet* **34**, 303-307.

Kimmel, C. B., Ballard, W. W., Kimmel, S. R., Ullmann, B. and Schilling, T. F. (1995). Stages of embryonic development of the zebrafish. *Dev Dyn* **203**, 253-310.

Korinek, V., Barker, N., Moerer, P., van Donselaar, E., Huls, G., Peters, P. J. and Clevers, H. (1998). Depletion of epithelial stem-cell compartments in the small intestine of mice lacking Tcf-4. *Nat Genet* **19**, 379-383.

Koyama, E., Golden, E. B., Kirsch, T., Adams, S. L., Chandraratna, R. A., Michaille, J. J. and Pacifici, M. (1999). Retinoid signaling is required for chondrocyte maturation and endochondral bone formation during limb skeletogenesis. *Dev Biol* **208**, 375-391.

Kurose, H., Bito, T., Adachi, T., Shimizu, M., Noji, S. and Ohuchi, H. (2004). Expression of Fibroblast growth factor 19 (Fgf19) during chicken embryogenesis and eye development, compared with Fgf15 expression in the mouse. *Gene Expr Patterns* **4**, 687-693.

Lacy, S. E., Bonnemann, C. G., Buzney, E. A. and Kunkel, L. M. (1999). Identification of FLRT1, FLRT2, and FLRT3: a novel family of transmembrane leucine-rich repeat proteins. *Genomics* **62**, 417-426.

Lavial, F., Acloque, H., Bertocchini, F., Macleod, D. J., Boast, S., Bachelard, E., Montillet, G., Thenot, S., Sang, H. M., Stern, C. D. et al. (2007). The Oct4 homologue PouV and Nanog regulate pluripotency in chicken embryonic stem cells. *Development* **134**, 3549-3563.

Lee, J. T., Jr. and McCubrey, J. A. (2002). The Raf/MEK/ERK signal transduction cascade as a target for chemotherapeutic intervention in leukemia. *Leukemia* **16**, 486-507.

Lewandoski, M., Sun, X. and Martin, G. R. (2000). Fgf8 signalling from the AER is essential for normal limb development. *Nat Genet* **26**, 460-463.

Li, Y. Q. (2010). Master stem cell transcription factors and signaling regulation. *Cell Reprogram* **12**, 3-13.

Lim, J., Yusoff, P., Wong, E. S., Chandramouli, S., Lao, D. H., Fong, C. W. and Guy, G. R. (2002). The cysteine-rich sprouty translocation domain targets mitogen-activated protein

kinase inhibitory proteins to phosphatidylinositol 4,5-bisphosphate in plasma membranes. *Mol Cell Biol* **22**, 7953-7966.

Lin, W., Furthauer, M., Thisse, B., Thisse, C., Jing, N. and Ang, S. L. (2002). Cloning of the mouse Sef gene and comparative analysis of its expression with Fgf8 and Spry2 during embryogenesis. *Mech Dev* **113**, 163-168.

Liu, A. and Joyner, A. L. (2001). Early anterior/posterior patterning of the midbrain and cerebellum. *Annu Rev Neurosci* **24**, 869-896.

Lizarraga, G., Ferrari, D., Kalinowski, M., Ohuchi, H., Noji, S., Kosher, R. A. and Dealy, C. N. (1999). FGFR2 signaling in normal and limbless chick limb buds. *Dev Genet* **25**, 331-338.

Logan, C., Hornbruch, A., Campbell, I., and Lumsden, A. . (1997). The role of of Engrailed in establishing the dorsoventral axis of the chick limb. *Development* **124**, 2317-2324.

Logan, M. (2003). Finger or toe: the molecular basis of limb identity. *Development* **130**, 6401-6410.

Loh, Y. H., Wu, Q., Chew, J. L., Vega, V. B., Zhang, W., Chen, X., Bourque, G., George, J., Leong, B., Liu, J. et al. (2006). The Oct4 and Nanog transcription network regulates pluripotency in mouse embryonic stem cells. *Nat Genet* **38**, 431-440.

Lonai, P. (2003). Epithelial mesenchymal interactions, the ECM and limb development. *J Anat* **202**, 43-50.

Loomis, C. A., Kimmel, R. A., Tong, C. X., Michaud, J. and Joyner, A. L. (1998). Analysis of the genetic pathway leading to formation of ectopic apical ectodermal ridges in mouse Engrailed-1 mutant limbs. *Development* **125**, 1137-1148.

Loomis, C. A., Kimmel, R. A., Michaud, J., Wurst, W., Hanks, M., and Joyner, A. L. (1996). The mouse Engrailed-1 gene and ventral limb patterning. *Nature* **382**, 360-363.

Lovicu, F. J. and McAvoy, J. W. (2001). FGF-induced lens cell proliferation and differentiation is dependent on MAPK (ERK1/2) signalling. *Development* **128**, 5075-5084.

Lunn, J. S., Fishwick, K. J., Halley, P. A. and Storey, K. G. (2007). A spatial and temporal map of FGF/Erk1/2 activity and response repertoires in the early chick embryo. *Dev Biol* **302**, 536-552.

Maatouk, D. M., Choi, K. S., Bouldin, C. M. and Harfe, B. D. (2009). In the limb AER Bmp2 and Bmp4 are required for dorsal-ventral patterning and interdigital cell death but not limb outgrowth. *Dev Biol* **327**, 516-523.

Maddika, S., Ande, S. R., Panigrahi, S., Paranjothy, T., Weglarczyk, K., Zuse, A., Eshraghi, M., Manda, K. D., Wiechec, E. and Los, M. (2007). Cell survival, cell death and cell cycle pathways are interconnected: implications for cancer therapy. *Drug Resist Updat* **10**, 13-29.

Mahmood, R., Bresnick, J., Hornbruch, A., Mahony, C., Morton, N., Colquhoun, K., Martin, P., Lumsden, A., Dickson, C. and Mason, I. (1995). A role for FGF-8 in the initiation and maintenance of vertebrate limb bud outgrowth. *Curr Biol* **5**, 797-806.

Maretto, S., Muller, P. S., Aricescu, A. R., Cho, K. W., Bikoff, E. K. and Robertson, E. J. (2008). Ventral closure, headfold fusion and definitive endoderm migration defects in mouse embryos lacking the fibronectin leucine-rich transmembrane protein FLRT3. *Dev Biol* **318**, 184-193.

Mariani, F. V. and Martin, G. R. (2003). Deciphering skeletal patterning: clues from the limb. *Nature* **423**, 319-325.

Marin, F. and Puelles, L. (1994). Patterning of the embryonic avian midbrain after experimental inversions: a polarizing activity from the isthmus. *Dev Biol* **163**, 19-37.

Marshman, E., Booth, C. and Potten, C. S. (2002). The intestinal epithelial stem cell. *Bioessays* **24**, 91-98.

Martin, G. R. (1998). The roles of FGFs in the early development of vertebrate limbs. *Genes Dev* **12**, 1571-1586.

Mason, I. (2007). Initiation to end point: the multiple roles of fibroblast growth factors in neural development. *Nat Rev Neurosci* **8**, 583-596.

McCabe, K. L., McGuire, C. and Reh, T. A. (2006). Pea3 expression is regulated by FGF signaling in developing retina. *Dev Dyn* **235**, 327-335.

McGlinn, E., van Bueren, K. L., Fiorenza, S., Mo, R., Poh, A. M., Forrest, A., Soares, M. B., Bonaldo Mde, F., Grimmond, S., Hui, C. C. et al. (2005). Pax9 and Jagged1 act downstream of Gli3 in vertebrate limb development. *Mech Dev* **122**, 1218-1233.

McQueeney, K., Soufer, R. and Dealy, C. N. (2002). Beta-catenin-dependent Wnt signaling in apical ectodermal ridge induction and FGF8 expression in normal and limbless mutant chick limbs. *Dev Growth Differ* **44**, 315-325.

Mercader, N. (2007). Early steps of paired fin development in zebrafish compared with tetrapod limb development. *Dev Growth Differ* **49**, 421-437.

Mercader, N., Leonardo, E., Piedra, M. E., Martinez, A. C., Ros, M. A. and Torres, M. (2000). Opposing RA and FGF signals control proximodistal vertebrate limb development through regulation of Meis genes. *Development* **127**, 3961-3970.

Merino, R., Rodriguez-Leon, J., Macias, D., Ganan, Y., Economides, A. N. and Hurle, J. M. (1999). The BMP antagonist Gremlin regulates outgrowth, chondrogenesis and programmed cell death in the developing limb. *Development* **126**, 5515-5522.

Mic, F. A., Sirbu, I. O. and Duester, G. (2004). Retinoic acid synthesis controlled by Raldh2 is required early for limb bud initiation and then later as a proximodistal signal during apical ectodermal ridge formation. *J Biol Chem* **279**, 26698-26706.

Mima, T., Ohuchi, H., Noji, S. and Mikawa, T. (1995). FGF can induce outgrowth of somatic mesoderm both inside and outside of limb-forming regions. *Dev Biol* **167**, 617-620.

Minowada, G., Jarvis, L. A., Chi, C. L., Neubuser, A., Sun, X., Hacohen, N., Krasnow, M. A. and Martin, G. R. (1999). Vertebrate Sprouty genes are induced by FGF signaling and can cause chondrodysplasia when overexpressed. *Development* **126**, 4465-4475.

Mitsuhashi, T. and Takahashi, T. (2009). Genetic regulation of proliferation/differentiation characteristics of neural progenitor cells in the developing neocortex. *Brain Dev* **31**, 553-557.

Mitsui, K., Tokuzawa, Y., Itoh, H., Segawa, K., Murakami, M., Takahashi, K., Maruyama, M., Maeda, M. and Yamanaka, S. (2003). The homeoprotein Nanog is required for maintenance of pluripotency in mouse epiblast and ES cells. *Cell* **113**, 631-642.

Mohanty-Hejmadi, P., Dutta, S. K. and Mahapatra, P. (1992). Limbs generated at site of tail amputation in marbled balloon frog after vitamin A treatment. *Nature* **355**, 352-353.

Montero, J. A., Ganan, Y., Macias, D., Rodriguez-Leon, J., Sanz-Ezquerro, J. J., Merino, R., Chimal-Monroy, J., Nieto, M. A. and Hurle, J. M. (2001). Role of FGFs in

the control of programmed cell death during limb development. *Development* **128**, 2075-2084.

Movassagh, M. and Philpott, A. (2008). Cardiac differentiation in Xenopus requires the cyclin-dependent kinase inhibitor, p27Xic1. *Cardiovasc Res* **79**, 436-447.

Nakagawa, M., Koyanagi, M., Tanabe, K., Takahashi, K., Ichisaka, T., Aoi, T., Okita, K., Mochiduki, Y., Takizawa, N. and Yamanaka, S. (2008). Generation of induced pluripotent stem cells without Myc from mouse and human fibroblasts. *Nat Biotechnol* **26**, 101-106.

Naveiras, O. and Daley, G. Q. (2006). Stem cells and their niche: a matter of fate. *Cell Mol Life Sci* **63**, 760-766.

Naylor, R. W., Collins, R. J., Philpott, A. and Jones, E. A. (2009). Normal levels of p27 are necessary for somite segmentation and determining pronephric organ size. *Organogenesis* **5**, 201-210.

Nelson, C. E., Morgan, B. A., Burke, A. C., Laufer, E., DiMambro, E., Murtaugh, L. C., Gonzales, E., Tessarollo, L., Parada, L. F. and Tabin, C. (1996). Analysis of Hox gene expression in the chick limb bud. *Development* **122**, 1449-1466.

Nichols, J., Zevnik, B., Anastassiadis, K., Niwa, H., Klewe-Nebenius, D., Chambers, I., Scholer, H. and Smith, A. (1998). Formation of pluripotent stem cells in the mammalian embryo depends on the POU transcription factor Oct4. *Cell* **95**, 379-391.

Niederreither, K., Ward, S. J., Dolle, P. and Chambon, P. (1996). Morphological and molecular characterization of retinoic acid-induced limb duplications in mice. *Dev Biol* **176**, 185-198.

Niederreither, K., Vermot, J., Schuhbaur, B., Chambon, P. and Dolle, P. (2002). Embryonic retinoic acid synthesis is required for forelimb growth and anteroposterior patterning in the mouse. *Development* **129**, 3563-3574.

Niehrs, C. and Pollet, N. (1999). Synexpression groups in eukaryotes. *Nature* **402**, 483-487.

Niswander, L. (2003). Pattern formation: old models out on a limb. *Nat Rev Genet* **4**, 133-143.

Niswander, L., and Martin, G. R. Development (1992). Fgf-4 expression during gastrulation, myogenesis, limb and tooth development. **114** 755-768.

Niwa, H. (2007). How is pluripotency determined and maintained? *Development* **134**, 635-646.

Ogata, S., Morokuma, J., Hayata, T., Kolle, G., Niehrs, C., Ueno, N. and Cho, K. W. (2007). TGF-beta signaling-mediated morphogenesis: modulation of cell adhesion via cadherin endocytosis. *Genes Dev* **21**, 1817-1831.

Ohnuma, S., Philpott, A., Wang, K., Holt, C. E. and Harris, W. A. (1999). p27Xic1, a Cdk inhibitor, promotes the determination of glial cells in Xenopus retina. *Cell* **99**, 499-510.

Ohnuma, S., Hopper, S., Wang, K. C., Philpott, A. and Harris, W. A. (2002). Co-ordinating retinal histogenesis: early cell cycle exit enhances early cell fate determination in the Xenopus retina. *Development* **129**, 2435-2446.

Ohuchi, H., Nakagawa, T., Yamamoto, A., Araga, A., Ohata, T., Ishimaru, Y., Yoshioka, H., Kuwana, T., Nohno, T., Yamasaki, M. et al. (1997). The mesenchymal

factor, FGF10, initiates and maintains the outgrowth of the chick limb bud through interaction with FGF8, an apical ectodermal factor. *Development* **124**, 2235-2244.

Okamoto, K., Okazawa, H., Okuda, A., Sakai, M., Muramatsu, M. and Hamada, H. (1990). A novel octamer binding transcription factor is differentially expressed in mouse embryonic cells. *Cell* **60**, 461-472.

Okumura-Nakanishi, S., Saito, M., Niwa, H. and Ishikawa, F. (2005). Oct-3/4 and Sox2 regulate Oct-3/4 gene in embryonic stem cells. *J Biol Chem* **280**, 5307-5317.

Ong, S. H., Hadari, Y. R., Gotoh, N., Guy, G. R., Schlessinger, J. and Lax, I. (2001). Stimulation of phosphatidylinositol 3-kinase by fibroblast growth factor receptors is mediated by coordinated recruitment of multiple docking proteins. *Proc Natl Acad Sci U S A* **98**, 6074-6079.

Osterloh, J. M. and Freeman, M. R. (2009). Neuronal death or dismemberment mediated by Sox14. *Nat Neurosci* **12**, 1479-1480.

Pajni-Underwood, S., Wilson, C. P., Elder, C., Mishina, Y. and Lewandoski, M. (2007). BMP signals control limb bud interdigital programmed cell death by regulating FGF signaling. *Development* **134**, 2359-2368.

Panman, L. and Zeller, R. (2003). Patterning the limb before and after SHH signalling. *J Anat* **202**, 3-12.

Parr, B. A., and McMahon, A. P. (1995). Dorsalizing signal Wnt-7a required for normal polarity of D-V and A-P aves of mouse limb. *Nature* **374**, 350-353.

Pesce, M. and Scholer, H. R. (2001). Oct-4: gatekeeper in the beginnings of mammalian development. *Stem Cells* **19**, 271-278.

Pikarsky, E., Sharir, H., Ben-Shushan, E. and Bergman, Y. (1994). Retinoic acid represses Oct-3/4 gene expression through several retinoic acid-responsive elements located in the promoter-enhancer region. *Mol Cell Biol* **14**, 1026-1038.

Pizette, S. and Niswander, L. (1999). BMPs negatively regulate structure and function of the limb apical ectodermal ridge. *Development* **126**, 883-894.

Pizette, S., Abate-Shen, C. and Niswander, L. (2001). BMP controls proximodistal outgrowth, via induction of the apical ectodermal ridge, and dorsoventral patterning in the vertebrate limb. *Development* **128**, 4463-4474.

Popovic, J. and Stevanovic, M. (2009). Remarkable evolutionary conservation of SOX14 orthologues. *J Genet* **88**, 15-24.

Popovic, J., Klajn, A., Petrovic, I. and Stevanovic, M. (2010). Tissue-specific Forkhead protein FOXA2 up-regulates SOX14 gene expression. *Biochim Biophys Acta* **1799**, 411-418.

Pott, U. and Fuss, B. (1995). Two-color double in situ hybridization using enzymatically hydrolyzed nonradioactive riboprobes. *Anal Biochem* **225**, 149-152.

Potten, C. S., Gandara, R., Mahida, Y. R., Loeffler, M. and Wright, N. A. (2009). The stem cells of small intestinal crypts: where are they? *Cell Prolif* **42**, 731-750.

Powers, C. J., McLeskey, S. W. and Wellstein, A. (2000). Fibroblast growth factors, their receptors and signaling. *Endocr Relat Cancer* **7**, 165-197.

Raible, F. and Brand, M. (2001). Tight transcriptional control of the ETS domain factors Erm and Pea3 by Fgf signaling during early zebrafish development. *Mech Dev* **107**, 105-117.

Raible, F. and Brand, M. (2004). Divide et Impera--the midbrain-hindbrain boundary and its organizer. *Trends Neurosci* **27**, 727-734.

Rancourt, D. E., Tsuzuki, T. and Capecchi, M. R. (1995). Genetic interaction between hoxb-5 and hoxb-6 is revealed by nonallelic noncomplementation. *Genes Dev* **9**, 108-122.

Riddle, R. D., Jonhson, R. L., Laufer, E., and Tabin, C. . (1993). Sonic hedgehog mediates the polarizing activity of the ZPA. *Cell* **75**, 1041-1416.

Robinson, M., Parsons Perez, M. C., Tebar, L., Palmer, J., Patel, A., Marks, D., Sheasby, A., De Felipe, C., Coffin, R., Livesey, F. J. et al. (2004). FLRT3 is expressed in sensory neurons after peripheral nerve injury and regulates neurite outgrowth. *Mol Cell Neurosci* **27**, 202-214.

Rodriguez-Esteban, C., Tsukui, T., Yonei, S., Magallon, J., Tamura, K. and Izpisua Belmonte, J. C. (1999). The T-box genes Tbx4 and Tbx5 regulate limb outgrowth and identity. *Nature* **398**, 814-818.

Rodriguez-Leon, J., Merino, R., Macias, D., Ganan, Y., Santesteban, E. and Hurle, J. M. (1999). Retinoic acid regulates programmed cell death through BMP signalling. *Nat Cell Biol* **1**, 125-126.

Rodriguez-Leon, J., Rodriguez Esteban, C., Marti, M., Santiago-Josefat, B., Dubova, I., Rubiralta, X. and Izpisua Belmonte, J. C. (2008). Pitx2 regulates gonad morphogenesis. *Proc Natl Acad Sci U S A* **105**, 11242-11247.

Sandberg, M., Kallstrom, M. and Muhr, J. (2005). Sox21 promotes the progression of vertebrate neurogenesis. *Nat Neurosci* **8**, 995-1001.

Sato, N., Meijer, L., Skaltsounis, L., Greengard, P. and Brivanlou, A. H. (2004). Maintenance of pluripotency in human and mouse embryonic stem cells through activation of Wnt signaling by a pharmacological GSK-3-specific inhibitor. *Nat Med* **10**, 55-63.

Saunders J. W., J. (1948). The proximo-distal sequence of origin of the chick wing and the role of ectoderm. *J Exp Zool* **108**, 363-403.

Savage, M. P. and Fallon, J. F. (1995). FGF-2 mRNA and its antisense message are expressed in a developmentally specific manner in the chick limb bud and mesonephros. *Dev Dyn* **202**, 343-353.

Savatier, P., Lapillonne, H., van Grunsven, L. A., Rudkin, B. B. and Samarut, J. (1996). Withdrawal of differentiation inhibitory activity/leukemia inhibitory factor up-regulates D-type cyclins and cyclin-dependent kinase inhibitors in mouse embryonic stem cells. *Oncogene* **12**, 309-322.

Scherz, P. J., Harfe, B. D., McMahon, A. P. and Tabin, C. J. (2004). The limb bud Shh-Fgf feedback loop is terminated by expansion of former ZPA cells. *Science* **305**, 396-399.

Schoorlemmer, J., van Puijenbroek, A., van Den Eijnden, M., Jonk, L., Pals, C. and Kruijer, W. (1994). Characterization of a negative retinoic acid response element in the murine Oct4 promoter. *Mol Cell Biol* **14**, 1122-1136.

Schulte-Merker, S., Ho, R. K., Herrmann, B. G. and Nusslein-Volhard, C. (1992). The protein product of the zebrafish homologue of the mouse T gene is expressed in nuclei of the germ ring and the notochord of the early embryo. *Development (Cambridge, England)* **116**, 1021-1032.

Sekine, K., Ohuchi, H., Fujiwara, M., Yamasaki, M., Yoshizawa, T., Sato, T., Yagishita, N., Matsui, D., Koga, Y., Itoh, N. et al. (1999). Fgf10 is essential for limb and lung formation. *Nat Genet* **21**, 138-141.

Shaker, A. and Rubin, D. C. (2010). Intestinal stem cells and epithelial-mesenchymal interactions in the crypt and stem cell niche. *Transl Res* **156**, 180-187.

Sharp, P. A. (1999). RNAi and double-strand RNA. *Genes Dev* **13**, 139-141.

Sharrocks, A. D. (2001). The ETS-domain transcription factor family. *Nat Rev Mol Cell Biol* **2**, 827-837.

Sivak, J. M., Petersen, L. F. and Amaya, E. (2005). FGF signal interpretation is directed by Sprouty and Spred proteins during mesoderm formation. *Dev Cell* **8**, 689-701.

Smith, T. G. and Tickle, C. (2006). The expression of Flrt3 during chick limb development. *Int J Dev Biol* **50**, 701-704.

Snippert, H. J., van der Flier, L. G., Sato, T., van Es, J. H., van den Born, M., Kroon-Veenboer, C., Barker, N., Klein, A. M., van Rheenen, J., Simons, B. D. et al. (2010). Intestinal crypt homeostasis results from neutral competition between symmetrically dividing Lgr5 stem cells. *Cell* **143**, 134-144.

Soshnikova, N., Zechner, D., Huelsken, J., Mishina, Y., Behringer, R. R., Taketo, M. M., Crenshaw, E. B., 3rd and Birchmeier, W. (2003). Genetic interaction between Wnt/beta-catenin and BMP receptor signaling during formation of the AER and the dorsal-ventral axis in the limb. *Genes Dev* **17**, 1963-1968.

Spence, J. R., Madhavan, M., Aycinena, J. C. and Del Rio-Tsonis, K. (2007). Retina regeneration in the chick embryo is not induced by spontaneous Mitf downregulation but requires FGF/FGFR/MEK/Erk dependent upregulation of Pax6. *Mol Vis* **13**, 57-65.

Stavridis, M. P., Collins, B. J. and Storey, K. G. (2010). Retinoic acid orchestrates fibroblast growth factor signalling to drive embryonic stem cell differentiation. *Development* **137**, 881-890.

Stefanovic, S. and Puceat, M. (2007). Oct-3/4: not just a gatekeeper of pluripotency for embryonic stem cell, a cell fate instructor through a gene dosage effect. *Cell Cycle* **6**, 8-10.

Stratford, T., Horton, C. and Maden, M. (1996). Retinoic acid is required for the initiation of outgrowth in the chick limb bud. *Curr Biol* **6**, 1124-1133.

Stratford, T. H., Kostakopoulou, K. and Maden, M. (1997). Hoxb-8 has a role in establishing early anterior-posterior polarity in chick forelimb but not hindlimb. *Development* **124**, 4225-4234.

Summerbell, D. (1974). A quantitative analysis of the effect of excision of the AER from the chick limb-bud. *J Embryol Exp Morphol* **32**, 651-660.

Summerbell, D., Lewis, J. H. and Wolpert, L. (1973). Positional information in chick limb morphogenesis. *Nature* **244**, 492-496.

Sun, X., Mariani, F. V. and Martin, G. R. (2002). Functions of FGF signalling from the apical ectodermal ridge in limb development. *Nature* **418**, 501-508.

Suzuki, T., Hasso, S. M. and Fallon, J. F. (2008). Unique SMAD1/5/8 activity at the phalanx-forming region determines digit identity. *Proc Natl Acad Sci U S A* **105**, 4185-4190.

Suzuki-Hirano, A., Harada, H., Sato, T. and Nakamura, H. (2010). Activation of Ras-ERK pathway by Fgf8 and its downregulation by Sprouty2 for the isthmus organizing activity. *Dev Biol* **337**, 284-293.

Swindell, E. C., Thaller, C., Sockanathan, S., Petkovich, M., Jessell, T. M. and Eichele, G. (1999). Complementary domains of retinoic acid production and degradation in the early chick embryo. *Dev Biol* **216**, 282-296.

Tabin, C. and Wolpert, L. (2007). Rethinking the proximodistal axis of the vertebrate limb in the molecular era. *Genes Dev* **21**, 1433-1442.

Takahashi, K. and Yamanaka, S. (2006). Induction of pluripotent stem cells from mouse embryonic and adult fibroblast cultures by defined factors. *Cell* **126**, 663-676.

Takeuchi, J. K., Koshiba-Takeuchi, K., Suzuki, T., Kamimura, M., Ogura, K. and Ogura, T. (2003). Tbx5 and Tbx4 trigger limb initiation through activation of the Wnt/Fgf signaling cascade. *Development* **130**, 2729-2739.

Takeuchi, J. K., Koshiba-Takeuchi, K., Matsumoto, K., Vogel-Hopker, A., Naitoh-Matsuo, M., Ogura, K., Takahashi, N., Yasuda, K. and Ogura, T. (1999). Tbx5 and Tbx4 genes determine the wing/leg identity of limb buds. *Nature* **398**, 810-814.

Tavares, A. T., Tsukui, T. and Izpisua Belmonte, J. C. (2000). Evidence that members of the Cut/Cux/CDP family may be involved in AER positioning and polarizing activity during chick limb development. *Development* **127**, 5133-5144.

te Welscher, P., Fernandez-Teran, M., Ros, M. A. and Zeller, R. (2002). Mutual genetic antagonism involving GLI3 and dHAND prepatterns the vertebrate limb bud mesenchyme prior to SHH signaling. *Genes Dev* **16**, 421-426.

ten Berge, D., Brugmann, S. A., Helms, J. A. and Nusse, R. (2008). Wnt and FGF signals interact to coordinate growth with cell fate specification during limb development. *Development* **135**, 3247-3257.

Teo, A. K. and Vallier, L. (2010). Emerging use of stem cells in regenerative medicine. *Biochem J* **428**, 11-23.

Thisse, B. and Thisse, C. (2005). Functions and regulations of fibroblast growth factor signaling during embryonic development. *Dev Biol* **287**, 390-402.

Thisse, B., Heyer, V., Lux, A., Alunni, V., Degrave, A., Seiliez, I., Kirchner, J., Parkhill, J. P. and Thisse, C. (2004). Spatial and temporal expression of the zebrafish genome by large-scale in situ hybridization screening. *Methods Cell Biol* **77**, 505-519.

Thisse, C. and Thisse, B. (2008). High-resolution in situ hybridization to whole-mount zebrafish embryos. *Nat Protoc* **3**, 59-69.

Tickle, C. (2002a). Molecular basis of vertebrate limb patterning. *Am J Med Genet* **112**, 250-255.

Tickle, C. (2002b). Vertebrate limb development and possible clues to diversity in limb form. *J Morphol* **252**, 29-37.

Todt, W. T. and Fallon, J. F. (1984). Development of the apical ectodermal ridge in the chick wing bud. *J. Embryol. Exp. Morph* **80**, 21-41.

Tomás, A. R. (2006). Papel do gene flrt3 no desenvolvimento do membro dos vertebrados. In *Departamento de Zoologia, Faculdade de Ciências e Tecnologia*, vol. MSc in Cell Biology, pp. 95. Coimbra: Universidade de Coimbra.

Tomás, A. R., Certal, A. C. and Rodríguez-Léon, J. (2010). Flrt3 as a key player on chick limb development. *(submitted)*.

Towers, M. and Tickle, C. (2009a). Generation of pattern and form in the developing limb. *Int J Dev Biol* **53**, 805-812.

Towers, M. and Tickle, C. (2009b). Growing models of vertebrate limb development. *Development* **136**, 179-190.

Trokovic, R., Trokovic, N., Hernesniemi, S., Pirvola, U., Vogt Weisenhorn, D. M., Rossant, J., McMahon, A. P., Wurst, W. and Partanen, J. (2003). FGFR1 is independently required in both developing mid- and hindbrain for sustained response to isthmic signals. *EMBO J* **22**, 1811-1823.

Tsang, M. and Dawid, I. B. (2004). Promotion and attenuation of FGF signaling through the Ras-MAPK pathway. *Sci STKE* **2004**, pe17.

Tsang, M., Friesel, R., Kudoh, T. and Dawid, I. B. (2002). Identification of Sef, a novel modulator of FGF signalling. *Nat Cell Biol* **4**, 165-169.

Tsuji, L., Yamashita, T., Kubo, T., Madura, T., Tanaka, H., Hosokawa, K. and Tohyama, M. (2004). FLRT3, a cell surface molecule containing LRR repeats and a FNIII domain, promotes neurite outgrowth. *Biochem Biophys Res Commun* **313**, 1086-1091.

Uchikawa, M., Kamachi, Y. and Kondoh, H. (1999). Two distinct subgroups of Group B Sox genes for transcriptional activators and repressors: their expression during embryonic organogenesis of the chicken. *Mech Dev* **84**, 103-120.

Van Vactor, D., O'Reilly, A. M. and Neel, B. G. (1998). Genetic analysis of protein tyrosine phosphatases. *Curr Opin Genet Dev* **8**, 112-126.

Velkey, J. M. and O'Shea, K. S. (2003). Oct4 RNA interference induces trophectoderm differentiation in mouse embryonic stem cells. *Genesis* **37**, 18-24.

Verheyden, J. M., Lewandoski, M., Deng, C., Harfe, B. D. and Sun, X. (2005). Conditional inactivation of Fgfr1 in mouse defines its role in limb bud establishment, outgrowth and digit patterning. *Development* **132**, 4235-4245.

Vernon, A. E. and Philpott, A. (2003). A single cdk inhibitor, p27Xic1, functions beyond cell cycle regulation to promote muscle differentiation in Xenopus. *Development* **130**, 71-83.

Vernon, A. E., Devine, C. and Philpott, A. (2003). The cdk inhibitor p27Xic1 is required for differentiation of primary neurones in Xenopus. *Development* **130**, 85-92.

Vogel, A., Rodriguez, C. and Izpisua-Belmonte, J. C. (1996). Involvement of FGF-8 in initiation, outgrowth and patterning of the vertebrate limb. *Development* **122**, 1737-1750.

Wang, C. K., Omi, M., Ferrari, D., Cheng, H. C., Lizarraga, G., Chin, H. J., Upholt, W. B., Dealy, C. N. and Kosher, R. A. (2004). Function of BMPs in the apical ectoderm of the developing mouse limb. *Dev Biol* **269**, 109-122.

Wegner, M. and Stolt, C. C. (2005). From stem cells to neurons and glia: a Soxist's view of neural development. *Trends Neurosci* **28**, 583-588.

Wei, Z., Yang, Y., Zhang, P., Andrianakos, R., Hasegawa, K., Lyu, J., Chen, X., Bai, G., Liu, C., Pera, M. et al. (2009). Klf4 interacts directly with Oct4 and Sox2 to promote reprogramming. *Stem Cells* **27**, 2969-2978.

Weston, A. D., Rosen, V., Chandraratna, R. A. and Underhill, T. M. (2000). Regulation of skeletal progenitor differentiation by the BMP and retinoid signaling pathways. *J Cell Biol* **148**, 679-690.

Wilkinson, D. G. (1992). In Situ Hybridization. Oxford: Oxford Univ. Press.

Wilson, V., Olivera-Martinez, I. and Storey, K. G. (2009). Stem cells, signals and vertebrate body axis extension. *Development* **136**, 1591-1604.

Wolpert, L. (1969). Positional information and the spatial pattern of cellular differentiation. *J Theor Biol* **25**, 1-47.

Xu, X., Weinstein, M., Li, C., Naski, M., Cohen, R. I., Ornitz, D. M., Leder, P. and Deng, C. (1998). Fibroblast growth factor receptor 2 (FGFR2)-mediated reciprocal regulation loop between FGF8 and FGF10 is essential for limb induction. *Development* **125**, 753-765.

Yang, Y. and Niswander, L. (1995). Interaction between the signaling molecules WNT7a and SHH during vertebrate limb development: dorsal signals regulate anteroposterior patterning. *Cell* **80**, 939-947.

Yashiro, K., Zhao, X., Uehara, M., Yamashita, K., Nishijima, M., Nishino, J., Saijoh, Y., Sakai, Y. and Hamada, H. (2004). Regulation of retinoic acid distribution is required for proximodistal patterning and outgrowth of the developing mouse limb. *Dev Cell* **6**, 411-422.

Ying, Q. L., Nichols, J., Chambers, I. and Smith, A. (2003). BMP induction of Id proteins suppresses differentiation and sustains embryonic stem cell self-renewal in collaboration with STAT3. *Cell* **115**, 281-292.

Yonei-Tamura, S., Endo, T., Yajima, H., Ohuchi, H., Ide, H. and Tamura, K. (1999). FGF7 and FGF10 directly induce the apical ectodermal ridge in chick embryos. *Dev Biol* **211**, 133-143.

Yu, J., Vodyanik, M. A., Smuga-Otto, K., Antosiewicz-Bourget, J., Frane, J. L., Tian, S., Nie, J., Jonsdottir, G. A., Ruotti, V., Stewart, R. et al. (2007). Induced pluripotent stem cell lines derived from human somatic cells. *Science* **318**, 1917-1920.

Zeller, R., Lopez-Rios, J. and Zuniga, A. (2009). Vertebrate limb bud development: moving towards integrative analysis of organogenesis. *Nat Rev Genet* **10**, 845-858.

Zhan, M., Zhao, H. and Han, Z. C. (2004). Signalling mechanisms of anoikis. *Histol Histopathol* **19**, 973-983.

Zhang, D., Schwarz, E. M., Rosier, R. N., Zuscik, M. J., Puzas, J. E. and O'Keefe, R. J. (2003). ALK2 functions as a BMP type I receptor and induces Indian hedgehog in chondrocytes during skeletal development. *J Bone Miner Res* **18**, 1593-1604.

Zhang, J. and Li, L. (2005). BMP signaling and stem cell regulation. *Dev Biol* **284**, 1-11.

Zhang, S., Lin, Y., Itaranta, P., Yagi, A. and Vainio, S. (2001). Expression of Sprouty genes 1, 2 and 4 during mouse organogenesis. *Mech Dev* **109**, 367-370.

Zhao, X., Sirbu, I. O., Mic, F. A., Molotkova, N., Molotkov, A., Kumar, S. and Duester, G. (2009). Retinoic acid promotes limb induction through effects on body axis extension but is unnecessary for limb patterning. *Curr Biol* **19**, 1050-1057.

Zuniga, A., Haramis, A. P., McMahon, A. P. and Zeller, R. (1999). Signal relay by BMP antagonism controls the SHH/FGF4 feedback loop in vertebrate limb buds. *Nature* **401**, 598-602.

Zuzarte-Luis, V., Montero, J. A., Rodriguez-Leon, J., Merino, R., Rodriguez-Rey, J. C. and Hurle, J. M. (2004). A new role for BMP5 during limb development acting through the synergic activation of Smad and MAPK pathways. *Dev Biol* **272**, 39-52.

INDEX OF FIGURES

INDEX OF TABLES

ANNEXES

I Supplementary data

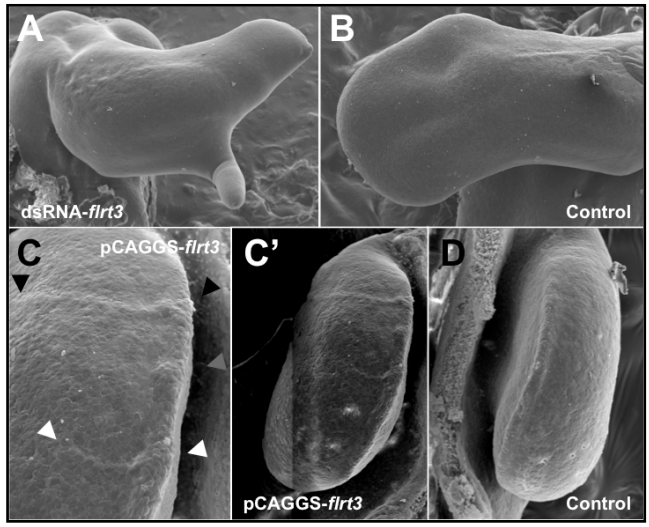

Figure 44. Scanning electron microscopy of *flrt3* gain and loss-of-function experiment embryos. A, Scanning Electron Micrograph of a *flrt3*-dsRNA electroporated limb; note that a small cluster of isolated AER cells is still able to promote outgrowth of part of the limb; **B**, control limb. **C**, Scanning Electron Micrograph of pCAGGS-*flrt3* electroporated embryos 72h after manipulation; **C'** is a detail of the phenotype shown in **C**, zooming on the projections towards the dorsal side of the limb bud and enlargement of the pre-existing AER. **D**, control limb.

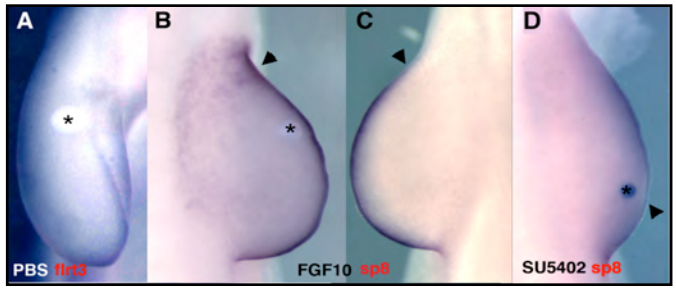

Figure 45. Control experiments of *flrt3* regulation by bead implantation. A, *In situ* hybridisation showing unaltered expression of *flrt3* 10h after treatment with a PBS bead. **B-D**, Example of the effect of FGF bead application; from (Kawakami et al., 2004). **B, C**, *sp8* induction 8h after FGF10 bead implantation. **D**, *in situ* hybridisation for *sp8* showing inhibition of *sp8* expression 12h after treatment with SU5402-soaked beads. *****, Bead location.

II Embryonic stages of the animal models used

II.1 *Gallus gallus*

HH Stage	Somite number	Incubation period
1	—	< 6 hours
2	—	6-7 hours
3	—	12-13 hours
4	—	18-19 hours
5	—	19-22 hours
6	—	23-25 hours
7	1 somite	23-26 hours
8	4 somites	26-29 hours
9	7 somites	29-33 hours
10	10 somites	33-38 hours
11	13 somites	40-45 hours
12	16 somites	45-49 hours
13	19 somites	48-52 hours
14	22 somites	50-53 hours
15	24-27 somites	50-55 hours
16	26-28 somites	51-56 hours
17	29-32 somites	52-64 hours
18	30-36 somites	63-79 hours
19	37-40 somites	68-72 hours
20	40-43 somites	70-72 hours
21	43-44 somites	3 1/2 days
22	—	3 1/2 days
23	—	3 1/2-4 days
24	—	4 days
25	—	4 1/2 days
26	—	4 1/2-5 days
27	—	5 days
28	—	5 1/2 days
29	—	6 days
30	—	6 1/2 days
31	—	7 days
32	—	7 1/2 days
33	—	7 1/2-8 days
34	—	8 days
35	—	8-9 days
36	—	10 days

HH Stage	Somite number	Incubation period
37	—	11 days
38	—	12 days
39	—	13 days
40	—	14 days
41	—	15 days
42	—	16 days
43	—	17 days
44	—	18 days

II.2 *Danio rerio*

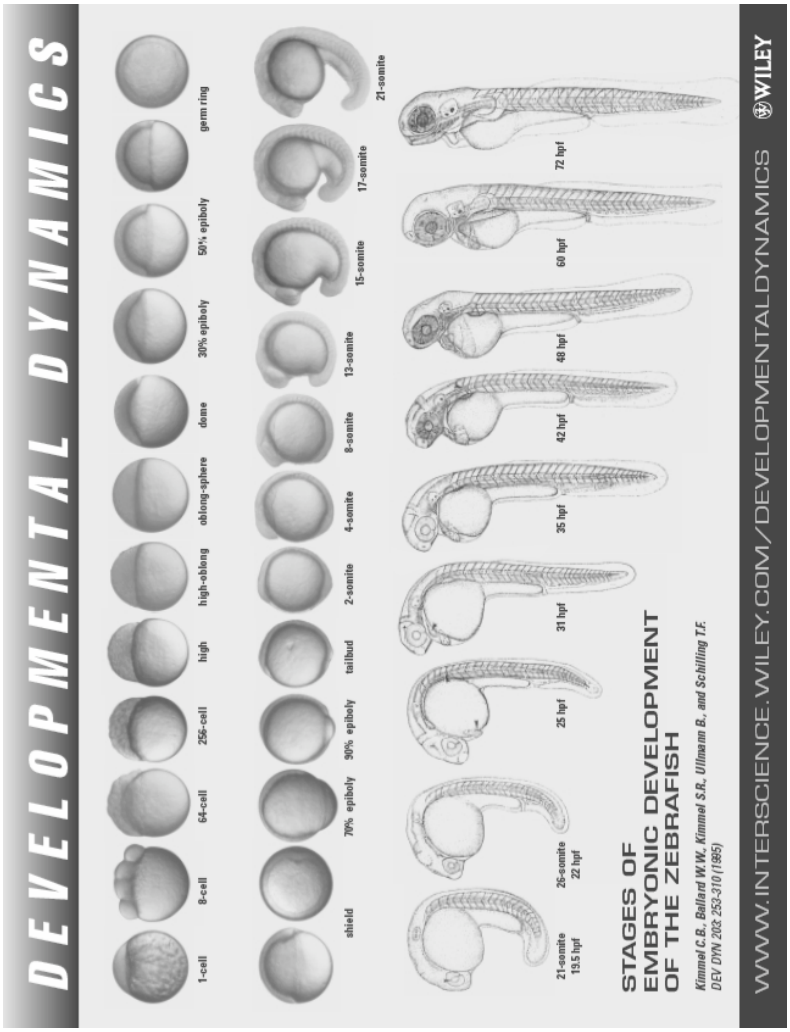

III Detailed Protocols

III.1 Wholemount *in situ* hybridisation protocol for chicken embryos

RNA probe transcription

Transcription buffer (5X)	4µL
Linearized DNA	1µg
Dig mix	2µL
RNasin, RNase inhibitor (Roche)	0,5µL
RNA polymerase (accordingly) (Roche)	1µL
RNase free MiliQ ddH2O	to 20µL

Leave the reaction at 37ºC for 2h30, control for efficient transcription with an electrophoresis gel, and precipitate accordingly, ressuspending in 20µl of ddH2O. Store at -20ºC or dilute in Hybmix buffer.

First day (hybridisation)

1. Rehydrate in decreasing concentrations of MetOH in PBT (PBS with 0,1% Tween-20), 5 min each, rocking
2. Wash in PBT, rocking at Room Temperature (RT) for 2 x 5 min
3. Wash in Hydrogen Peroxide 6% in PBT for 1hr at RT (protect from light).
4. Wash 3 x 5 min in PBT at RT
5. Digest with Proteinase K (10µg/mL) (see Table for time details)

Stage HH	PK time (min)	Stage HH	PK time (min)
9-11	6	22-24	10
12-14	7	25-27	12
15-17	8	28-30	13
19-21	9		

6. Wash with Glycine (2mg/mL in PBT), prepared fresh
7. Pos-fixate in 4% PFA, 0,2% Glutaraldeide for 20 min at RT
8. Wash 2 x 5 min in PBT at RT
9. Substitute PBT for Hybridisation mix (HybMix)
10. Pre-hybridize for at least 3h at 70ºC
11. Hybridize with RNA-Dig/RNA-Fluo probe, or both in case of a double *in situ* hybridisation, dissolved in hybridisation mix (20µL of transcription in 20mL of HybMix) ON at 70ºC

Second day (washes and antibody)

1. Wash 2 x 60 min in ISH sol I (pre-heated at hybridisation temperature)
2. Wash 2 x 30' in ISH sol III (pre-heated at hybridisation temperature of 70ºC)
3. Wash 2 x 5' in MABT
4. Block with blocking solution for at least 3 hrs RT
5. Incubate ON, rocking, at 4ºC with anti-DIG/FLUO diluted from 1:2000/ 1:4000 in 2% heat inactivated sheep serum (HISS)/ 10% blocking solution (Roche)/ MABT

Third day (washes and staining)

1. Wash 2 x 5 min in MABT, 2mM levamisole and then every other hour at RT
2. Wash 2 x 10 min with NTMT solution, freshly prepared
3. Add BM Purple AP Substrate (Roche), and monitor under a dissecting scope
4. Stop reaction with PBT (2 x 10 min) and fixate ON with 4% PFA at 4ºC
5. Wash in PBT
6. Store in a solution of 1% sodium azide in PBT at 4ºC

In case of a double *in situ* hybridisation, stop the reaction, inactivate AP enzymatic activity by heat (70ºC) in MABT for 1hour, block in antibody blocking solution for 1h, and incubate with the antibody against the reporter molecule of the second probe. Continue by redoing day 3 of the previous protocol, this time using a different substrate, like INT/BCIP (Roche) or Fast Red Tablets (Roche).

Solutions

HybMix
50% Formamide; 5x SSC pH 7.5; 10% Tween-20; 50 µg/ml tRNA; 50 µg/ml Heparin

In situ hybridisation solution I
50% Formamide; 5X SSC pH4,5; 0,2% Tween-20

In situ hybridisation solution III
50% Formamide; 2X SSC pH4,5

MAB 5X
500mM Maleic Acid; 450mM NaCl; Adjust pH to 7.5; Treat in an autoclave

MABT
MAB 1X, 0,1% Tween-20 (v/v)

MABT w/ Levamisole
0,4816g levamisol per litre of MABT

NTMT
0.1 M Tris-HCL pH 9.5; 0.1 M $MgCl_2$; 0.5 M NaCl; 1% Tween-20

III.2 Wholemount *in situ* hybridisation protocol for zebrafish embryos

First day (hybridisation)

1. Rehydrate in decreasing concentrations of MetOH 5' each, rocking
2. Wash in PBT, rocking at RT for 5' x 2
3. Dechorion (if necessary, depending on embryo stage)
4. Refix in 4% PFA/PBT, for 20' on ice
5. Wash in PBT, rocking at RT for 5' x 2
6. Incubate with Proteinase K (10µg/mL), see Table 13 for incubation times

Embryo age (hpf)	PK time (min)
<10 hrs embryos	3'
12 hrs embryos	5'
24 hrs embryos	7'
36 hrs embryos	8'
48 hrs embryos	9'
60 hrs embryos	11'
72 hrs embryos	12'

7. Wash in PBT, rocking at RT for 5' x 2
8. Refix in 4% PFA/PBT, for 20' on ice
10. Wash in PBT, rocking at RT for 5' x 2
11. Prepare Fish ISH Hybridisation mix (HM)
12. Rinse with sterile water
13. After removing the water, immediately add acetic anhidride/triethanolamine mix, leave for 10 min without rocking. Prepare mix just before use.
14. Wash in PBT, rocking at RT for 5' x 2
15. Pre-hybridize embryos in HybMix for a minimum of 1 hour at 70ºC
16. Remove HM and hybridize ON at 70ºC with RNA-Dig probe (100-200ng of transcription dissolved in 200 µL of HM)

Second day (washes and antibody)

1. Wash briefly with 5xSSC, 0,1% Tween-20, 50% Formamide at 70ºC
2. Wash for 30' with 5xSSC, 0,1% Tween-20, 50% Formamide at 70ºC
3. Wash for 30' with 2xSSC, 0,1% Tween-20, 50% Formamide at 70ºC
4. Wash for 30' with 2xSSC, 0,1% Tween-20, 25% Formamide at 70ºC
5. Wash for 2 x 30' with 2xSSC 0,1% Tween-20 at 70ºC
6. Wash in PBT, rocking at RT for 5' x 2
7. Incubate with blocking solution (5% HISS in PBT) for at least 1 hour
8. Incubate ON with anti-DIG antibody 1:8000 in blocking solution with agitation at 4ºC

Third day (washes and staining)

1. Remove the anti-DIG antibody solution
2. Wash in PBT, very briefly
3. Wash in PBT 6 x 15'
4. Wash 2 x 10' with NTMT solution
5. Incubate embryos in BM Purple AP Substrate at RT in the dark and monitor
6. Stop reaction with PBT
7. Fix ON in 4%PFA
8. Wash in PBT and store embryos in PBT azide

Solutions

Acetic anhidride/ Triethanolamine mix
Add 2,5µl acetic anhidride to 1ml 0,1M triethanolamine

HybMix
60% Formamide; 5x SSC pH 7.5; 0,1% Tween-20; 500 µg/ml tRNA; 50 µg/ml Heparin

NTMT
0.1 M Tris-HCL pH 9.5; 0.1 M MgCl2; 0.5 M NaCl; 1% Tween-20

III.3 Immunohistochemistry protocol for wholemount zebrafish embryos

First day

1. Rehydrate in decreasing concentrations of MetOH 5' each, rocking
2. Wash in PBT, rocking at RT for 5' x 2
3. Dechorion (if necessary, depending on embryo stage)
4. Incubate 30 min in 0,5% TPBS (PBS, 0,5% Triton X-100)
5. Rinse with sterile water
6. Fix in Acetone, for 10' on ice
7. Rinse with sterile water
8. Block in PBS/BSA/DMSO/Triton +FBS for 1 hour
9. Dilute the 1st Antibody in the blocking solution (w/o FBS) and leave it from 1h at (37ºC) to ON (4ºC) – adapt according to the antibodies

Second day

(save the 1st Antibody)

1. Wash in 4-5 x 30 min in 0,1% TPBS
2. (If not DAB jump to 3) If DAB, do Blocking of Endogenous Peroxidase with 6% H_2O_2 in PBT for 1 hour at RT

3. 2 x 5 min 0,1% TPBS
4. Dilute the 2st Antibody in the blocking solution (w/o FBS) and leave it from 1h at (37ºC) to ON (4ºC) – adapt according to the antibodies

Third day

1. Remove the antibody solution
2. Wash in 4-5 x 30 min in 0,1% TPBS
3. If DAB, Add substrate and develop. Stop reaction with PBT

Solutions

Acetic anhidride/ Triethanolamine mix
Add 2,5µl acetic anhidride to 1ml 0,1M triethanolamine

PBS/BSA/DMSO/Triton
10 ml 10 x PBS; 1g BSA; 1 ml DMSO; 0,5 ml 10% Triton X-100; H_2O to 100 ml. Add 15 µl FBS per ml of blocking solution.

III.4 RNAi cloning

Before transfection with pSuper plasmid it is necessary to: select target sequence and design primers, anneal primers, phosphorylate oligos, dephosphorylate pSuper, ligate and transform E. coli.
Specific oligo primers had to be constructed for each gene; these were made using iRNAi software (www.mekentosj.com). This program selects a target sequence for the gene we intent to silence, according to the following parameters: sequences as close as possible from to the initiation codon, GC content between 40-60%, no symmetry and a Thymine in the middle of the sequence. Oligos with 64bp were purchased from MWG-Biotech AG (Ebersberg, Germany).
Each primer was resuspended to 100pmol/µL, of DEPC water. Then 1µL of each (forward and reverse) primer was mixed with 48µL RNAi annealing buffer (100mM Potassium acetate, 30mM HEPES (KOH pH 7,4), 2 mM Magnesium acetate) in a PCR tube. To promote annealing of the two primers the termocycler was programmed for 4' at 95ºC, 10' at 70ºC and finally 4ºC.

Phosphorylation of primers and dephosphorylation of pSuper

To enhance the efficiency of the ligation the extremities of the primers were phosphorylated and those of pSuper dephosphorylated. Primers were phosphorilated using polynucleotide kinase (PNK) as follows:

Reaction mix	
Annealed primers	1µL
PNK buffer	1µL
ATP (1mM)	1µL
T4 PNK enzyme	1µL
H_2O	5µL

Reaction conditions	
37°C	30’
70°C (PNK inactivation temperature)	10’

pSuper vector was first linearized with BglII and HindIII, and then dephosphorilated with Shrimp Alkaline Phosphatase (SAP), this enzyme removes the phosphate group from 5’ ends, as follows:

Reaction mix	
pSuper	20ng
SAP (1000U)	1µL
SAP buffer	1µL
H_2O	4µL

Reaction conditions	
37 °C	45’
65 °C	20’

Primers and pSuper ligation

For ligation of primers into pSuper T4 DNA ligase was used, this enzyme has the ability to create phosphate bonds between the extremities. Reaction mix (see bellow) was incubated for 1 hour at RT.

Phosphorylated primers	2µL
Dephosphorylated pSuper	1µL
T4 DNA ligase buffer	1µL
T4 DNA ligase	1µL
H_2O	5µL

The plasmid was transfected to *E. coli* competent cells, colonies picked, and their pDNA extracted. To confirm the insertion the plasmid was double digested with EcoRI and HindIII. DNA was migrated in a 0,8% agarose gel. Positive recombinant clones should present a 360bp band and clones without insert should have a 300bp band. Positive clones were then sequenced, only clones with 100% homology in the 64bp where selected since a single nucleotide mismatch could abrogate the ability to suppress gene expression.

III.5 Production of RCAS virus

Previously, clone the full-length cDNA of the gene of interest into an empty RCAS vector.

1. Split chicken embryonic fibroblast (CEF).
   From a nearly confluent 10-cm dish, suspend cells in 20 mL, and plate 1 mL into a 6cm dish.
2. Let the cells grow until they reach 50-70% confluence in a (normally in 12-16 hours).
3. Transfect RCAS construct using Fugene6 (Roche).The following condition is for a 6-cm dish.
   a) add 3 mg of RCAS construct, 0.5 mg of pCAGGS-GFP and opti-MEM to a total of 100 mL.
   b) 9 mL of Fugene6, opti-MEM to a total of 100 mL.
   c) add b) to a), mix, spin briefly, and leave at RT for 15 min.
   d) while waiting, change media to fresh growth media (2 mL).
   e) add DNA-Fugene6 complex, by dropping onto cells.
4. Confirm the transfection efficiency by the GFP signal after 24 hours.
5. Wait until 48 hours post-transfection, then trypsinize cells and transfer into a 10cm dish.
6. When the cells reach confluence, trypsinize cells, suspend in 10-mL media, and transfer 2.5mL into a new 10cm dish.
   Also transfer 5 mL of old media, and add ~8 mL of fresh media.
7. When the cells reach confluence, expand the cells into a 15cm dish. Transfer all the old media containing RCAS virus to the 15cm dish.

8. When the cells reach confluence, expand the cells into 4 x 15cm dishes.
   Transfer all the old media containing RCAS virus to the 4 x 15cm dish.

9. When the cells reach confluence, change the media to harvesting media (11mL/dish).
10. Collect the media and feed the cells with fresh collecting media every day.
    Spin the media at 1,500 rpm at RT, collect the supernatant and keep it at 4ºC (only for a few days).
11. Repeat step 10 for 3-4 days.

12. Combine all supernatant, and filter 0.45 mm using a filter unit plus a glassfiber filter.
13. Spin the supernatant
    Beckman SW28 rotor, 22000 rpm, 4ºC, 2 hours, Accel=1, decel=7
14. Decant the sup. Wipe 1/2 of the tube using kimwipe with the tube inverted.
15. Stand the tubes on ice for 30-60 min. Suspend virus in the remaining media, and combine them. Transfer the virus solution into a 1.5mL tube.

16. Spin at 12,000 rpm at 4ºC for 5 min, and take the supernatant to a new tube. Calculate the degree of concentration by the volume.
17. Divide into 10 mL aliquot, and store at -80ºC.
18. If necessary, determine the titer by serial dilution and immunostaining using anti-gag antibody (AMV3C2).

Media

growth media
D-MEM (high glucose) + 10% FBS, 1% chicken serum, Glutamine, antibiotics

harvesting media
Opti-MEM + 2% FBS, 0.1% chicken serum, Glutamine, antibiotics

IV Sequences

Gallus Gallus*'s *Flrt2 (ChEST873n14; 816 pb)

GGATTATGATCGGTGCCGGCGAGGGATTCCCAGACACTGTCAGGCAGGCCAGAT
CCAGCTGATAGCTGTTATGAGGACTTTGCTGACTTCAGAAAGCTGAGCATAACAT
CAACAGACTTCAGTGAAAGGAAATATTATCACTCCAAGCAACTTGTACACAGAC
AACTTTTGGTAGCTTTAAATTAACTGGTTGCTCACCTACAAGGACACAGCTAGTG
TTTCTTTCGGCACAAATGGAGGAAAGCAACAAGATTTGTAACCCTGGCTAATAGG
ACTGTGGCTTTCTTATCAAAAGTAGGAGGTGGGCCAAGTGTAAAAGGATTATTTT
ATACTTAGCCTGAACACTGGACATAAACTGAAGCCAATTTTAATGACCTGAGATT
TTGCTACTTGTCCTTTATTATTGTTATCAGTTCTTTAACACTTTGATACTTTCTTTC
TTTAAATTGGACATGGGTTCCTGGACTAGAATGTGGCCCTCAGACTGGGCTGTTC
TCATGAAATCATGGCTTATCTTTTCCCTGGGGCTCTACATGCAGGTCTCCAAAACT
TTGGCCTGTCCAAAAGTGTGCCGCTGTGACCGAAACTTTGTCTACTGTAATGAGC
GAAGCTTGACCTCAGTGCCTCTTGGGATACCAGAGGGTGTAACCGTCCTCTACTC
CATAATAACCAAATTAATAATGCTGGATTTCCTGCAGAGTTGCACAGTGTCCAGT
CTGTGCACACAGTCTATCTGTATGGCACCAATTGGATGATTCCCAATGAACCTGC
CCAAAAATGTCAGGGTTCTCCACTTGCAGGAAAACAATATCAGAC

Gallus Gallus*'s *Flrt3 (ChEST840j5; 730 pb)

TCCAAGATCATTACAATATTTGTGAAATCGGTGAGCACAGAGACCATCCACATCT
CCTGGAAAGTTGCGCTGCCAATGACAGCCTTACGGCTCAGCTGGCTCAAGATGGG
CCACAGCCCTGCCTTTGGATCTATAACTGAAACCATCGTAACAGGGGACAGGAGT
GACTACCTGCTTACAGCACTCGAACCAGAGTCGCCATACCGCGTCTGCATGGTCC
CCATGGAAACCAGCAACATCTATCTCTCTGACGAGACACCTGAATGCATCGAGAC
CGAGACAGCTCCCCTCAAGATGTACAACCCGACAACCACACTCAACCGGGAGCA
GGAAAAGGAGCCCTACAAGAACTCCAGCGTGCCTCTGGCCGCCATCATCGGTGG
CGCGGTGGCACTGGTGGCCCTGGCACTGCTGGCCCTGGTGTGCTGGTACGTCCAC
AGGAATGGGGCCCTCTTCTCCCGGCACTGCGCCTACAGCAAGGGGCGCAGGAGG
AAGGACGACTATGCTGAGGCGGGTACCAAGAAGGACAACTCCATTCTAGAAATC
AGGGAGACTTCTTTTCAGATGATACCCATCACTAACGACCAGGTGTCCAAGGAGG
AGTTTGTAATACACACCATTTTCCCCCCTAATGGCATGAATCTGTATAAGAACAG
CCACAGTGAAAGCAGTAGTAACAGGAGCTACAGAGACAGTGGTATTCCAGATTC
AGATCATTCACACTCATGAT

Danio rerio*'s *Flrt3 (710 pb)

CTGAAGCGACTGGTTCTGGATGGCAACCTCCTGAACAACAGGGGCATCGGGGAG
ATGGCCTTGGTGAATTTAGTAAATCTGACCGAGCTCTCATTGGTACGAAACTCCC
TGACGTCCCCACCAGCCAACTTGCCTGGCTCAAGCCTAGAGAAGCTAAATCTTCA
AGACAACCACATCAATCACGTACCACCAGGTGCCTTTGCTTTTCTGCGACAGCTG
TACCGCTTGGATTTGTCAGGCAACAACTTGAGCAGTCTGCCCATGGGGGTATTTG
AGGACCTGGATAACCTTACCCAACTGCTCTTGCGCAACAACCCCTGGCATTGCAA
CTGCAGGATGAAGTGGGTACGTGATTGGCTGCGCACTCTTCCATCTAAGGTCAAT
GTGCGTGGCTTCATGTGCCAGGGTCCCGATAAGGTCAAAGGGATGGCCATCAAA
GACTTATCCACTGAGCTGTTTGGCTGTTCAGACACAGAGATTCCAACCACATACG
AGACCAGCACAGTCTCAAACACTTTGCCTCCCTCTCGACCCCAGTGGCCCTCATA

TGTAACTAAAAGACCTGTGGTTAAGGGTCCAGATCTAGGAAGAAACTATCGTAG
CACGACACCGTCTAGTCGTAAGATCATCACAATAAGTGTCAAATCAAGTAGCGCT
GAGACAGTGCACATATCTTGGAGAGTATCTCAGCCCATGACAGCCCTGAGGCTC

Gallus Gallus*'s *Oct4 (probe=full length, 742bp)

ATGCATGTAAAAGCCAAAAACCTGCTGCGAATGTGTAAATGGCTTAAAGGATTG
CGAAATGCCCGCGGCAGCACTTGGGGCCGTAGCGGTGGCAGGAAGCCGATGCGC
TCGAGTGAGCGGCTGCCCCGAAGTGCGGATCCTGGCTGGGGGAACCACGCGAAC
CGCGCGGCTGTTGTCACCCGCGGTATCTCGAGCCATTCACCGCGTGTCTGCCTCT
GCCTCTGCCAGGATGCGCCAACCTCAGAGGAGCTGGAGCAGTTTGCCAAGGACC
TCAAGCACAAGCGCATCATGCTGGGCTTCACTCAGGCTGACGTGGGGCTGGCTCT
GGGCACGCTCTATGGGAAGATGTTCAGCCAGACCACCATCTGCCGCTTCGAAGCT
CTCCAGCTCAGCTTTAAGAACATGTGCAAGCTGAAGCCACTGCTGCAGCGTTGGC
TCAATGAGGCAGAGAACACGGACAACATGCAGGAGATGTGCAATGCAGAGCAA
GTGCTGGCCCAAGCCCGGAAGAGAAAACGCAGGACCAGCATCGAGACCAACGTG
AAGGGAACGCTGGAGAGCTTCTTCCGCAAATGTGTGAAGCCCAGTCCCCAGGAG
ATCTCCCAGATCGCTGAGGACCTCAACCTGGACAAAGACGTTGTCCGGGTCTGGT
TCTGCAACCGGCGTCAGAAAGGCAAGCGGCTGCTGCTGCCCTTTGGCAACGAGTC
GGAGGGGGTGATGTACGACATGAACCAGTCCCTGGTGCCCCCTNGTCTGCCCATC
CCAGTGACATCCCAGGGCTACAGCCTGGCGCCGTCCCCCCCCGTCTACATGCCAC
CTTTCCACAAGGCCGAGATGTTCCCCCCGCCTCTGCAGCCCGGGATCTCCATGAA
CAACAGCAGCCAC**TAA**

Gallus Gallus*'s *Lgr5 (ChEST999g16; 355 bp)

GCTGCGGCGGGCAGGAGGGCATGCTGCTCTGCGCCGACTGCTCCGACCTGGGGC
TGACGGCCGTGCCCGCCAACCTCAGTGCCTTCACCTCCTACCTTGATCTCAGTATG
AACAACATTACTAAGCTGCCCTCGAACCCCGTGCACAATCTCCGCTTCCTGGAAG
AGCTACGTCTTGCAGGAAATGGCTTGACATACATTCCTAAGGGAGCATTTGCTGG
CCTTTTCAGTCTTAAAGTGCTAATGCTGCAGAATAACCAACTACGCCAGGTTCCT
ACTGAAGCACTCCAGAACTTGCGCAGCCTGCAGTCTCTACGCCTGGATGCCAACC
ACATCAACTACGTGCCCCCCAAAAA

Gallus Gallus*'s *flrt3 (full length, 2028bp)

ATGGCAACCATCACAAAATTTACTCTTACCTTTAAATACGATTTTGAAGATCAGA
ACTGTATACAGATCTCATCATTCCTGACCATGATTACTGTACCCTGGAGCGTCTTC
CTAATTTGGACTAAAATAGGGCTGTTACTTGACATGGCACCTTATTCTGTCGCTGC
CAAACCGTGCCCATCAGTATGTCGCTGTGATGTGGGTTTCATATATTGTAATGAT
CGCGATTTGACATCTATTCCTACAGGAATCCCAGAGGATGCTACTAACCTCTTCC
TTCAGAACAATCAAATAAATAATGCTGGGATTCCGTCCGAACTGAAGAACTTGCG
TAGGGTGGAGAGAATATTTTTATACCACAACAGCCTAGATGAATTCCCCACTAAC
CTCCCTAAGTACGTCAAAGAACTGCATTTGCAGGAGAATAATATAAGGACCATC
ACTTACGATTCACTTTCACAAATTCCTTATCTGGAAGAACTGCATTTGGATGATA
ATTCTGTTTCCGCTGTTAGCATTGAAGATGGAGCTTTCAGGGACAACATCTATCTC
AGACTTCTTTTTCTCTCTCGAAATCACCTTAGCACCATTCCCTGGGGTTTGCCTAA
AACAATAGAAGAGCTACGCTTGGATGATAATCGTATTTCCACGATTTCAGAGCTG
TCCCTTCAAGACCTTACAAATCTAAAACGCCTTGTTCTAGATGGAAATCTTCTAA

ATAACCACGGATTAGGAGACAAGGTCTTTATGAATCTAGTCAATCTTACAGAACT
GTCATTGGTTCGCAATTCACTTACAGCCGCACCAGTAAATTTGCCAGGAACAAAC
CTAAGGAAGCTTTATCTGCAAGAAAACCATATCAATCACGTGCCACCCAATGCTT
TCTCTTACTTAAGGCAGTTGTATCGACTAGATATGTCCAATAACAATCTCAGCAA
TTTACCTCAGGGTGTCTTTGATGACCTGGACAACATAACTCAGCTGTTTCTTCGCA
ACAACCCTTGGCACTGTGGGTGCAAAATGAAGTGGGTCCGTGACTGGTTACAGTC
ATTGCCTTTGAAAGTGAACGTACGTGGGCTGATGTGCCAGGCGCCGGAAAAAGT
GCGCGGAATGGCTATCAAAGACCTGAACGCGGAACTGTTCGATTGTAAGGATGA
CATGAGCACCATCCAGATCACTACTGCGGTACCCAACACGCTGTACCCGGCCCAG
GGACACTGGCCGGTTTCTGTGACCAAACAACCAGACATCAAGACCCCCAACCTA
AACAAGAACTACAGAACCACGGCCAGCCCAGTACGCAAGATCATTACAATATTT
GTGAAATCGGTGAGCACAGAGACCATCCACATCTCCTGGAAAGTTGCGCTGCCA
ATGACAGCCTTACGGCTCAGCTGGCTCAAGATGGGCCACAGCCCTGCCTTTGGAT
CTATAACTGAAACCATCGTAACAGGGGACAGGAGTGACTACCTGCTTACAGCAC
TCGAACCAGAGTCGCCATACCGCGTGTGCATGGTCCCCATGGAAACCAGCAACA
TCTATCTCTCTGACGAGACACCTGAATGCATCGAGACCGAGACAGCTCCCCTCAA
GATGTACAACCCGACAACCACACTCAACCGGGAGCAGGAAAAGGAGCCCTACAA
GAACTCCAGCGTGCCTCTGGCCGCCATCATCGGTGGCGCGGTGGCACTGGTGGCC
CTGGCACTGCTGGCCCTGGTGTGCTGGTACGTCCACAGGAATGGGGCCCTCTTCT
CCCGGCACTGCGCCTACAGCAAGGGGCGCAGGAGGAAGGACGACTATGCTGAGG
CGGGTACCAAGAAGGACAACTCCATCCTAGAAATCAGGGAGACTTCTTTTCAGAT
GATACCCATCACTAACGACCAGGTGTCCAAGGAGGAGTTTGTAATACACACCATT
TTCCCCCCTAATGGCATGAATCTGTATAAGAACAGCCACAGTGAAAGCAGTAGTA
ACAGGAGCTACAGAGACAGTGGTATTCCAGATTCAGATCATTCACACTCA**TGA**

Gallus Gallus*'s *Sox14 (ChEST847i12; probe, 742bp; full length, 723bp)

GCAGC**ATG**TCCAAACCCAGCGACCACATCAAGCGCCCCATGAACGCCTTCATGG
TGTGGTCCCGCGGCCAGCGGCGCAAGATGGCCCAGGAGAACCCCAAAATGCACA
ACTCGGAAATCAGCAAGCGGCTGGGCGCGGAGTGGAAGCTGCTCTCCGAGGCGG
AGAAGCGGCCCTACATCGACGAGGCCAAGCGGCTGCGGGCGCAACACATGAAGG
AACACCCCGACTACAAGTACCGGCCCCGGCGCAAGCCCAAGAACCTGCTCAAAA
AGGACAGGTATGTCTTCCCTTTGCCTTACCTGGGGGAAACCGATCCCTTAAAGGC
TGCCGGGCTTCCCGTGGGGGCCACTGACTCGCTGCTGAGCTCCCCGGAGAAGGCC
AGGGCTTTCCTGCCCCCCACCTCAGCACCTTACTCCTTACTTGACCCCAGCCAGTT
CAGCTCCAGCGCCATTCAGAAGATGACCGAGGTTCCTCACACCTTGGCCACCGGC
ACCCTGCCCTACGCCTCCACCTTGGGATACCAGAACGGGGCGTTCGGCAGCCTGA
GCTGCCCCAGCCAACACACCCACACCCACCCCTCGCCGACCAACCCGGGCTACGT
GGTGCCGTGTAACTGTACCGCTTGGTCGGCCTCCAGTTTGCAGCCTCCGGTTGCCT
ACATATTATTCCCGGGCATGACCAAGACTGGCATAGACCCCTATTCTTCAGCACA
CGCGACTGCTATG**TAA**CACCCGCCCACAAC

Gallus Gallus*'s *p27 (ChEST639l5; probe, 742bp; full length, 594bp)

CGAGAAAACCCACCGCCATCGGTGACGGCAGAAAGGGAGGGGGAG**ATG**TCAAA
CGTCCGCATTTCTAATGGGAGCCCTACCCTGGAGCGCATGGAGGCGCGGCAGTCG
GAGTACCCGAAGCCGTCGGCCTGCAGGAACCTCTTCGGGCCGGTAAACCACGAA
GAGTTAAACAGGGACTTGAAGAAGCACCGCAAGGAAATGGAAGAGGCATGCCA
GAGGAAGTGGAATTTCGATTTCCAGAACCACAAGCCGCTGGAAGGCAGGTACGA

GTGGCAAGCCGTGGAGAAGGGGAGCTCGCCCGACTTCTACTTCAGGCAGCCGAG
GCTATCCAAAGCCGTCTGCAAGTCCGCCGGCCGTCAGAGCCTGGATGTAAACGG
GAATTGCCAAACCGCGATTTGCGCCGCTTCTCAGGGAATCTCAGAGGACACTCAC
TGTGTAGGCCGAAAGACTGATGTTGCTGGCAGTCAGACGGACTTTGCAGAGCAG
TGCGCCGGGCAGAGGAAAAGACCCGCCGCCGACGATTCCTCTCCTCAAAATAAA
AGAGCCAACACAACAGAAGAGGAGGTTTCAGAAGACTCCCCCAGTGCCAGTTCA
GTGGAGCAAACACCCAAGAAATCGAGCCCGAGACGACATCAA**ACG**TAAACTCCC
TAAGGCGGAGGACTCGCGTTTCCTTGCTCATCGGGGGGGCGGTGAAGCCAGGAA
GATATAAGTTGTAGTAGAGATGAATACCTATCGTCGGTCTCCATGGGATTGGGGA
CCCTGTGCAAGCACTTGAAAAACAACGACCGAAAAC

V Plasmids vectors

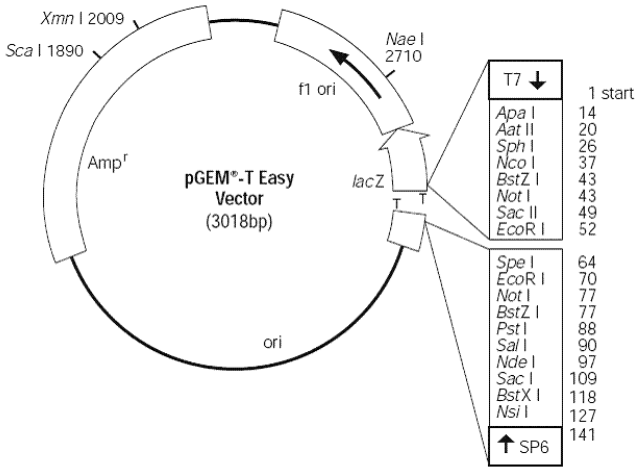

Map 1 – pGEM-T easy plasmid map.

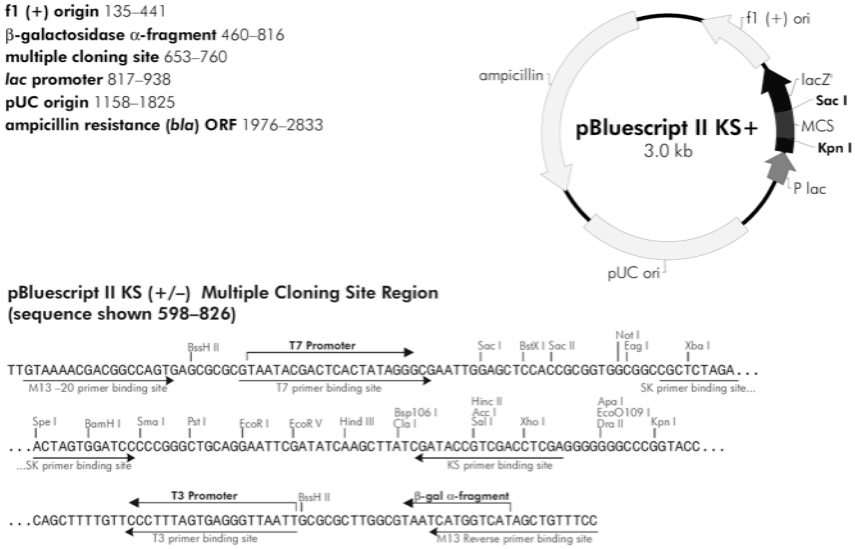

Map 2 – pBluescript II KS+ plasmid map.

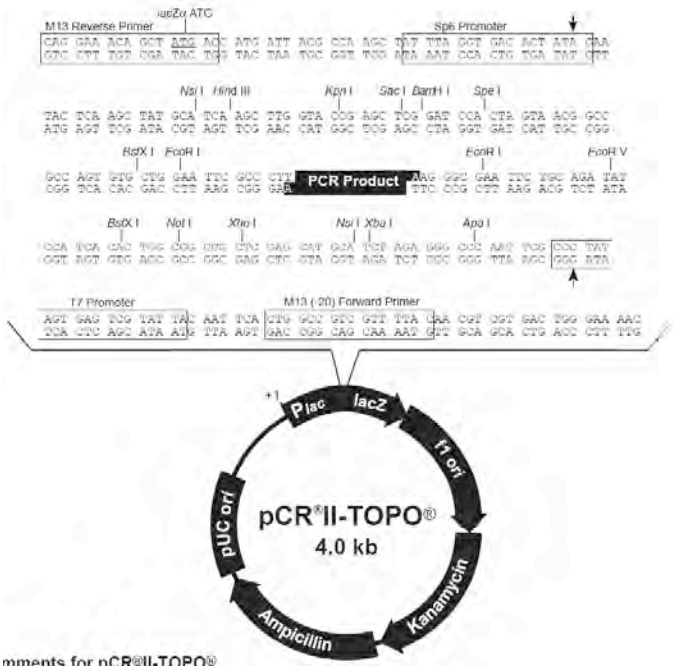

Map 3 – pCR®II-TOPO plasmid map.

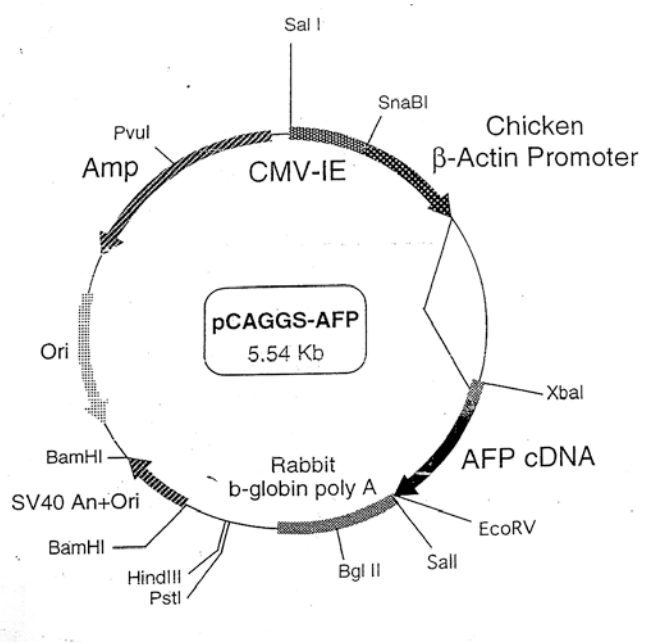

Map 4 – pCAGGS AGFP plasmid map.

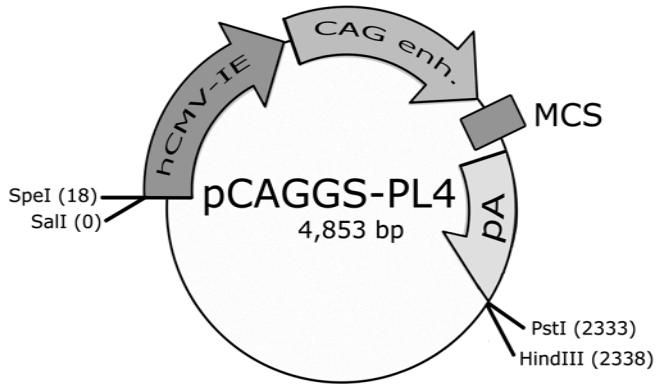

GCGTGTGACCGGCGGCTCTAGAGCCTCTGCTAACCATGTTCATGCCTTCTTCTTTTTCCTACAGCTCCTGGGCAACGTGCTGGTTATT
XbaI
GTGCTGTCTCATCATTTTGGCAAAGAATTGGTACCGCGGCCGCTTCGAACCCGGGAGATCTGATATCATCGATGCTCGAGGCTAGCGAATTCACTCCTCAG
KpnI BglII ClaI XhoI EcoRI
NotI XmaI/SmaI EcoRV

Map 5 – pCAGGS-PL4 modified plasmid map.

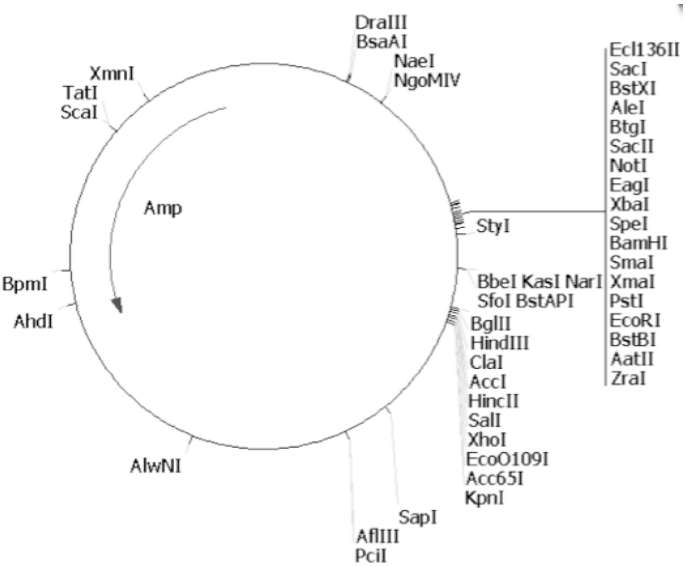

Map 6 – pSuper plasmid map.

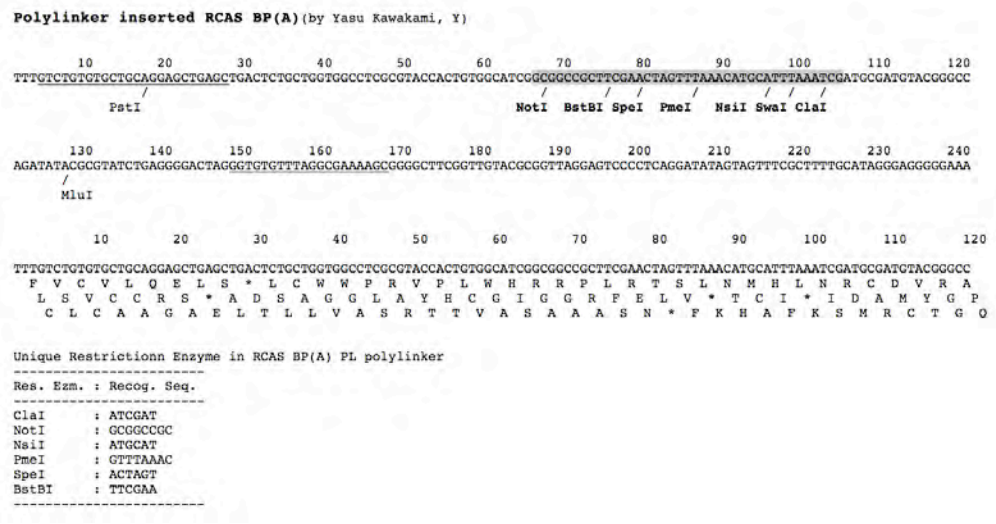

Map 7 – RCAS BP (A) plasmid.